Validation of a sensor setup and interpretation method for in situ degradation studies of coated metals with electrochemical impedance spectroscopy.

J.C.G. Pieterse

Delft University of Technology

TUDelft
Delft University of Technology

C·Cube international bv
Coating *and* Corrosion in Control

Challenge the future

Validation of a sensor setup and interpretation method for in situ degradation studies of coated metals with electrochemical impedance spectroscopy.

By

J.C.G. Pieterse

Course code MK 5903

in partial fulfilment of the requirements for the degree of
Master of Science
in Material Science and Engineering

at the Delft University of Technology,
to be defended publicly on Tuesday April 1, 2014 at 10:00 AM.

Supervisor:	Dr. ir. A. Mol,	TU Delft
Thesis committee:	Prof. dr. ir. H.A. Terryn,	TU Delft
	Dr. ir. D.A. Koleva,	TU Delft
	Dr. ir. A.S. 't Hoen-Velterop,	NLR
	Ir. G. Coolegem,	C-Cube

Partial copy due to confidentiality reasons

TUDelft Delft University of Technology

Preface

The title of this thesis report is "Validation of a sensor setup and interpretation method developed for in situ degradation studies of coated metals with electrochemical impedance spectroscopy".

The thesis project completes the Master of Material Science and Engineering at the faculty of Mechanical, Maritime and Materials Engineering, Delft university of Technology. For their help and guidance during this thesis research, I would like to thank ir. G. Coolegem, ing. G. Harteveld. I like to also thank Dr.ir. J.M.C Mol and Dr. P. Taheri for their supervision and feedback.

Delft University of Technology   J.C.G. Pieterse
March 18, 2014   (1115588)

Contents

1 Summary

Corrosion has a large negative effect on the service life of metallic substrates, such as cars, bikes and boats. To reduce the corrosion rate, the bare metal can be isolated from the corrosive environment by applying an organic coating (paint). As metals corrode, organic coatings degrade. Temperature, wet-dry cycles and UV-light all have an effect on the lifetime of an organic coating. Maintenance of these systems is therefore of vital importance to guarantee the coating still provides sufficient protection against corrosion.

While in theory Electrochemical Impedance Spectroscopy (EIS) can give valuable insight in the condition of a applied in situ coating system, this method is seldom used outside laboratory mainly due to the complexity of the setup. In this master thesis, a new EIS setup and interpretation method are introduced to reduce the complexity of EIS method for in situ measurements. To validate this new method, laboratory coupons with different aircraft coatings were degraded in salt-spray and UV-condensation cabinets. These coupons were frequently measured during the degradation process with a normal EIS setup and the new handheld setup. With these measurements, the interpretation methods and setups were compared. The same procedure was executed on a location outside the laboratory, the Oosterscheldekering, the measurements were compared with result values of measurements performed five years ago.

The result values of the measured laboratory coupons showed comparable degradation trend with both measurement setups. The same was observed with the measurements on the Oosterscheldekering. The interpretation method exhibited an easy way to present the coating condition, although is not able to show complex physical processes occurring when the corrosion process starts. Overall, it can be concluded that the handheld sensor setup with the simplified interpretation method is very good technique for in situ organic coating assessment on metal substrates. With the condition that the measurements are performed by someone who is experienced in the use of Electrochemical Impedance Spectroscopy and who understands the discussed shortcomings of the system.

2 Introduction

2.1 General

All items made of a metal like cars, bikes and boats suffer from corrosion which has a large negative effect on the service life of our possessions. Large infrastructural structures like bridges and sluices also suffer from corrosion as they are often made of metal. Corrosion can be defined as used in Ref. [1] seems best applicable for this study and is defined as "Corrosion is the electrochemical degradation, occurring at the metal-solution interface where the metal is oxidized (anodic reaction) and species from the solution such as oxygen (cathodic reaction) are reduced". Corrosion can have some very serious side effects such as catastrophic failures, system shut downs, etc.

To reduce the rate of the corrosion reactions the bare metal can be isolated from the aggressive environment by applying an organic coating. Organic coatings (paints) are widely used to offer a protection against corrosion. In 2011 archaeologists discovered a finding of a 100,000 year old ochre-based mixture, which may have been used as paint [2]. Besides protection it can have several other functions like lubrication and good aesthetics.

Electrochemical Impedance Spectroscopy (EIS) is a scientific measure method that can provide a detailed insight in the protective properties of an organic coating by measuring the overall protective properties of the coating. This technique is well known for over 15 years for lots of research on coating behavior, quality and accelerated degradation. Although the technique can potentially provide an insight on the condition of coatings outside laboratory these researches are mainly limited to laboratory environments. Primarily due to limitations of the electrochemical impedance spectroscopy setup.

In order to make electrochemical impedance measurements interesting for in situ application it is important that two important requirements are met:
1. Measure setup is easy to use quick and applicable in various configurations (eg. upside-down).
2. The interpretation should be quick and the results should be easy to understand for everyone.

C-Cube international BV company is a specialist in the area of corrosion and coating assessment. C-Cube develops a sensor suitable for the in situ use of Electrochemical Impedance Spectroscopy. In the processes monitoring, it is crucial to follow what happens, in laboratory, and also in practice. Electrochemical measurements are able to describe coating behavior qualitatively and quantitatively. This gives an insight in coating quality and therefore helps to make accurate maintenance schedules, which are of great importance to the life cost of for example large infrastructure.

2.2 Field of application

This research is performed in collaboration with the Dutch Laboratory for Aerospace (NLR). NLR is doing a research to commercially available sensor setups that can give insight in the quality of a protective coating. The Dutch military is interested in this information to be able to make more accurate maintenance schedules for their F16 aircrafts and Apache helicopters. The focus will

therefore be on specialized military aircraft coatings used on F16 aircrafts and Apache helicopters. These coating systems are all artificial degraded in different degradation cabinets and tested in a laboratory. Since these are specialized coating systems used for specific applications, another simplified coating system widely used for infrastructures, is evaluated in this study. Measurements are performed on the Oosterscheldekering sluice and the results are compared with measurements conducted in the past. The Oosterscheldekering is the largest part of the world famous Deltawerken and protects a large part of the Netherlands against the North Sea.

2.3   Research question

The research question is built up in two parts. The first is to verify if the handheld sensor setup produces similar results as a traditional laboratory setup. The second is to compare the simplified interpretation method with two traditional interpretation methods.

Since the research question is divided into two parts the experimental set up is as following:
1. In collaboration with the National Aerospace Laboratory of the Netherlands (NLR) two sets of laboratory coupons are coated with different aircraft coatings and are labeled. These coupons are then artificially degraded in a salt spray cabinet and a cyclic UV-condensation cabinet and periodically measured (roughly every 2 weeks).
   Since these datasets are all artificially degraded, a coating system that is naturally aged is used. C-Cube performed EIS measurements on the Oosterscheldekering sluices in 2008. These measurements are repeated in the same locations. To answer the first part of the research question, the data of the EIS measurements are interpreted with the simplified interpretation method and compared.
2. To verify the second part of the research question, the data generated as described above are analyzed with the simplified interpretation and the phenomenological interpretation methods. These are compared with each other to find boundaries of the simplified interpretation method.

2.4   Research approach

To answer the first part of the research question, the measurement results collected with the laboratory setup for all specimen sets are interpreted and a comparison is made between the interpretation methods used in literature and the simplified interpretation method. To answer the second part, a comparison between the measurement setups is made. The comparison is made with the results generated by the simplified interpretation method. Table 1 shows a schematic overview of the approach followed to answer the research question.

Table 1. Interpretation scheme

	Traditional interpretation	Simplified interpretation	
Laboratory	X	X	
Handheld sensor		X	

It is crucial to know that the different sets of laboratory coupons were not measured simultaneously. First the measurements of the coupons degraded by salt spray were performed after the specimens degraded with the UV condensation cabinet were measured. By performing the measurements, experience was gained and the result data became more accurate. This means that the data collected from the UV condensation cabinet coupons are likely more controlled and with a higher accuracy.

2.5   Outline of the report

In the introduction an overview is given of the research subject, the research questions are presented and the research approach is discussed. Theoretic background of the corrosion process and the electrochemical reactions that take place is explained in Chapter 2. Chapter 3 background of coatings, degradation methods and Electrochemical Impedance Spectroscopy measurement method is given. Chapter 4 the experimental setup and research approach is discussed, the used test setups are described and the interpretation methods are explained. Results and discussion are presented in Chapter 5. The conclusions of the research are summed up in Chapter 6. In chapter 7 called "remarks" describes some phenomena observed during the research. The recommendations are given in Chapter 8. Finally, chapter 9 winds up the report with a measurement protocol based on the experience gained during this research.

3   Background

3.1   Corrosion process

In the production of metals natural ores are processed in several process steps. In the conversation process of natural ores their energetic state is increased. This means that metals have the inherent tendency to revert to its more or less natural state. Corrosion is the chemical re-combination of the metals to form ore like compounds. These corrosion products have very little mechanical strength and a severely corroded metal part is therefore often not useable for its original goal. This thermodynamic reversion process of metals into their ores is schematically shown in Figure 1 as the life cycle from metallic ore to the finished product (metal) [3].
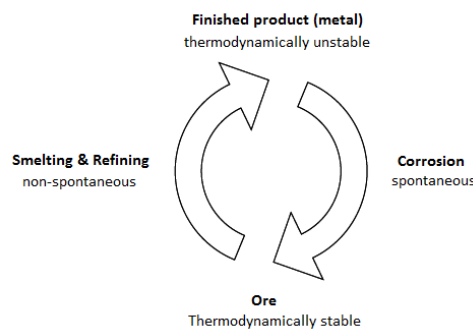

Figure 1. Life cycle metals

As mentioned in the introduction corrosion can be defined as "the electrochemical degradation, occurring at the metal-solution interface where the metal is oxidized (anodic reaction) and species from the solution such as oxygen (cathodic reaction) are reduced". In order for corrosion to take place four components must be present and active.

- *Anode*, the anode is the site where electrons are produced through the chemical activity of the metal. The anode is the area where the metal dissolves into the electrolyte.
- *Cathode*, the cathode is the site where the electrons are consumed and the reduction reaction takes place. For each electron that is produced at an anodic site, an electron must be consumed at a cathodic site. No metal loss occurs at sites that are totally cathodic.
- *Electron path*, in order for electrons to flow from the anodic sites to cathodic sites, the electrons migrate through a metallic path. This migration occurs due to a voltage difference between the anodic and cathodic reactions. Electrons can move easily through metals and some non-metals such as graphite. Electrons from electrochemical reactions cannot move through insulating materials such as most plastics nor can they directly enter water or air. In some cases, the electron path is the corroding metal itself, in other cases, the electron path is through an external material.
- *Electrolyte*, electrolytes are solutions that can conduct electrical currents through the movement of charged chemical constituents called ions. Positive and negative ions are present in equal amounts. Positive ions tend to migrate away from anodic areas and toward cathodic areas. Negative ions tend to migrate away from cathodic sites and towards anodic sites. This closes the electrical circuit between these sites.

Corrosion phenomena are of an electrochemical nature. This means that two or more electrode reactions need to occur, the oxidation and reduction reaction. Oxidation is the process of losing electrons, the metal atoms release electrons (are oxidized) and become positive ions. The oxidation step is called the corrosion reaction and takes place at the anodic site. Its general chemical reaction is shown in 3.1.

$$Fe \rightarrow Fe^{n+} + ne^-$$

3.1

Electrons produced at the anodic site are consumed by the reduction reaction at the cathodic site, which is not the same as the site where the corrosion reaction takes place. The reduction reaction of water or counter reaction is shown in 3.2.

$$O_2 + 2H_2O + 4e^- \rightarrow 4OH^-$$

3.2

After the corrosion reaction, the products of corrosion reactions can precipitate. In the precipitation step the corrosion product is formed, in the case of corroding iron, the formation of iron(II)hydroxide as shown 3.3.

$$Fe^{2+} + 2OH^- \rightarrow Fe(OH)_2$$

3.3

The formation of rust iron(III)oxide is a result of a series of reactions where iron(II)hydroxide is converted. First iron(III)oxide is formed by the further oxidation of iron(II)oxide. The formed iron(III)oxide changes to rust through a dehydration reaction. The overall reaction of the formation of rust from iron(II)oxide is shown in equation 3.4.

$$4Fe(OH)_2 + O_2 \rightarrow 2Fe_2O_3 \cdot H_2O + 2H_2O$$

3.4
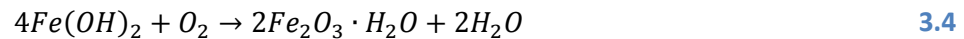
The adhesion of rust on metal is very low, which exposes the metal to more water and oxygen allowing rust to continue to the corrosion. Figure 2 gives a schematic representation of the formation of rust on a unprotected piece of iron.
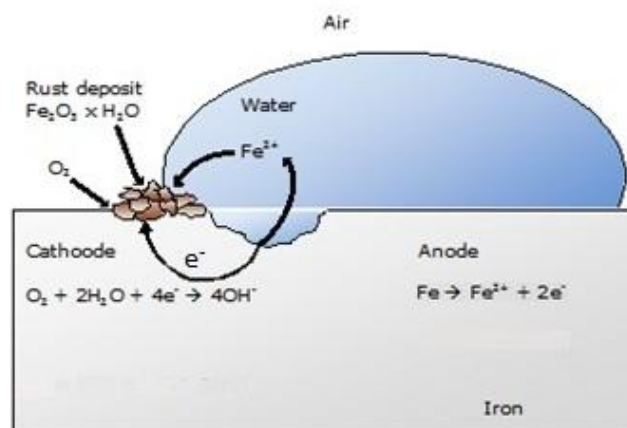
Figure 2. Schematic representation of the formation of rust on iron.

3.2 Organic coating and constituents

Metal structures need to have excellent mechanical properties and machinability at a low price, while retaining good corrosion properties. This combination is nearly impossible to achieve in one and the same material. To overcome this often organic coatings are applied for the protection of metal structures in outdoor environments. Organic coatings form an barrier against ionic migration to the metal and therefore corrosion is retarded. Other reasons to use organic coatings, besides corrosion protection, are providing good aesthetics, lubrication or any other purpose. Organic coatings contain a film-forming organic or inorganic material, after application this may form a hard, impervious film, a soft porous film or a combination [4].

Organic coatings are composed of a dispersion of pigments, fillers, additives and solvents in a binder matrix. These constituents will be introduced in the following paragraphs [5].

Binder
The binder material may be clear (un-pigmented) or a variety of different pigments may be added to provide for example color or increase the corrosion resistance. The binder material acts as a matrix to keep the pigment in place and to connect the coating to the substrate. When the binder (resin plus pigment) is dissolved in a solvent to make it liquid, the combination (solvent, binder, and pigment) is applied to the substrate to form a physical barrier. Binder matrix creates a continuous film on the substrate, by transforming from a liquid phase when applied into a solid state as end product. Three different types of curing can be categorized:

- *Physical drying*, the evaporation of the solvents after application from the liquid.
- *Chemical network formation*, in general two component, resin and harder, coatings that polymerize by a chemical reaction after mixing.
- *Coalescence*, these coatings are often water based, the binder is not non-soluble and is dispersed in small particles. When the solvent evaporates the polymer particles blend together and form a protective film.

A combination of above named curing principles is also possible in organic coatings [6]. For application on military aircrafts the two important binders are epoxy, and polyurethane. Table 2 shows a general guide to the performance of two exponent epoxy and polyurethane systems [7].

Table 2. General guide to the performance of two component epoxy and polyurethane systems.

Properties	Epoxy	Polyurethane
Adhesion	Excellent	Good
Water Resistance	Excellent	Good
Cure Speed	Good	Excellent
Susceptibility to moisture during curing	Little to considerable	Considerable
Gloss Retention	Poor	Very good
Abrasion Resistance	Good	Excellent

Pigments and fillers

Pigments are primarily added to give the coating color and to make the coated substrate more attractive. Another very important property of pigments is added corrosion resistance, also mechanical properties can be influenced with the addition of certain pigments. Three different types of pigments are:

- *Organic pigments*, are mainly used to give the coating color, by selective absorption of some frequencies of light.
- *Inorganic pigments*, primarily function is to increase the coating corrosive resistivity properties, they are also used to give color.
- *Metallic pigments*, are also added for better corrosion resistance. Metal pigments can act as cathodic protection, when in electrical contact with the steel substrate.

Coatings may contain a combination of these pigments to achieve the best properties possible [8]. Fillers represent a large group of different additives that can all have different functions in the coating. They are used to increase the volume of the coating, abrasion and impact resistance and water permeability may be changed with addition of the right filler.

Additives

Pigments and binder are the most important components of a coating, but sometimes hard to incorporate due to incompatibility with the binder; therefore additives are used. Additives are primarily related to the manufacturing, application and curing processes of the coating. Additives are also used to achieve special properties: anti-foamers, fire retarding agents, anti coalescence agents, UV-absorbers [6].

Solvents

Solvents are added to the coating to reduce viscosity, for a good dispersion of the pigments and to make a thin smooth continuous film possible when applied on the substrate. Solvents are also added to vary the drying and curing characteristics of the coating [9].

3.2.1 Organic coating functions and protection mechanisms

In this survey only the properties that are relevant for the corrosion protection properties of an organic coating are presented. Other functions like color, wear resistance, formability, noise reduction and electronic insulation are not discussed. Literature shows that for organic coatings that are typically used in corrosion protection the diffusion rate of H_2O and O_2 far exceeds the diffusion limited value for oxygen reduction [10], which implies that adhesion of the coating plays a very important role in the corrosion protection properties of a coating. Some important coating protection mechanisms are described below:

- *Barrier protection*; to form a relatively impermeable barrier to moisture and electrolytes to prevent corrosion. Barrier for ions leading to an extended diffusive double layer, blocking of ionic paths between local anodes and cathodes along the metal/polymer interface. An ideal coating should be as impermeable and continuous as possible. Sometimes this is achieved by for example adding flakes of aluminium, like in metallic coatings on cars.

- *Adhesion*; the maintenance of adhesion to the substrate under chemical and electrochemical conditions imposed by the environment stops corrosion development over the surface and thereby limits the impact of local failure of the coating.
- *Cathodic protection*; by adding a high volume fraction of metallic (zinc or aluminum) particles to the coating the underlying steel can be protected by cathodic protection.
- *Corrosion inhibitors*; pigments and inhibitors are added to primers to inhibit corrosion at the coating/metal interface or get released in case of a coating damage. These additives can also change the dielectric properties of a coating.

3.2.2   Organic coating failure modes

Modern organic coatings are of a very high quality and for most applications a special coating is developed. No matter how good these coatings are they will always suffer from degradation and failure. The most important factor in extending the lifespan of a coating is in the hands of the applicator. The applicator should make the right coating selection, follow manufacturer instructions for mixing, conduct the proper surface preparation, take into account drying, curing and over coating times and proper application under the right environment conditions. Other factors affecting the lifespan of a coating are temperature extremes, chemical and light exposure and mechanical forces [11]. These effects result in the degradation of the coating; the binder, pigments or the adherence between them or between binder and substrate. The degradation of the coating results in visually detectable deflection of the coating. These deflections are described as failure modes for visual examinations in ISO standards, for example:

- *Blistering*; loss of adhesion between coating layers or between coating and substrate may be caused by:
  a. Poor surface preparation. Poor adhesion of the coating to the substrate or poor undercoat adhesion.
  b. Inadequate release of solvent during both application and drying of the coating system.
  c. Moisture vapor that passes through the film and condenses at a point of low paint adhesion.
  d. A coating within the paint system that is not resistant to the environment.
  e. Application of a relatively fast drying coating over a relatively porous surface.
  f. Failure due to chemical or solvent attack.
  g. Over-protection by cathodic protection
- *Chalking*; typically caused by attack of UV radiation in sunshine. As a result the coating deteriorate by powdering.
- *Erosion*; large similarity with chalking in appearance, it occurs due surface weathering by agents like air, water etc.
- *Cracking*; due to continued polymerization/oxidation stresses can occur in the coating.

3.2.3   Organic coating application methods

There are a lot of different methods to apply a coating to its substrate. In this section some common application technologies are shortly introduced.

- *Brush*, the most common used way of applying a coating is by brush. The results depend largely brushing techniques, also the quality of the brush used plays an important role. This

way of application is the most expensive way due to the high labor costs. A big advantage of brush application is it ensures complete wetting of the surface and surface irregularities.

- *Air spraying*, specially designed guns atomize paint into a fine spray, typically the paint is fed into the spray gun using compressed air. Air gun spraying equipment can be either automated or hand-held and has relatively low cost per square meter applied coating.
- *Electro coating*, is a dipping method whereby coatings are electrophoretic deposited onto parts from an aqueous medium. The particles migrate under influence of an electric field. The substrate needs to act as cathode or anode and therefore needs to be electrically conductive. Some advantages of electro coating are reduction of air pollution from solvents and the good covering properties. Disadvantages are the difficult to operate and high investment costs.
- *Powder coating*, is applied as a free-flowing dry powder and is applied electrostatic or by fluidized bed. The powder is then cured by heating to their melt temperatures to create a hard finish that is tougher than conventional paint.
- *Roll and coil coating*, is highly automated way to coat sheets and coiled metals before fabrication. In this method, coatings are rolled onto surfaces by resilient rollers. The roller motion can be the same as the substrate (direct roller) or contrary the substrate (reverse roller). Metals can be coated with polyesters, epoxies, vinyls, plastisols, acrylics, water-born emulsions, fluorocarbons, dry lubricants, treatment and primer combinations.

3.2.4   Typical organic coating systems used in industry

Coating systems:
- Aircraft
  a. *Conversion coating;* are coatings for metals where the part surface is converted into the coating with a chemical or electro-chemical process.
  b. *Primer*; often the first coating which has extra binding molecules to increase adhesion. Since a higher amount of binding molecules makes a coating more liable for water penetration, a topcoat with water barrier properties is applied over the primer.
  c. *Topcoat*; a transparent or translucent coat of paint applied over the underlying material as a sealer.
- Infrastructure (bridges, sluices, etc.) ships
  d. *Primer*; the adhesion layer with an increased binding molecule portion, often epoxy based to limit water penetration.
  e. *Mid coat*; the water barrier sometimes applied in more than one layer to achieve high dry film thickness, often epoxy or vinyl ester based.
  f. *Topcoat;* often a polyurethane with good UV-resistant properties.

3.3   Organic coating degradations methods

3.3.1   General

There are two ways to degrade coatings reproducibly for scientific research, the first is outdoor exposure and the second is artificially accelerated degradation tests. Degradation tests are often used to test the quality of organic coatings for certain applications. When results of such test are interpreted it is important to consider that when these coatings are used in their normal

environment the property changes and failure modes are reproduced by the accelerated test conditions. In case outdoor exposure is used as degradation method, translation to practice becomes much easier. The acceleration of degradation mechanisms in these tests is done by exaggerating the natural situation. Therefore modern accelerated degradation methods are not capable to fully simulate coating degradation of organic coatings in natural environments. This makes translation of the acquired test results to the relative lifespan of organic coatings in situ very difficult and can be influenced by difference in UV radiation, probation time, relative humidity, temperature, pollutants, and other factors [12, 13].

3.3.2   Outdoor exposure

Outdoor exposure is the most reliable way of studying a coating for a specific application [14]. Because modern coatings are of a very high quality, outdoor exposure is a very time consuming test method. These time frames can frequently run up to 10 or even 20 years which makes these test commercially only acceptable for verification, not for coating development. The test setup generally consist of a rack were the coated panels are mounted on as shown in Figure 3.
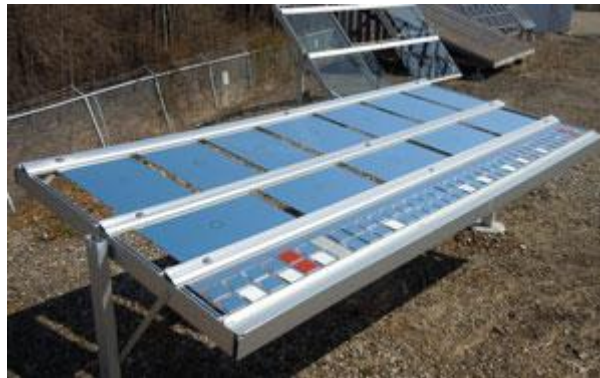

Figure 3. Test setup for outdoor exposure testing.

3.3.3   Salt spray test

The salt spray test is the most common of all accelerated degradation test methods and is widely used for coating research [15]. Salt spray tests was first used around 1914 for corrosion testing on coated panels. The test was incorporated in ASTM B117 in 1939 [16]. Salt spray cabinets (Figure 4) traditionally spray salt fog of 5% NaCl at 35˚C on the test specimen. This exposure enhances existing small failures in the coating and on the coating/substrate surface. These conditions are of such extreme level, that the general idea was that a coating which performed well in the test would perform well in extreme outside conditions. In literature several examples can be found that indicate that the correlation between test and service are very little [17, 18, 19].

Figure 4. Ascott salt spray cabinet.

The biggest reason of this failure in correlation is general thought the constant stress imposed during salt spray testing, whereas in normal use periods of drying out occur. This lead to the demand for more accurate test methods and the development of cyclic testing which will be discussed in the next section.

3.3.4 Cyclic testing

In accelerated degradation methods such as the salt spray test the failure of the coatings tested are often in correlation with the constant stress imposed during such a test. In normal outdoor environment this stress is often interspersed with period of drying. This lead to the demand for more accurate test methods and the development of cyclic testing. Cyclic corrosion test are based on the fact that actual outdoor exposures usually include both wet and dry conditions. By this a more realistic way of performing a salt spray test can be achieved. Several research articles [15, 20, 21] show that better correlation between the test and outdoor is achieved. Relative corrosion rates, structure and morphology seem all more similar. Cyclic corrosion test can be used for evaluating several corrosion mechanisms, including general, galvanic and crevice corrosion. Modern salt spray cabinets may simulate several different environments like:

- *Ambient environment*, is a laboratory ambient condition, which is normally used as a way to very slowly change the test sample condition. Typical in ambient conditions there is little movement of air and is free of corrosive vapors and fumes. Temperature is around 25˚C and relative humidity is 50% or less.
- *Humid environment*, cyclic corrosion test procedures often call for high humidity environments. Relative humidity's are around 95% to 100%. These may be achieved either by using ASTM D2247 [22] or as an alternative ASTM B117 chamber may be used to apply a pure water fog.
- *Dry-Off environment*, this environment can be achieved in an open laboratory or inside a chamber. Enough air circulation must be present to allow drying of the sample. When corrosion product start to build up the drying time may increase. This environment can only be used after a wetting environment.

- *Corrosion immersion environment*, this environment would normally consist of an aqueous solution with an electrolyte at a specified concentration, typically up to 5%. The pH can be chosen between pH 4 and pH 8 and temperature is usually specified. The solution will become contaminated with use, so it should be changed on a regular basis.
- *Water immersion environment*, this environment uses distilled or de-ionized water. ASTM D1193 [23] can be consulted which gives a useful guidance on water purity. Typical pH is in the range of 6 to 8 and temperature should be 24˚C ±3°C.

Ultraviolet radiation (UV)/condensation cabinets is another very important cyclic environment. Cyclic testing with the combination of salt fog and UV radiation proved to give better correlation between test and outdoor service [24, 25, 26]. These papers show that cyclic testing with the combination salt fog/UV radiation is more effective in reproducing failure modes that are observed in outdoor situations then continuous salt fog or cyclic salt fog. In 1996 the ASTM D5894 [27] norm was published which describes a standardized cyclic UV/condensation and UV/salt fog procedure.
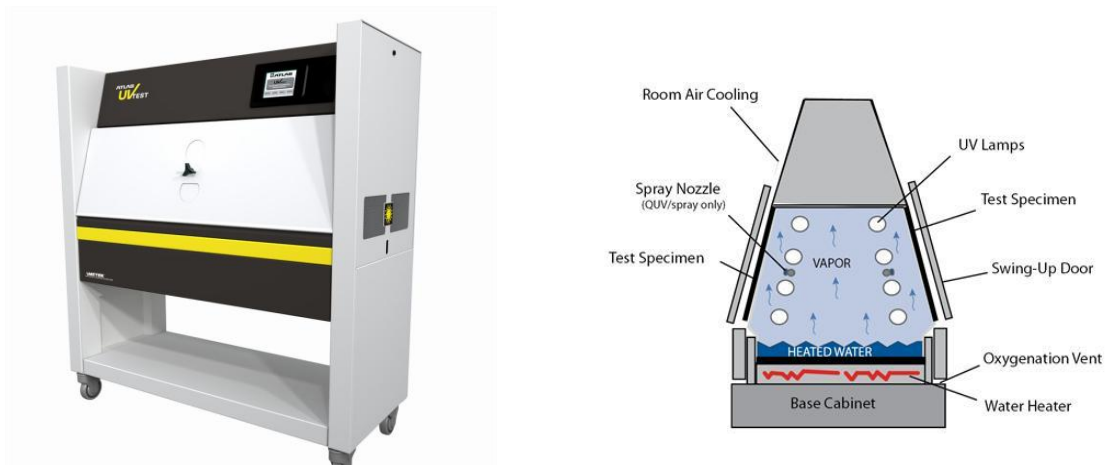

Figure 5. UV condensation cabinet.

3.3.5   Acceleration factor

The acceleration factor is used in accelerated degradation test to get a feel of how much degradation takes place in the test. The acceleration factor for a specific degradation test can be calculated with equation 3.5 [9].

$$A = \frac{x_{test}}{x_{field}} * \frac{t_{field}}{t_{test}}$$

3.5

here:

A   acceleration factor

x_{test} response from accelerated test

x_{field} response from field exposure

t_{field} duration of field exposure [h]

t_{test} duration of accelerated test [h]

There are several factors that play an important role in the calculation of acceleration factors and the use of it.

- Acceleration factors are material dependent and can be significantly different for each material and for different formulations of the same material [27].

- Variability in the rate of degradation in both actual use and laboratory accelerated exposure test can have a significant effect on the calculated acceleration factor [27].
- Acceleration factors calculated based on the ratio of irradiance between a laboratory light source and solar radiation, even when identical band passes are used, do not take into consideration the effects on a material of irradiance, temperature, moisture, and differences in spectral power distribution between the laboratory light source and solar radiation [27].

When using acceleration factors it is important to first verify literature for known factors, before calculating.

3.4   Electrochemical impedance spectroscopy (EIS)

3.4.1   History

Electrochemical impedance spectroscopy measurements are well known over a hundred years and is now a well established powerful tool used for [28, 29]:

- Investigating the mechanisms of electrochemical reactions;
- Measuring the dielectric and transport properties of materials;
- Exploring the properties of porous electrodes;
- Investigating passive surfaces.

The rapid development of microcomputers and electronic devices accounted for a broader application of the technique.

Heaviside invented the concept of electrochemical impedance spectroscopy between 1880 and 1887 [30]. He derived a method of solving differential equations by transforming them into ordinary algebraic equations. These equations described the flow of current through a circuit with resistors, capacitors and inductors. In the same period he came up with the expressions of 'impedance', 'admittance' and 'reactance'. Heaviside controversial way of solving the differential was not proven until the next century [9]. Warburg was the first to extend the concept of impedance to electrochemical systems at the end of the 19th century, he derived the impedance function for a diffusion process that still bears his name [31].

The development of the potentiostat in the 1940s and the development of frequency response analyzers in the 1970s led to the beginning of exploring electrochemical and corrosion mechanisms, mainly due to the ability to probe electrochemical systems at very low frequencies. An explosion in the use of EIS in all kinds of fields was caused by these inventions [9].

3.4.2   Measurement principle

Electrochemical impedance spectroscopy is a technique is based on the application of an alternating current (AC) potential of a small amplitude (typically 10 mV), as a consequence an AC current is obtained. From the relation of both signals the impedance (Z) is obtained. The measurements are carried out at different AC frequencies and thus the name of impedance spectroscopy. The typical frequency range of an impedance scan is from 0.5 Hz to 100 kHz. To understand the concept of impedance it is good to first take a look at a direct current (DC) system. In a DC system a well known concept is electric resistance which can be defined as the ability to resist electrical current flow by a

circuit element. This resistance (R) is defined by Ohm's law as the ratio between voltage (E) and current (I) shown in equation 3.6. An ideal resistance has several simplifying properties:

- At all current and voltage levels it follows Ohm's law
- The value of resistance is independent of frequency
- AC current and voltage keep in phase with each other.

$$R = \frac{E}{I}$$ 3.6

To describe the more complex behavior other circuit parameters are necessary. Therefore the parameter impedance (Z) is introduced to extend the concept of resistance. The term impedance is derived from the Latin word 'impedire', which means in English 'to hinder' [14]. Impedance can be defined as the ability to resist flow in an alternating electric current.

Electrochemical impedance is measured by applying an alternating voltage to the system and measure the current response [32]. The response of the system is a current that differs in amplitude and phase (phase difference, Φ) with the applied voltage [33]. The impedance is a kind of generalized resistance, which behaves like a combination of a resistor and a capacitor in series. In the section below the concept of impedance is further explained using a resistance and capacitance in a linear system.

When an excitation signal expressed as a function of time of the form 3.7 is applied to a pure resistance R. Ohm's law always holds as shown in 3.8.

$$E_t = E_0 \sin(\omega t)$$ 3.7

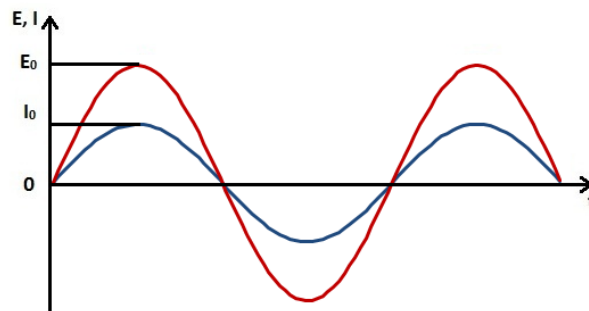$$R = \frac{E}{I} = \frac{E_0 \sin(\omega t)}{I_0 \sin(\omega t)}$$ 3.8

Figure 6. Current response of an AC voltage signal applied to pure resistance.

When this excitation signal is applied to a capacitance the response of the current is shifted with phase Θ (Figure 7).
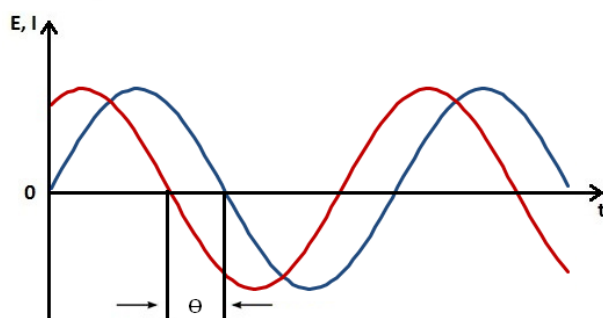
$$I_t = I_0 \sin(\omega t + \theta)$$ 3.9

Figure 7. Current response of an AC voltage signal applied to pure capacitance.

When this excitation signal is applied to a resistance and capacitance placed in series, which resembles electrochemical impedance, the response is shown in Figure 8. An expression analogous to Ohm's Law allows us to calculate the impedance of the system as described in 3.10.

$$Z = \frac{E_t}{I_t} = \frac{E_0 \sin(\omega t)}{I_0 \sin(\omega t + \theta)} = Z_0 \frac{\sin(\omega t)}{\sin(\omega t + \theta)} \qquad \textbf{3.10}$$

The impedance is therefore expressed in terms of a magnitude Z_0 and a phase shift Ө.
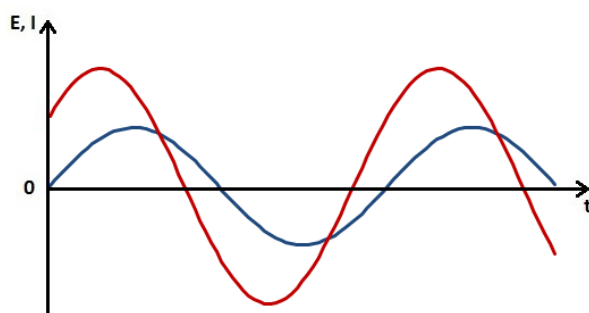
Figure 8. Current response of an AC voltage signal applied to a resistance and capacitor in series.

The systems above the current response is purely linear. In practice electrochemical systems rarely show pure linearity. In electrochemical systems phenomena like passivation and polarization are observed which leads to non-linear behavior. Electrochemical Impedance is normally measured using a small excitation signal. This is done so that the cell's response is pseudo-linear. In a linear (or pseudo-linear) system, the current response to a sinusoidal potential will be a sinusoid at the same frequency but shifted in phase. The response of the applied sinusoidal on such a system can be presented in a graph called a 'Lissajous figure' (Figure 9) [14, 34].
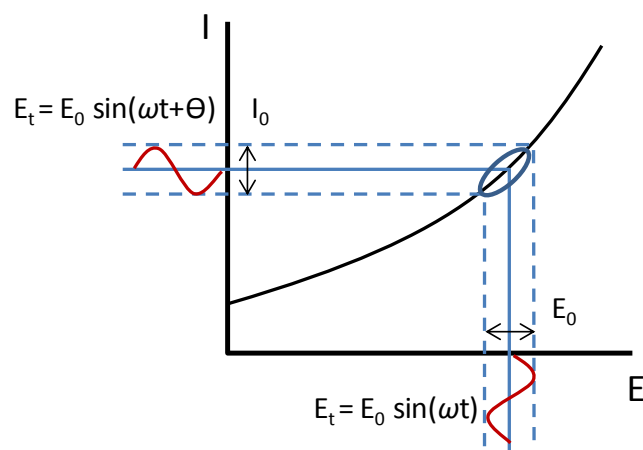
Figure 9. Origin of Lissajous figure.

Using Euler's relationship,

$$\exp(j\theta) = cos\theta + jsin\theta \qquad \text{3.11}$$

the potential and the current response can be described as a complex function.

$$E_t = E_0\exp{(j\omega t)} \qquad \text{3.12}$$

$$I_t = I_0\exp{(j\omega t - \theta)} \qquad \text{3.13}$$

The impedance is then represented as a complex number, with $j^2 = -1$.

$$Z(\omega) = \frac{E}{I} = \frac{E_0\exp{(j\omega t)}}{I_0\exp{(j\omega t - \theta)}} = Z_0\exp(j\theta) = Z_0(cos\theta + jsin\theta) = Z' + jZ'' \qquad \text{3.14}$$

In equation 3.14 the expression for Z(ω) is composed of a real and an imaginary part. For representing the data a Nyquist plot can be used. On a Nyquist plot the impedance can be represented as a vector of length |Z| with the argument angle ϴ (Figure 10). Notice that in this plot the y-axis is negative and that each point on the Nyquist plot is the impedance at one frequency, this means that you cannot tell what frequency was used to record that point, one major shortcoming of the Nyquist plot. Low frequency data are on the right side of the plot and higher frequencies are displayed on the left. This is true for electrochemical impedance spectroscopy data where impedance usually falls as frequency rises (this is not true of all circuits).

The Nyquist plot in Figure 10 results from the electrical circuit shown in Figure 11. The semicircle is characteristic of a single "time constant". Electrochemical Impedance plots can contain several time constants, each representing certain physical behavior.
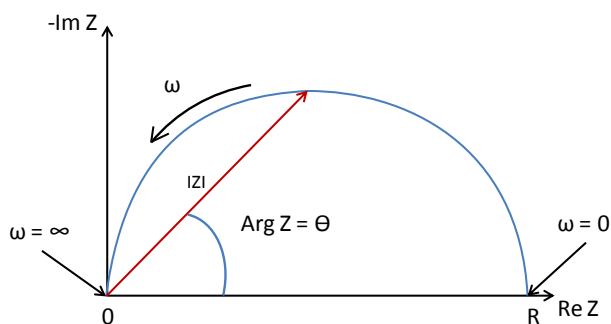
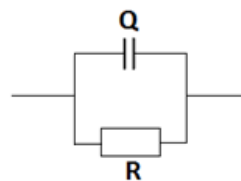**Figure 10 Nyquist plot with impedance vector**

Figure 11. Simple equivalent circuit with one time constant

To character impedance the 'Bode plot' is another method that is often used. In this representation the magnitude of the impedance, |Z| and phase Ө as function of the frequency is plotted. Because the frequency can range from 100,000 Hz to 0.001 Hz or less, the frequency axis is plotted logarithmically. Since |Z| can also change by a factor of a million or more in a simple experiment, the |Z|-axis is also plotted on a logarithmic axis. In the bode plot the impedance data, which are frequency independent, represent the behavior of the resistive processes (phase angles close to 0°) whereas the ones that are dependent on the frequency are more related to capacitive or diffusive processes (phase angles between -90° or -45°). The plot is very useful to get information of the number of significant processes that has to be used in the equivalent circuit. The Bode plot for the electric circuit of Figure 11 is shown in Figure 12. Unlike the Nyquist plot, the Bode plot explicitly shows frequency information.
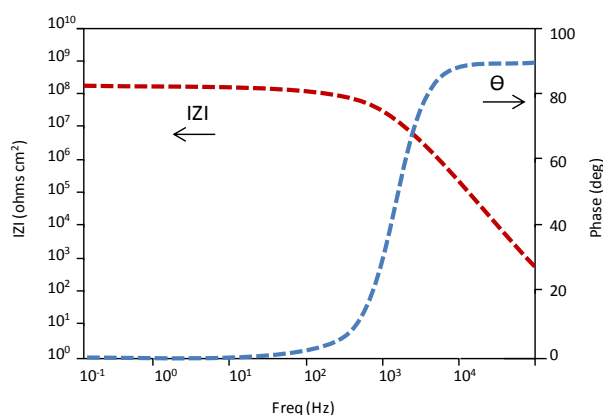

Figure 12. Bode plot

3.4.3   Data analysis

For the analysis and interpretation of EIS data there are different approaches can be used to translate a EIS spectrum to a coating condition.

Fundamental approach

In the fundamental approach it is important to have the reaction mechanism. A charge transfer function may be calculated which couples, in a mathematical representation, a relation between the input and output of a system. This charge transfer function can for example contain the kinetics of the reactions and the diffusion equations and is directly obtained from the impedance data and

fitted. To get an accurate charge transfer function the reaction mechanism should be almost fully understood, this is a major disadvantage of this interpretation approach.

Phenomenological approach
To find the correct electric circuit the collected EIS spectrum can be modeled, the MPEC (most probable equivalent circuit) have to be constructed. A problem with this method is that different electric circuit models can produce the same fit and therefore can result in a wrong interpretation of the coating condition. To make sure the electric circuit is as accurate as possible it is important to construct these models with great care and according to a certain set of guidelines. Tom Bos [9] described a comprehensive set of guidelines to perform this data analysis:

- Normally one starts with a qualitative circuit based on other research results.
- Based on graphic analysis of the Nyquist and Bode plot a basic model can be obtained, this is only possible with simple circuit models. The values and combinations of the different components can be determined from these plots.
- The hierarchical structure of the different components in the circuit should be brought in accordance with a theoretically meaningful model [14, 28, 35] in this research only circuits are used that are described by the process changes in the unified coating degradation model of Nguyen and Hubbard [36].
- If after a reasonable fit is achieved the remaining error should not follow a recognizable pattern but must be randomly distributed, otherwise a different electric circuit must be chosen or extended with a additional time constant.
- Although better fit results can be achieved by adding components, the physical meaning of these extra components is often unresolved. A fit with the least amount of electric components is what must be aimed for [6, 30, 37, 1].
- After a reasonable fit has been obtained the impedance at the frequencies 0 and ∞ Hz can be checked. Normal systems cannot contain singularities and should have finite impedance for all frequencies [30, 38, 37].
- The final fit should contain values for components that are reasonable according to literature [37] and show systematic change with time [6, 1]

Coating capacitance (C_t)
A method that recently gained in popularity to characterize water uptake of a coating system, is to calculate the coating capacitance at fixed high frequency, usually $1 \cdot 10^4$ Hz. Since at high frequency the constant phase element is proportional to the impedance modulus |Z| the coating capacitance can be directly calculated and complex modeling is unnecessary. The coating capacitance is related to the magnitude of the impedance |Z| by 3.15. The coating capacitance values are plotted versus the exposure time with the electrolyte.

$$|Z| = \frac{1}{(2\pi f C_c)}$$
3.15

Where:
f   Frequency of applied AC voltage

Electrolyte consist of primarily water which has a dielectric constant in the range of 80.2 − 82.2 at typical ambient temperatures (i.e., 293-298 K). The dielectric constant of a polymeric coating is on the other hand much lower in the same temperature range between 3 and 8 [39]. This means that the coating capacitance increases as the electrolyte penetrates the coating according to equation 3.16.

$$C_c = \varepsilon_0 \varepsilon_r \frac{A}{d}$$

3.16

Where:

C_c coating capacitance [F]

ε_0 permittivity of vacuum $8,85*10^{-12}$ F/m

ε_r dielectric constant

A coating surface [m^2]

d coating thickness [m]

The penetrated electrolyte causes swelling of the coating, which would have the opposite effect and lead to a lowering of the capacitance. In comparison with the high dielectric constant this effect can usually be neglected. The uptake of water is therefore strongly related to the coating capacitance, to qualify this uptake of water Brasher and Kingsbury [36] derived equation 3.17.

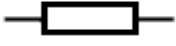$$\emptyset = \frac{K \, log\left(C_t/C_0\right)}{log(\varepsilon_w)}$$

3.17
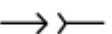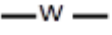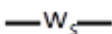
Where:

C_0 coating capacitance of dry coating [F]

ε_w dielectric constant of water

Φ volume fraction water

3.4.4 Common equivalent circuit models

Equivalent circuit modeling of electrochemical impedance spectroscopy data is used to extract physically meaningful properties of the electrochemical system by modeling the impedance data in terms of an electrical circuit composed of ideal resistors (R), capacitors (C), and inductors (L). Table 3 lists the common used circuit elements with their impedance expressions.

Table 3. Components that are used in equivalent circuit modeling.

Component	Symbol	Impedance
Resistor	R	$Z = R$
Capacitor	C	$Z = \dfrac{1}{\omega C}$
Inductor	L	$Z = j\omega L$
Constant Phase Element	C	$Z = \dfrac{1}{(j\omega)^n Y_0}$
Warburg (semi-infinite diffusion)	W	$Z = \dfrac{1}{\sqrt{(j\omega)} Y_0}$
Warburg (finite diffusion length)	W_s	$Z = R_d \left[\dfrac{\tanh(j\omega B)^n}{(j\omega B)^n}\right]$ with $B = \dfrac{\delta_N}{\sqrt{D}}$

Solution resistance (R_e)
Solution resistance is often a significant factor in the impedance of an electrochemical cell. A modern three electrode potentiostat compensates for the solution resistance between the counter and reference electrodes. An electrolyte is usually very conductive (1-50 ohms) and can be ignored.

Coating resistance (R_c)
Coating resistance is the resistance that charge carriers encounter in a organic coating. It corresponds to electron transfer reaction such as corrosion reactions. R_c is also often used as a measure for effectiveness of corrosion protection.

Coating capacitance (C_c)
Most coatings are relatively thick and therefore the coating capacitance is in the beginning rather low, around 1 nF/cm^2. For the identification of coating failure the parameter The coating capacitance is a very useful parameter to measure during coating failure.

Constant Phase Element (Q)
Real corrosion and polymer degradation systems do not necessarily behave ideally with processes that occur distributed in time and space. Therefore, specialized circuit elements are used. The most important one for this study is the generalized constant phase element (CPE) that models the behavior of a double layer, that is an imperfect capacitor. CPE is defined as described in equation 3.18

$$Z = \frac{1}{(j\omega)^n Y_0}$$

3.18

The Constant Phase element is used to represent a wide variety of elements. With n=-1 it represents an inductance (L), with n=0 a resistor (then Y_0 becomes 1/R), Warburg (W) impedance with n=$^1/_2$ and

a capacitor (C) if n=1 (then Y_0 becomes C). So, the n value and the Y_0 of the CPE are very important tools in relating measurement response to mechanisms. Different physical phenomena's are coupled with the constant phase element:

- Surface roughness
- Distribution of reaction rates
- Varying thickness or composition
- Non-uniform current distribution

Warburg

Diffusion can create an impedance known as the Warburg impedance. This impedance depends on the frequency of the potential perturbation. At high frequencies the Warburg impedance is small since diffusing reactants don't have to move very far. At low frequencies the reactants have to diffuse farther, thereby increasing the Warburg impedance. The Warburg element is used to model ideal semi-infinite diffusion. This occurs when the diffusion layer has infinite thickness. The equation for the Warburg impedance becomes:

$$Z = \frac{1}{\sqrt{(j\omega)Y_0}}$$

3.19

On a Nyquist plot the infinite Warburg impedance appears as a diagonal line with a slope of 0,5. On a Bode plot, the Warburg impedance exhibits a phase shift Φ of 45°.

This form of the Warburg impedance is only valid if the diffusion layer has an infinite thickness. Quite often this is not the case If the diffusion layer is bounded, the impedance at lower frequencies no longer obeys the equation above. Instead, we get the form:

$$Z = R_d \left[\frac{\tanh(j\omega B)^n}{(j\omega B)^n} \right] \; with \; B = \frac{\delta_N}{\sqrt{D}}$$

3.20

with,

δ_N Nernst diffusion layer thickness

D   Average value of the diffusion coefficients of the diffusing species

This more general equation is called the "finite" Warburg. For high frequencies where ω approaches infinity, or for an infinite thickness of the diffusion layer, the above equation simplifies to the infinite Warburg impedance.

To translate the modeled results of a electrochemical impedance spectroscopy measurement to a degradation state, the unified model for coating degradation is introduced by Nguyen and Hubbard [36]. The Nguyen and Hubbard model describes a four step degradation process of an defect-free organic coating on a steel substrate exposed to a neutral electrolyte solution. Nguyen and Hubbard combined two general ideas from literature to form this unified model. The first idea is that degradation of a coating starts with the sorption of water [36, 40] in a coating. The other is the formation of conductive paths by the interconnection of hydrophilic regions. Which makes it possible for ions to reach the metal surface [41, 42, 43]. If these two phenomena could somehow linked it would provide a unified view of the initial step in the degradation of an defect free organic coating.

The difference of these two views are not that different from each other if conductive pathways are the consequence of water uptake in the coatings. In numerous studies [43, 44, 45, 46, 47] was found that coatings naturally contain regions that are able to take up a large amounts of water and have a low resistance against ions. This may be the best evidence that supports the theory of Nguyen and Hubbard that the linkage of these two phenomena is justified. Is that in numerous studies. In two of these studies [44, 47] corrosion spots where found on the substrate which could be directly related to these regions.

Figure 13 gives a schematic overview of the four step degradation model described by Nguyen and Hubbard with the corresponding electric circuit model for each degradation step. Step 1 describes the attack of a coated metal by water in the hydrophilic regions. When these hydrophilic regions grow and form interconnections the formation of conductive paths in the coating will occur (Step 2). These conductive paths make it possible for ions to reach the substrate surface corrosion of the substrate (Step 3). Corrosion products building up under the coating leads to delaminating of the coating (Step 4). To keep the figure clear the hydrophilic regions are left out in step 2, 3 and 4.
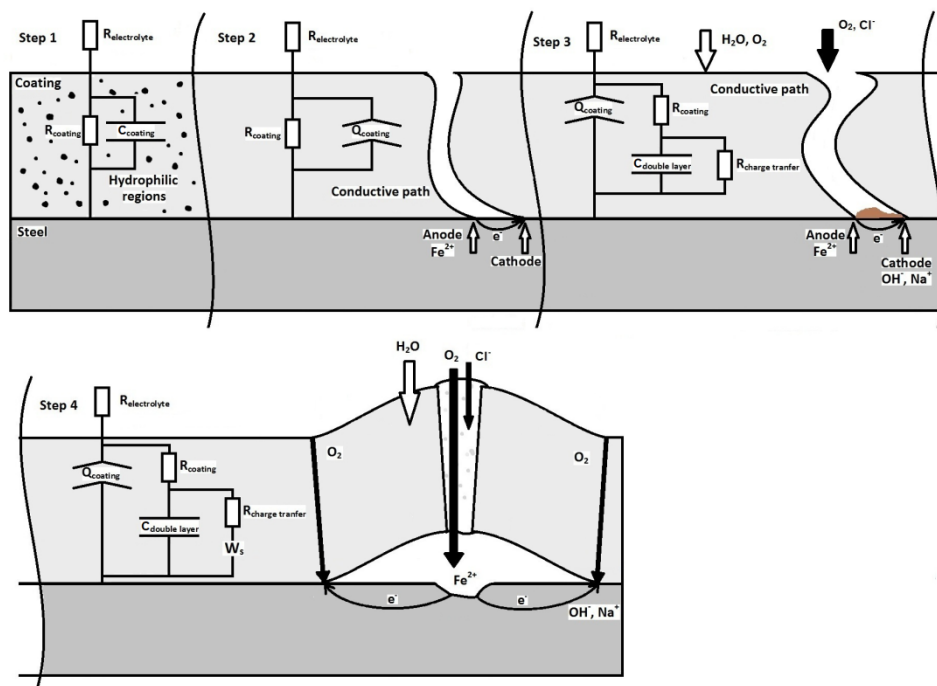

Figure 13. Four step degradation model for an intact organic coating on steel in a neutral NaCl solution and the corresponding electric circuit model.

In 1948 Bacon, Smit and Rugg [41] introduced a coating performance rating system based on the coating resistance. The coating resistance was recorded at a low frequency (0,01 Hz) and a ranking of the barrier properties of the coating was given. Numerous [33, 48, 13, 49, 50, 51] authors presented similar rankings systems based on the coating resistance. Based on these publications a general ranking of the barrier properties of an organic coating can be defined as:

> 10^8 Ω cm^2 good
$10^8 – 10^7$ Ω cm^2 fair (standard)
$10^7 – 10^6$ Ω cm^2 doubtful
< 10^6 Ω cm^2 poor

For special coatings this general qualification might not be valid for example coatings containing conductive materials like conductive polymers and carbon.

3.4.1 Result interpretation electrochemical impedance spectroscopy scheme for in situ applications

When corrosion starts, the coating actually fails; corrosion is then limited mainly by the adhesion of the coating to the substrate, and the aggressiveness of the environment. When the coating degradation is followed in order to determine the time to over-coat, especially Step 1 and Step 2 in the degradation of a coating are the most interesting. In this section the results of a impedance measurement is coupled with a coating degradation state. For this representation the Bode plot and the Nyquist plot are used which are obtained with an electrochemical impedance measurement.
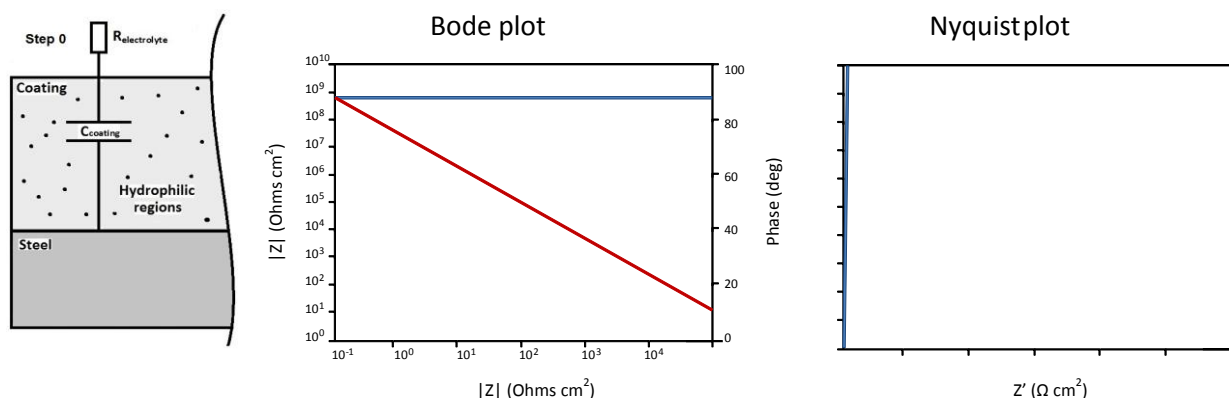

Figure 14. 'Perfect coating' and its representing Bode plot and Nyquist plot

When a coating shows merely capacitive behavior it can be described as 'the perfect coating'. The phase angle (displayed in blue), representing the capacitive behavior, is slightly under 90˚ due to the fact that a perfect coating does not exist. The equivalent circuit for this type of coating behavior can be described by a model consisting a resistor, for the electrolyte resistance, and the coating capacitance in series (Figure 14).
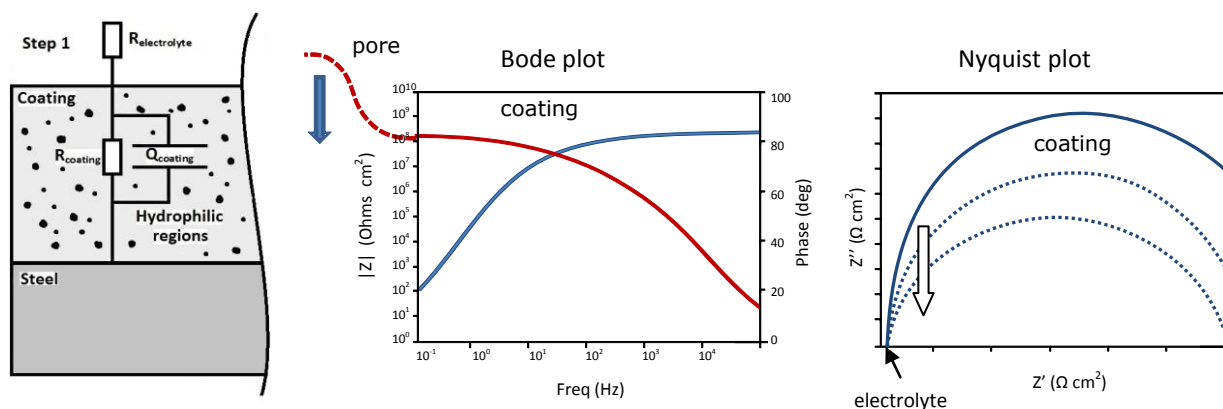
Figure 15. Degradation step 1 and its representing Bode plot and Nyquist plot

The first step in the degradation process of a coating (Figure 15) is the absorption of molecular water by the polymer and recombination of this water in the hydrophilic regions of a coated metal. The increase of water recombination in hydrophilic regions is responsible for the decrease of the coating resistance (R_c) which is recorded in the Bode plot at the lower frequencies. Since this effect first occurs in the top of the coating, the rest of the coating is still a perfect capacitor and therefore no effect is seen in the high frequency spectrum. As the water penetrates deeper into the coating the semi-circle in the Nyquist plot starts to get smaller.

The Nyquist plot shows two time constants one for the electrolyte and one for coating. The time constant of the electrolyte can be represented in the electrical circuit model as a resistor (R_e) and is represented in the high-frequency area on the left side of the Nyquist plot. Since the electrolyte that is used during electrochemical impedance spectroscopy has very little resistance it is barely visible in the Nyquist plot. The second time constant gives an indication of the coating protection behavior and can be represented by a resistance (R_c) and a constant phase element (Q_c) placed parallel to each other. A rough estimation of R_c is related with the diameter of the semicircle. When the hydrophilic regions grow and become interconnected, conductive pathways are formed which enable ion transport by diffusion to the substrate. This process is shown by the arrow in Figure 15 and leads to step 2 of the degradation process. As the quality of the coating drops the semi-circle becomes smaller and less perfect semi-circle shape. The resulting electric circuit will therefore have a smaller value for R_c and the CPE represents a more and more leaking capacitor (n-value is decreasing, Y_0 is changing from C to R).
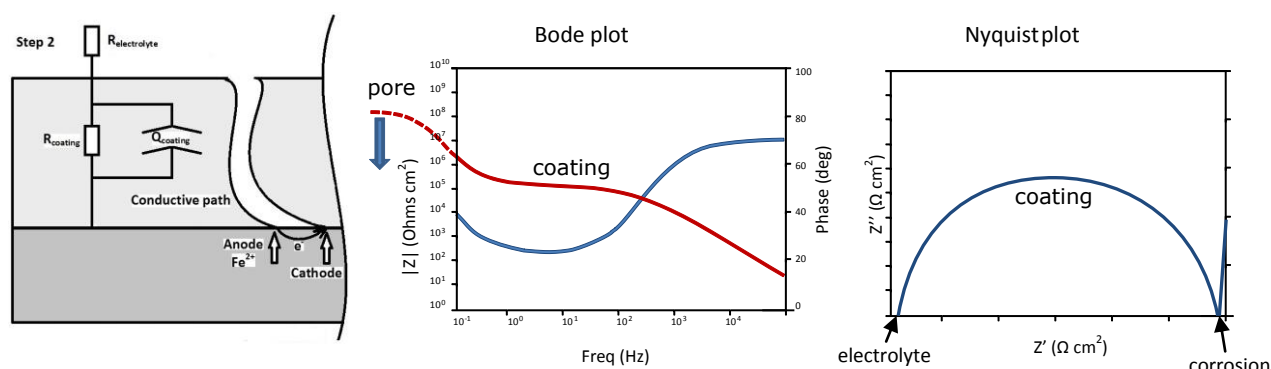
Figure 16. Degradation step 2 and its representing Bode plot and Nyquist plot.

When the diffused ions reach the substrate, corrosion reactions can take place. This introduces a third time-constant as showed in the Nyquist plot at the low-frequencies. Figure 16 shows the start of this third time-constant on the right side of the Nyquist plot indicated by the corrosion arrow. Since this third time constant describes the corrosion processes which are outside the scope of this study it will not be further discussed. For more detail about this subject [6] or [9] can be consulted.

3.4.2 Basic electrochemical impedance spectroscopy setup

In an electrochemical impedance measurement the setup typically consists of a three electrode set-up. The working counter (WE), reference electrode (RE) and a counter electrode (CE). An electrochemical cell is placed on the coated substrate and filled with an suitable electrolyte. The specimen with the protective coating must be electrically conducting and is used as the working electrode. A reference electrode along with a counter electrode is placed inside the cell. Together with the working electrode they are connected to an EIS frequency response analyzer with a computer. A larger electrochemical cell surface will make the setup more sensible for defects and will give a better signal to noise ratio. The sample with the protective coating must be electrically conducting and is used as the working electrode. The WE, CE and Re should be placed in an electrolyte.
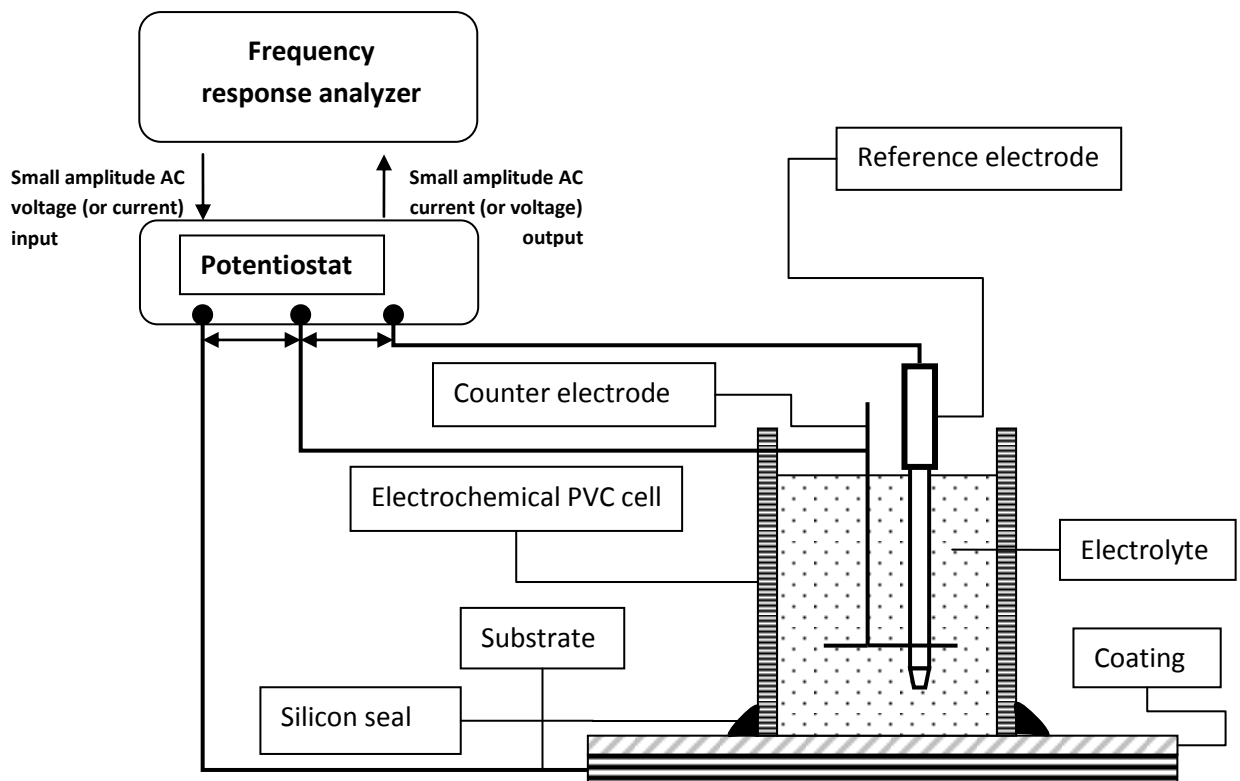

Figure 17. Three electrode set-up for FT-EIS testing of corrosion protective coating on metals and alloys. The working, counter and reference electrodes are respectively denoted as WE, CE and RE.

4 Approach and experimental setup

4.1 Approach

To get the best answers to the two research questions formulated in the introduction, a broad selection of coating systems and accelerated degradation methods are used, to compare the measurement setups and interpretation methods. The focus is on specialized coatings used for military aircrafts, which are degraded in salt spray and UV-condensation cabinets located in the NLR facility in Marknesse and were measured approximately every two weeks. But for completeness of the research a more simple coating system typically used to protect large infrastructure is added. These measurements were performed on the Oosterscheldekering sluices. The results are compared with EIS measurements that C-Cube performed in 2008.

4.2 Test materials

4.2.1 Laboratory coupons

All substrates are made of aluminum 2024-T3 and are all grinded the with Scotch-Brite 7447 [52] (Figure 18) and degreased before application of the coating system. The dimensions of the coupons put in the salt-spray cabinet are 100mm x 100mm that of the coupons in the UV-condensation are 200mm x 100mm. All coatings systems are specially designed for the application on military airplanes and helicopters. Some of these coating systems are not commercially available and exact compositions are confidential.

Figure 18. Scotch-Brite 7447 abrasive hand pad.

On the laboratory coupons used in the salt-spray cabinet the coating system is only applied on one side the other side is protected with a epoxy coating as showed in Figure 19. The coupons that are put in the UV-condensation cabinet only the coating system is applied on one side and no protective coating on the other side. Due to the design of the UV-condensation cabinet only one side is exposed and is it a protective coating on the other side unnecessary.

Figure 19. Epoxy coating for the protection of underside and edges of the coupon.

In **Fout! Verwijzingsbron niet gevonden.** the information of laboratory coupons placed in the salt spray cabinet are described.

Fout! Verwijzingsbron niet gevonden. describes the coating systems that were placed in UV-condensation cabinet. All these coating systems are chromate free and comply with low volatile organic compounds (VOC) requirements (<350g/l in primer and <420g/l in the topcoat), with the exception of coating system 2-1-4-1. Some of these coatings are still in development and/or patented and details of the system and working pigments are not released the known pigments and coating systems are described in **Fout! Verwijzingsbron niet gevonden.**.

4.3   Degradation environments

4.3.1   Degradation cabinets

Salt spray cabinet and UV-condensation cabinet

An Ascott salt spray cabinet is used to perform a cyclic acidified salt spray test according to ASTM G85-A2 [53]. Figure 20 shows the laboratory coupons along with some other coupons used for a different research.

Figure 20. The laboratory coupons placed in the salt-spray cabinet.

An Atlas UV-condensation cabinet is used to perform a cyclic UV-condensation test according to ASTM G154 [54]. Figure 21 shows the coupons placed in the UV-condensation holders.
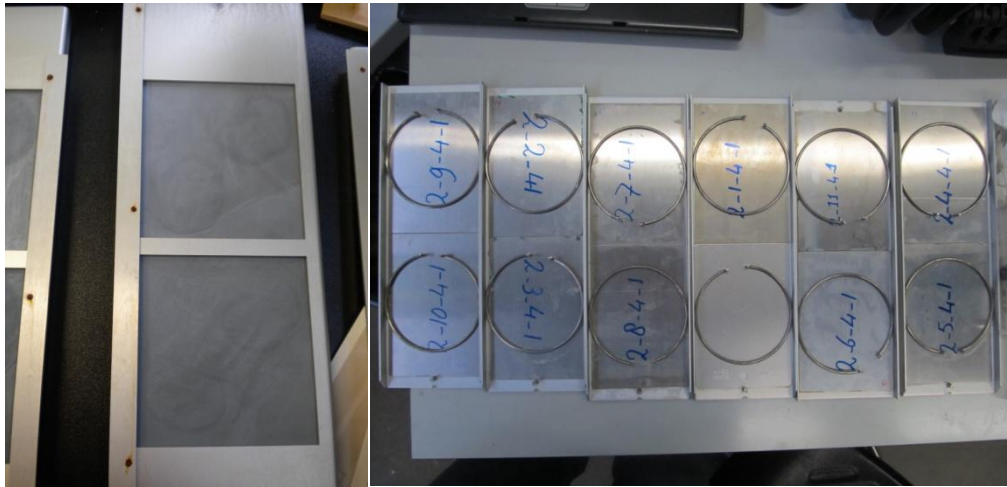

Figure 21. The laboratory coupons placed in the UV-condensation cabinet holders.

To be able to get information about the quality of the coating with a single EIS measurement, it is important that the coating is saturated. All the laboratory coupons were therefore periodically measured after the wetting cycle of the different degradation tests.

4.3.2   Oosterscheldekering

The measurements on the Oosterscheldekering sluices are added to this research, due to the fact that this coating system is naturally aged and EIS measurements performed in 2008 were available. The Oosterscheldekering is divided in three sections (Hammen, Schaar and Roompot). Each section contains around 30 separate sluices. On the left side of Figure 22, an overview of the Roompot section is given and on the right side a close-up of one sluice. One sluice is sandwiched between two pillars as schematically shown in Figure 23.

Figure 22. Left: Overview of a section of the Oosterscheldekering Right: Close-up of a single sluice.

Five years ago C-Cube performed measurements on a selection of sluices on every section. In order to get a good comparison between the old and the new measurements it was important to find the exact locations and types of measurements performed. After analyzing the old results a selection of

suitable measurement locations was made. These locations are characterized with a coordination label, Figure 23 is a schematic representation of the Schaar 9 and shows the measured locations. In Table 4 the locations selected to repeat the new measurements are presented with the coordination label.
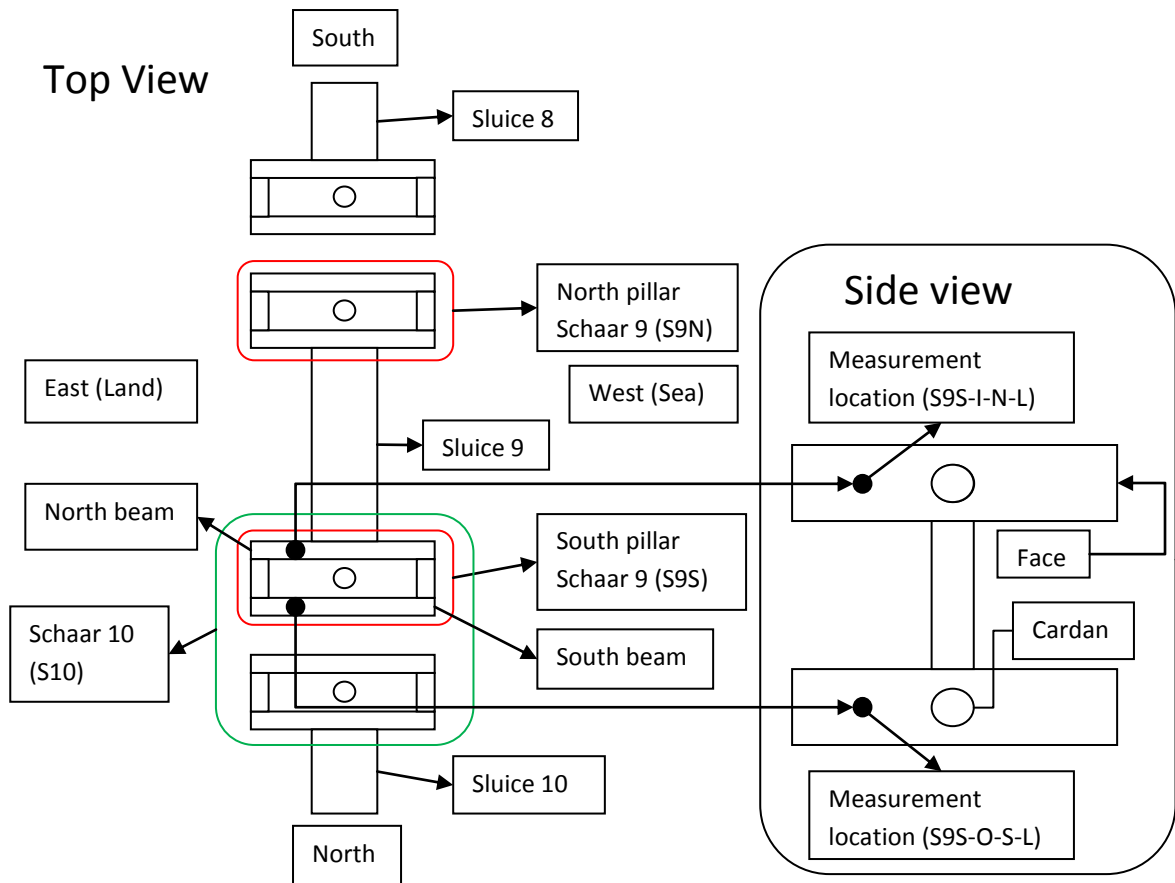

Figure 23. Schematic overview of Schaar 9 and the measure locations.

Table 4. Oosterscheldekering measurement locations.

Section	Location
Schaar 10	• Inside north beam left cardan (S9S-I-N-L) • Outside south beam left cardan (S9S-O-S-L)

4.4 Electrochemical impedance spectroscopy test setup

4.4.1 Electrochemical impedance spectroscopy analyzer

To perform an in situ EIS measurement it is important that the whole setup is portable. Therefore a laptop in combination with an Ivium compactstat is used shown in Figure 24. The Ivium is a mobile

potentiostat/galvanostat with built-in impedance analyzer. It is powered directly from the USB port of a PC/laptop and does not need a power-cord.

Figure 24. Ivium compactstat.

The Ivium compactstat is used in combination with the Iviumsoft software [55] to perform the Electrochemical impedance measurements. A single sine measurement from 10^5 Hz to 0.1 Hz with a resolution of 25 is performed. A relative high perturbation of 1 V is applied to create a high response.

4.4.2 Laboratory setup

A laboratory electrochemical impedance spectroscopy consists of a three-electrode setup which is placed in an electrochemical cell. This cell is placed on the coated substrate and filled with the electrolyte. An Ag/AgCl (gel) reference electrode along with a titanium counter electrode is placed inside the cell. Together with the working electrode, they are connected to an EIS frequency response analyzer and a computer as shown schematically in Figure 17. The used electrochemical cell is made of a PVC tube with a silicon seal of 2 cm diameter on the bottom. To prevent the electrolyte leaking, a piece of brass is put on the PVC tube. Figure 25 shows the used electrochemical cell.
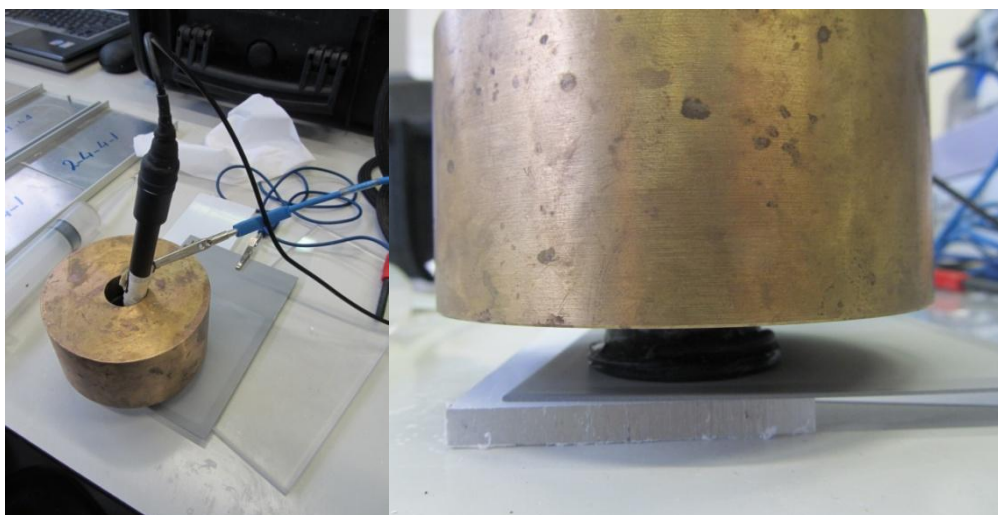

Figure 25. Electrochemical cell used with the laboratory setup.

4.4.3 Handheld sensor test setup

4.4.4 Built-in sensor setup

4.4.5   Application of EIS system on Oosterscheldekering

4.5   Interpretation methods

4.5.1   Interpretation method used with handheld setup

4.5.2   Example of a complete simplified result interpretation

5 Results and discussion

5.1 Introduction

In the upcoming paragraph, the results of the performed measurements are presented and discussed. For clarity, three result graphs batches are distinguished:

1. The result graphs from the coupons degraded by salt spray cabinet.
2. The result graphs from the coupons degraded by UV condensation cabinet.
3. The result graphs of the in situ measurements on the Oosterscheldekering.

The result graphs were used to compare the interpretation methods and the measurement setups for all different coatings. One important point has to be made before discussing the results. The EIS measurements performed on the laboratory coupons degraded in the salt spray cabinet were the first to be measured. This meant that in this batch everything was new and EIS measurements were performed for the first time. After performing numerous measurements the level of skill of performing EIS measurements improved and therefore the accuracy of the measurements increased. The measurement results that came from the UV condensation cabinet are more controlled. In the discussion section this will be described in more detail.

5.2 Data selection

The collected EIS spectra were interpreted with the simplified interpretation method, as described in section 4.5. The resulting Protective Value (PV) and Capacitive Value (CV) were plotted in graphs against time, with the PV on the primary axis and CV on the secondary axis. From these graphs a selection was made based on the degradation steps, as described in section 3.4. Table 5 shows the result of this selection procedure. All coupons are categorized and if a degradation step was present it was labeled green, it was labeled red if this step was not present and orange if it was not completely clear. The result graphs of the laboratory coupons outside this selection can be found in Appendix A. The reason that not all coupons show a reliable degradation profile can be largely attributed to inexperience performing EIS measurements at that stage, as described in the introduction. This selection was used to compare the different measurement setups. The batch of coupons degraded by UV condensation was much smaller and more controlled, since this was the second batch of measurements the increased experience led to more accurate results. All the result graphs are therefore used for the comparison.

Table 5. Laboratory coupons selection table.

Naam	Lab/sensor/hand	Initial state/step 1	Step 2	Step 3	Selection	Naam	Lab/sensor/hand	Initial state/step 1	Step 2	Step 3	Selection
NLR-10-A-A-C-L-1	Laboratory					NLR-10-A-A-C-A-1	Laboratory				
	Sensor						Sensor				
	Hand						Hand				
NLR-10-A-A-C-N-1	Laboratory					NLR-10-A-A-C-F-1	Laboratory				
	Sensor						Sensor				
	Hand						Hand				
NLR-10-A-D-C-L-1	Laboratory					NLR-10-A-D-C-A-1	Laboratory				
	Sensor						Sensor				
	Hand						Hand				
NLR-10-A-D-C-N-1	Laboratory					NLR-10-A-D-C-F-1	Laboratory				
	Sensor						Sensor				
	Hand						Hand				
NLR-10-A-K-C-L-1	Laboratory					NLR-10-A-K-C-A-1	Laboratory				
	Sensor						Sensor				
	Hand						Hand				
NLR-10-A-K-C-N-1	Laboratory					NLR-10-A-K-C-F-1	Laboratory				
	Sensor						Sensor				
	Hand						Hand				
NLR-10-A-S-C-L-1	Laboratory					NLR-10-A-S-C-A-1	Laboratory				
	Sensor						Sensor				
	Hand						Hand				
NLR-10-A-S-C-N-1	Laboratory					NLR-10-A-S-C-F-1	Laboratory				
	Sensor						Sensor				
	Hand						Hand				
NLR-10-C-A-C-L-1	Laboratory					NLR-10-C-A-C-A-1	Laboratory				
	Sensor						Sensor				
	Hand						Hand				
NLR-10-C-A-C-N-1	Laboratory					NLR-10-C-A-C-F-1	Laboratory				
	Sensor						Sensor				
	Hand						Hand				
NLR-10-C-S-C-L-1	Laboratory					NLR-10-C-S-C-A-1	Laboratory				
	Sensor						Sensor				
	Hand						Hand				
NLR-10-C-S-C-N-1	Laboratory					NLR-10-C-S-C-F-1	Laboratory				
	Sensor						Sensor				
	Hand						Hand				
NLR-10-S-P-C-L-1	Laboratory					NLR-10-S-P-C-A-1	Laboratory				
	Sensor						Sensor				
	Hand						Hand				
NLR-10-S-P-C-N-1	Laboratory					NLR-10-S-P-C-F-1	Laboratory				
	Sensor						Sensor				
	Hand						Hand				

For the comparison of the interpretation methods, all EIS spectra of a coupon generated with the laboratory setup are modeled with Z-View. From the modeled results the n-value and the R_c value are plotted against time with respectively the CV and the PV in the same graph. From the batch of coupons degraded by salt spray this is done for coupon ADCN since it showed a gradual degradation profile. From the batch of coupons degraded by UV condensation cabinet this is done for coupons 2-5-4-1 and 2-10-4-1 because they showed very different degradation behavior. From the Oosterscheldekering locations, S9S-I-N-L was used. This measurement position was inside the pillar (Figure 23) and was therefore better protected against wind present on measurement day. This protection made the measuring easier and more controlled.

5.3 Modelling versus simplified interpretation

Modeling

All data points of the selected coupons where modeled with Z-View to find the most probable equivalent circuit as described in section 3.4. Figure 27 shows the result of the first data point of

coupon 2-5-4-1 modeled. The recorded Bode and Nyquist plot of this modeled data point are shown in Figure 26.
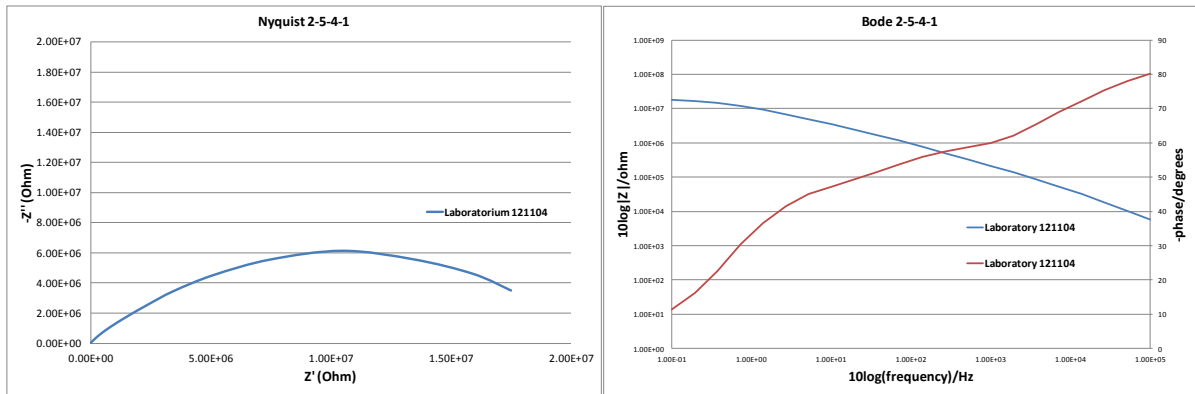

Figure 26. Left: Nyquist plot recorded for coupon 2-5-4-1 right: Bode plot recorded for coupon 2-5-4-1.
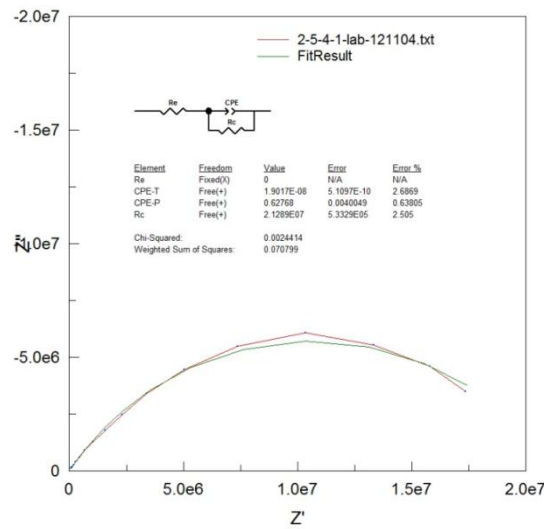

Figure 27. Modeled Z-View results.

Table 6 shows the values of the modeled elements that belong to the circuit shown in Figure 27. From these modeled results the value for R_c is plotted with the protective value from the simplified interpretation results against time. The CPE-P (n) values of the modeled results are plotted with the capacitive values from the simplified interpretation against time.

Table 6. Modeled results from coupon 2-5-4-1.

Element	Value
R_e	0
CPE-T	1.9017e-8
CPE-P (n-value)	0.62768
R_c	21289e7

Result comparison of the interpretation methods for coupon ADCN

The two graphs in Figure 28 show the result values of the simplified interpretation method and the result values R_c and n of the modeled circuits. The graph on the left shows both values follow the same degradation profile. First an increase in both the R_c and the PV is observed. Since these values are recorded at low frequencies it gives information on what happens on the interface of the substrate and the coating. It suggests electrochemical reactions take place at the interface and in time the reactions activity slows down, increasing the R_c value and the PV. This coating system consists of a chromate conversion coating that forms a passive chromium hydroxide $Cr(OH)_3$ layer. This activity results in a lower R_c value and PV. The point indicated with the red circle in Figure 28 shows a strong deviation of the original degradation pattern. This can be attributed by the fact that the coupons were taken out the salt-spray cabinet and transferred to another cabinet. This resulted in a 2 week break in which the coupons were kept outside the cabinet. This two break made it possible for the coating to dry, which results in mechanical stress in the coating and cracks may have been formed, although till this point no visible blisters were observed. The hexavalent chromium (Cr^{6+}) chromate is released and reduced reforming the $Cr(OH)_3$ barrier. This self-healing effect of the chromate conversion coatings may well be the reason of the increase of the result values.

The graph on the right shows that both values, the n-value and the CV follow a very gradual degradation profile. This means that the capacity of the coating slowly deteriorates and more and more conductive paths reach the substrate.
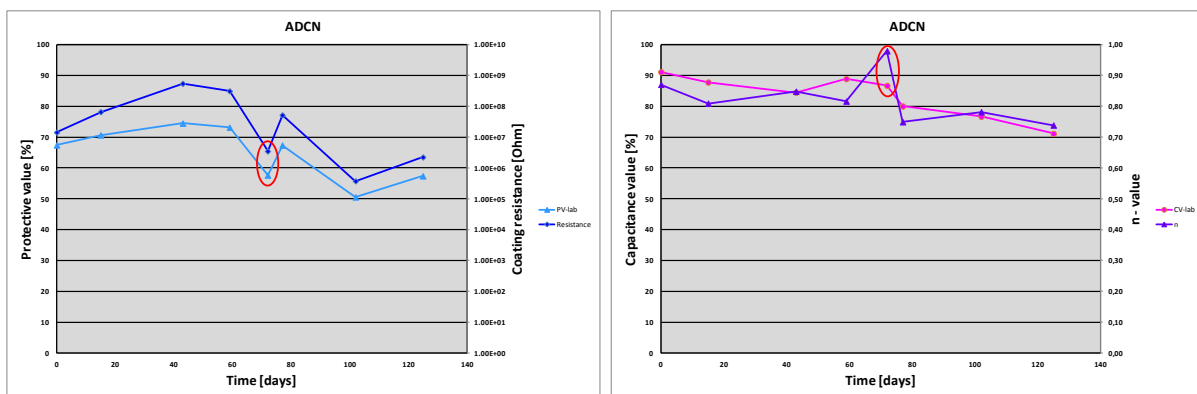
Figure 28. Left: ADCN PV - Corrosion resistance Right: ADCN CV – n-value.

The red circle in this figure indicates a strong deviation from the trend, with the important remark that only the n-value shows this deviation. Figure 29 shows the recorded bode and Nyquist plot of this measurement, some noise is recorded as shown in the 50Hz frequency range caused by the laptop charger connected to the grid, this phenomena will be discussed in more detail in section 7.1. This noise results in an inaccurate modeling of this n-value.
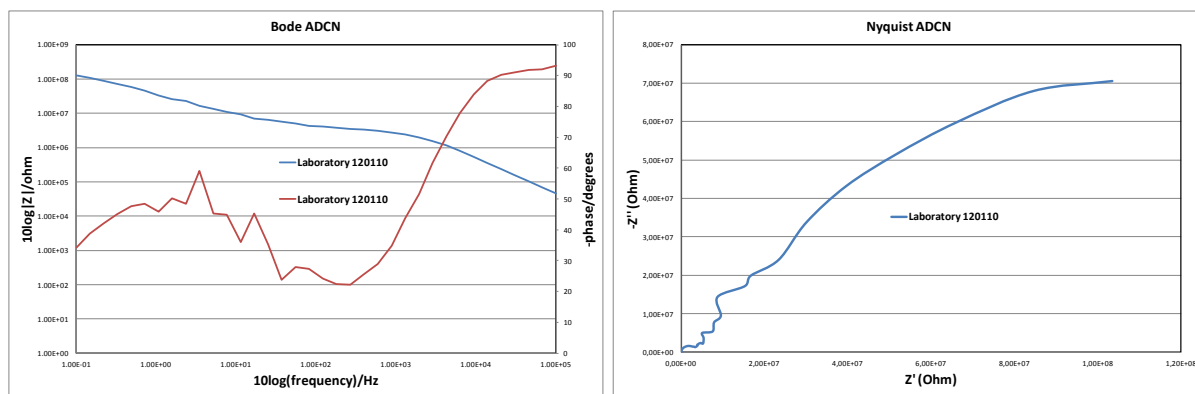
Figure 29. Bode and Nyquist recorded at t = 72 days.

Result comparison of the interpretation methods for coupon 2-5-4-1 and 2-10-4-1.

Both coupons are coated with coating systems containing magnesium. A key aspect of Mg-rich primers is the presence of a thin oxide layer that enables the particles to be handled in air similar to a conventional pigment or inorganic corrosion inhibitor [56]. The oxide layer also affects the rate of Mg consumption as water slowly penetrates the primer during exposure of a coating system to a corrosive environment.

The two graphs in Figure 30 show the result values of the simplified interpretation method and the result values R_c and n of the modeled circuits of coupon 2-5-4-1. Both graphs show that the result values follow very similar degradation profiles. The left graph shows very little difference between the degradation pattern generated by the values of PV and R_c. The graph on the right shows similar behavior for the CV and the n-value although there seems to be little more variation in the first 35 days of the experiment. From the start this coupon performed much worse compared to the other coupons. In the left graph the red line shows a logic degradation profile for the PV, the two result values for the PV indicated with the red circle deviate strong from this line. Two possible explanations for these higher values are:

1. The coupon stayed longer in the dry cycle of the UV-condensation cabinet, which may resulted in a dryer coating when the measurement was performed (further explained in section 7.3).
2. Magnesium present in the primer of this coating system to provide for sacrificial protection, may have formed magnesium oxides that blocked hydrophilic pathways.
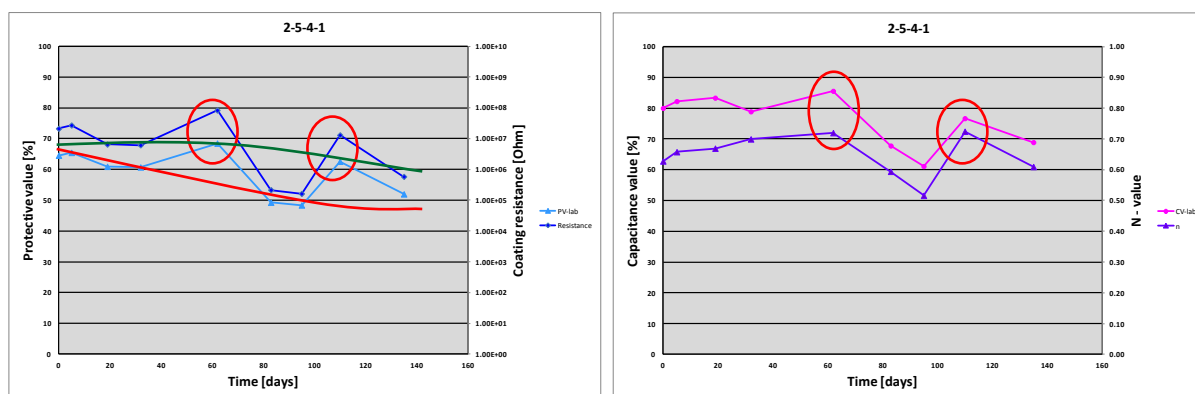
Figure 30. Left: 2-5-4-1 PV - Corrosion resistance Right: CV – n-value

Figure 31 shows coupon 2-5-4-1 after 110 days (second red circle in Figure 30) of exposure in the UV-condensation cabinet, clear blister formation is observed. Since the n-value and the CV are still reasonably high while clear blisters are visible is another indication that the coating was to dry for performing a correct measurement.

Since Mg is electrochemically very active and undergoes rapid oxidation in the presence of water to produce hydrogen gas as shown by reaction 5.1.

$$Mg + 2H_2O \rightarrow MgO + H_2 \qquad \textbf{5.1}$$

Rapid hydrogen gas evolution produce blisters as described in [57]. Its suggest that Mg-oxide layer is partially decomposing resulting in relatively rapid oxidation of the Mg particles. It is possible the blisters shown in Figure 31 are the result of this phenomena.

Figure 31. Blister formation on coupon 2-5-4-1 after 110 days of exposure in the UV condensation cabinet.

There is however also another possibility which is indicated with the green line. This reasoning stray current may cause lower result values, which can occur if the coating is still wet, water can be still present in the rough surface of the coating. Especially since this coupon is degraded by UV which is known to cause chalking [58]. Roughness of the coating could lead to leaking of the seal of the electrochemical cell as shown in Figure 32.
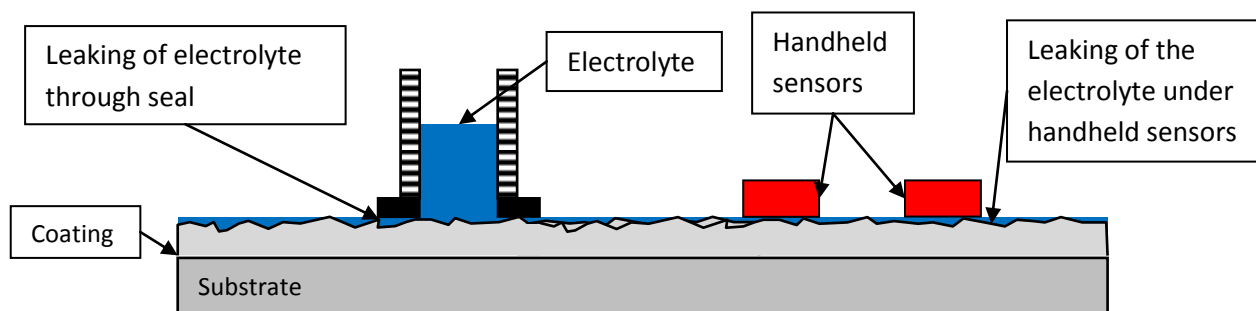
Figure 32. Basic idea of imperfect seal leads to stray current over rough surface.

The leaking electrolyte can have a large contribution on the result value especially if a local crack is present and a direct path to the substrate is possible. Although no visible cracks were visible, leaking electrolyte trough the seal effects the measurement and results in lower values.

Figure 33 shows the comparison of the result values of coupon 2-10-4-1 on the left the PV and R_c are shown, on the right the comparison between CV and the n-value is presented. The left graph shows very little difference between the degradation pattern generated by the values of PV and R_c. The same can be seen in the graph on the right with the values of CV and n. The strong improvement of the result values in the first 30 days of exposure in the UV-condensation cabinet can be explained by the working principle of the coating system. The MgO conversion coating in combination with the primer, a anticorrosive magnesium hydroxide film will grow according to reaction 5.2.

$$MgO + H_2O \rightarrow Mg(OH)_2 + H_2 \qquad \textbf{5.2}$$

The film forming process goes slow as water needs to diffuse through the coating and the hydrogen gas needs to escape.

The data point marked with the red circle deviates strongly from the degradation pattern. The Bode plot and Nyquist plots of this measurement are shown in Figure 34. The deviation could be caused by a local defect present under the measured surface. This defect makes it possible for the electrolyte to come in contact with the substrate and form a conductive pathway causing a decrease of the values. The increased values of the next measurement might be caused by magnesium containing primer in this coating system, or the electrochemical cell was not placed directly on the defect.
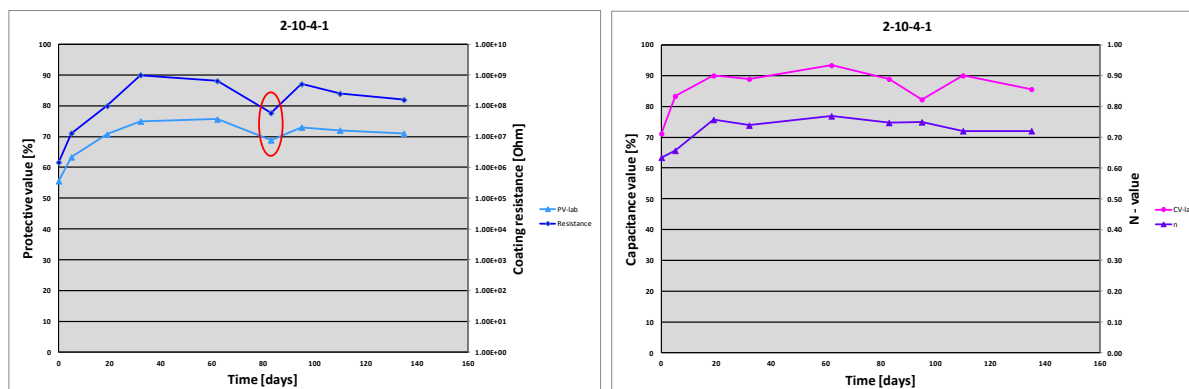
Figure 33. Left: 2-10-4-1 PV - Coating resistance Right: 2-10-4-1 CV – n-value
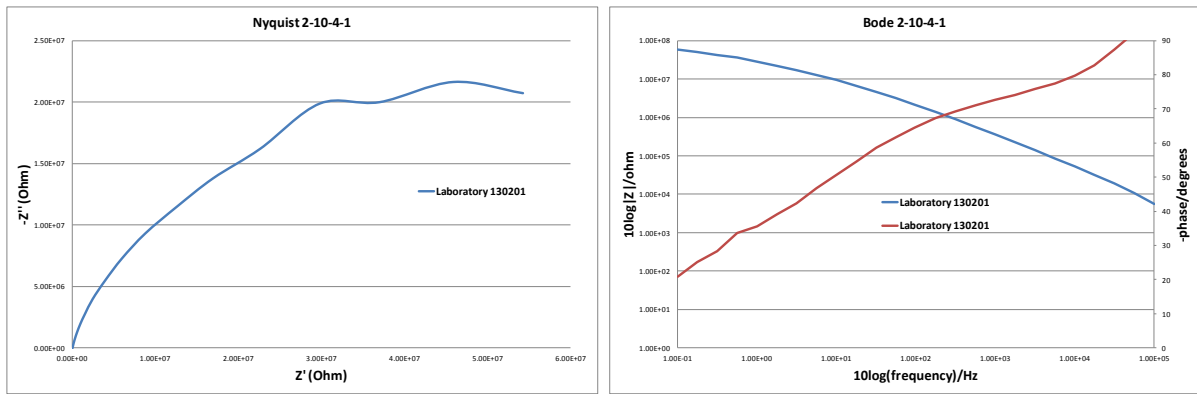
Figure 34. Bode and Nyquist recorded at T = 83 days

Result comparison of the interpretation methods for location S9S-I-N-L on the Oosterscheldekering.
Figure 35 shows the comparison of the result values of the Oosterscheldekering position S9S-I-N-L on the left the PV and R_c are shown, on the right the comparison between CV and the n-value is presented. This coating system was provided a new coating layer one year after the first measurements, indicated with the red line. The increase of the result values is in accordance with this new layer and shows an improvement of the overall coating properties.
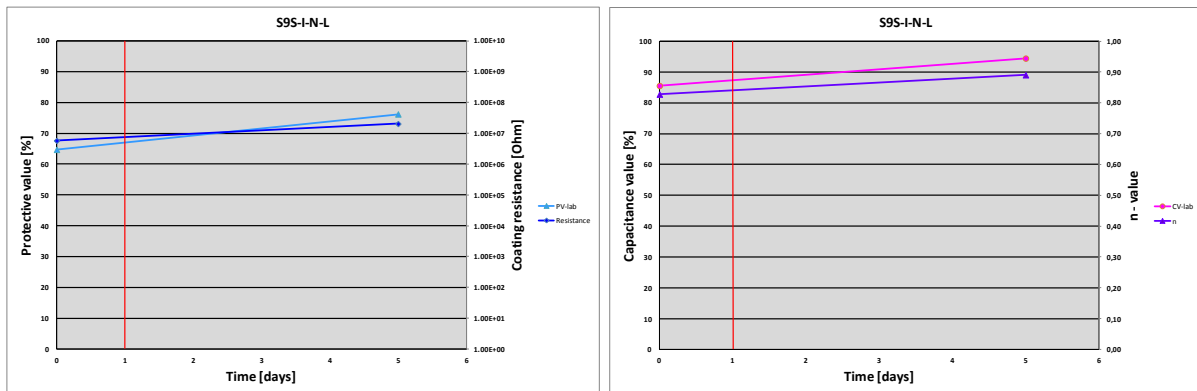
Figure 35. Left: OSK PV - Coating resistance Right: CV – n-value.

5.4 Coating capacitance versus simplified interpretation

The coating capacitance is extracted from the modulus of impedance at 10^4 Hz and plotted versus the exposure time. In Figure 36 the coating capacitance and the CV are plotted against time. These figures show little correlation between the CV and the coating capacitance.
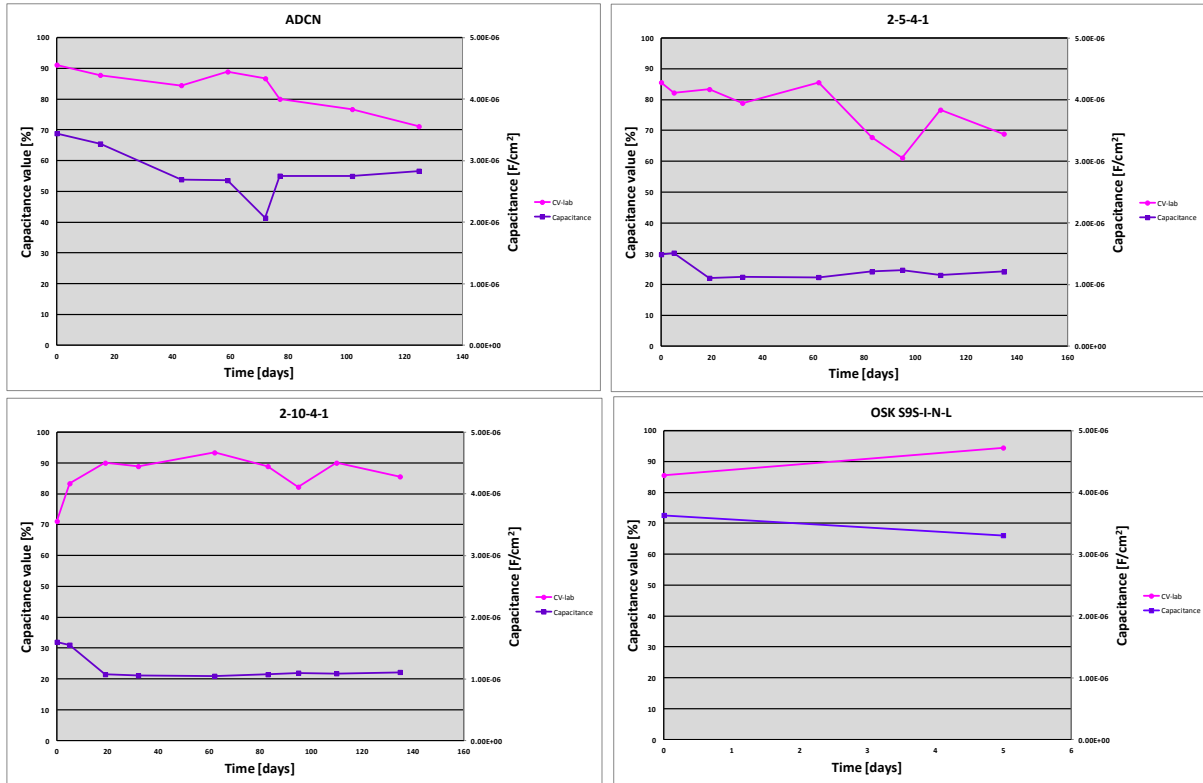
Figure 36. CV and Coating capacitance versus time.

It is important to note that in this situation the capacitance is not continue monitored meaning the coating is not continue exposed to an electrolyte column. Instead its exposed to an cyclic condensation stage. The measurement frequency is in days instead of hours. The used aircraft coating systems are only 100 µm thick and interesting water diffusion process happens in the first hours to maybe a few days of contact with water. In this period the coating capacitance should be monitored frequently to capture the diffusion characteristics of the coating. For the capacitance to be proportional to the impedance no contributions of the surface must be present.

5.5 Handheld setup versus laboratory setup

Result interpretation of the laboratory coupons degraded in the salt-spray cabinet.

In this section, the results of the two measurement setups are compared. Figure 37 shows the CV and PV results of the coupons degraded in the salt spray cabinet. The results for the PV are displayed in dark blue for the handheld measurements and in blue for the laboratory measurements. The results for the CV are displayed in purple for the handheld measurements and in pink for the laboratory measurements. The green line indicates the moment that both measurement methods simultaneous were performed, before this green line only handheld measurements were performed. In general these results show that both setups produce very similar degradation patterns.
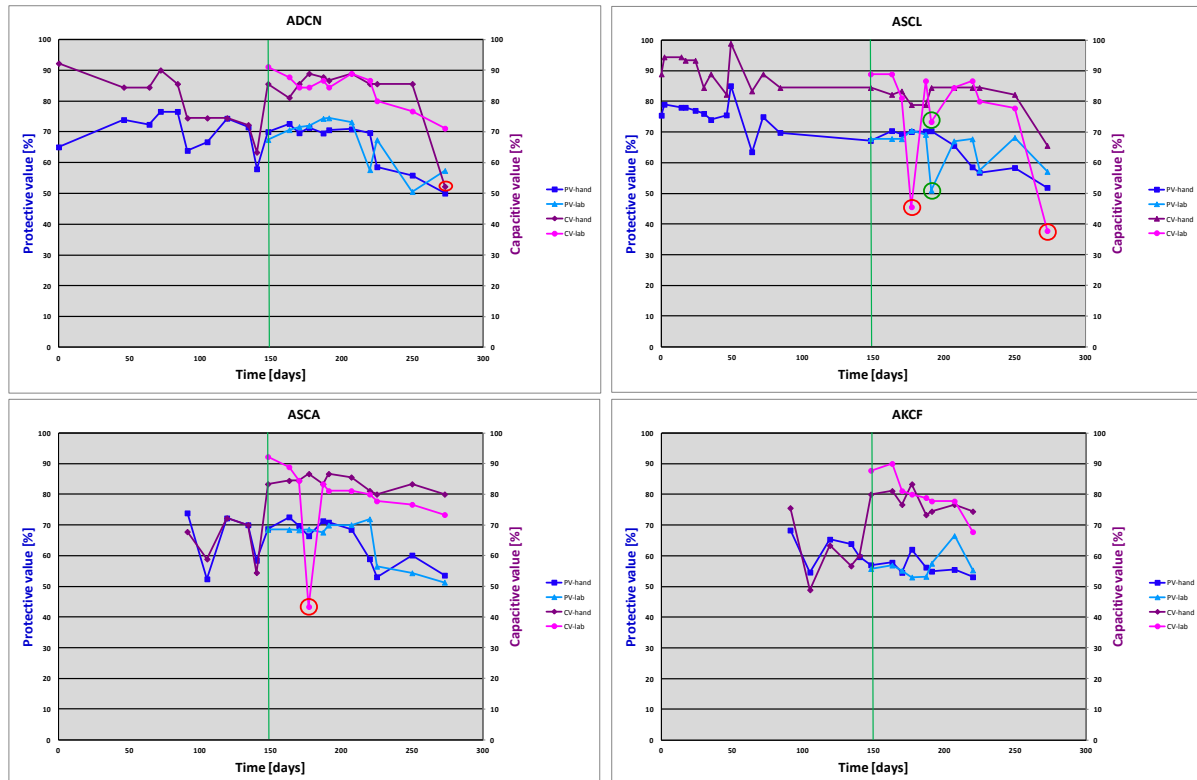
Figure 37. Handheld setup and laboratory setup comparison of the salt spray coupons.

A few data points need some further explanation. The data points indicated with a red circle strongly deviates from the general degradation pattern. The recorded Bode and Nyquist plot for these points are shown in Figure 38. Remarkably all these points were measured with the laboratory setup and not with the handheld sensor setup. This suggests that the handheld setup is less sensitive in detecting coating defects or the laboratory measurements were performed incorrect. These deviations can have several causes, one is the lack of experience as described in the introduction (5.1) what might have lead to an incorrect EIS measurement. Another more fundamental explanation could be that mechanical stresses that arise in cyclic salt spray tests caused cracks in the coating. If such a crack arises just before a measurement is performed and the electrochemical is placed over the crack, this can lead to a drop in capacitive behavior of the coating. Since this coating system contains a chromate conversion coating the passive oxide film prevents electrochemical reactions from taking place therefore the PV not affected. The unique 'self healing' ability off CCCs is responsible for the recovery of the CV in the next measurement. CCCs form via a redox reaction

between Al in the alloy and Cr(VI) species in the chromating solution. They are amorphous and mainly composed of hydrated mixed Cr(III)/Cr(VI) oxide [59]. The Cr(VI) species can be stored in CCCs and released as soluble chromate species when CCCs are exposed to solution.
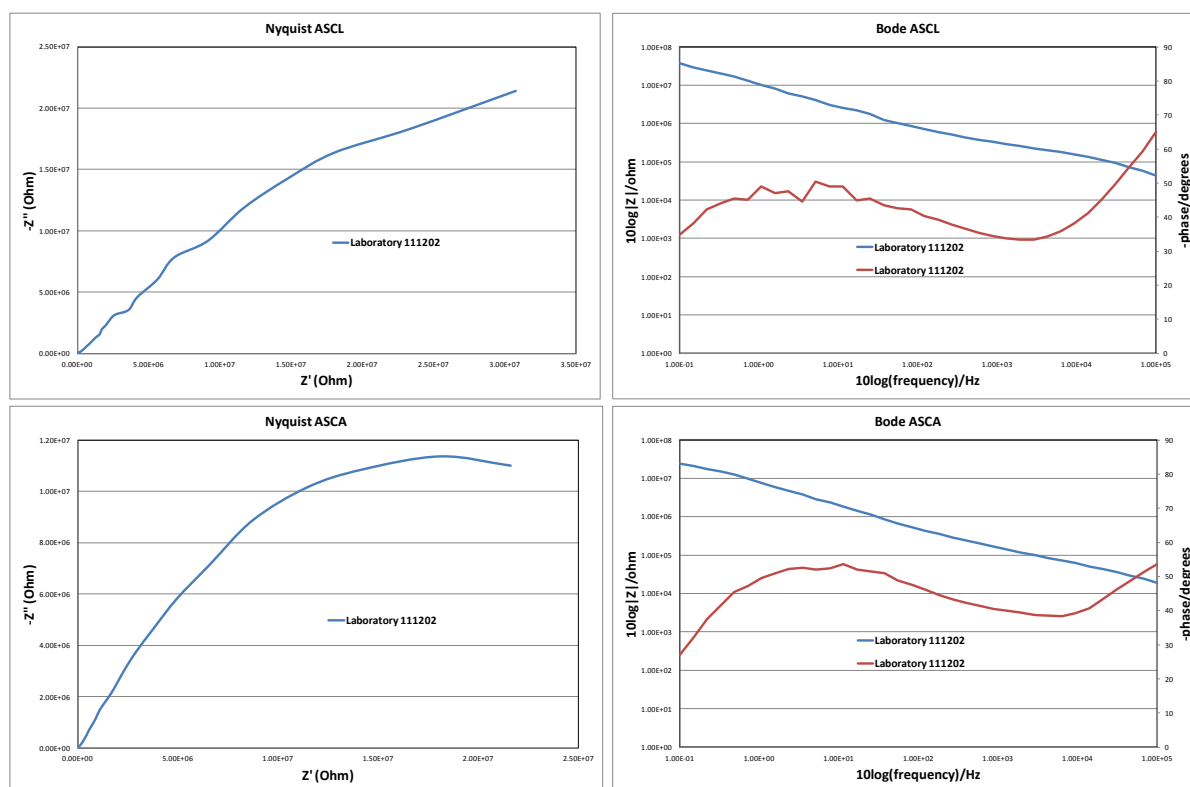

Figure 38. Nyquist + Bode (top ASCL, bottom ASCA) plot recorded at red circles.

The lower CV and PV of the data point circled green in the result graph of the laboratory coupon ASCL can be the result of a similar phenomena (Figure 39 shows the recorded Bode and Nyquist plot for this data point). In this case, the PV is also affected which suggest that the electrochemical activity at the interface is increased, caused by damage due to the stresses on the passive chromate film. The values recover by the released Cr(VI) species, as described above.
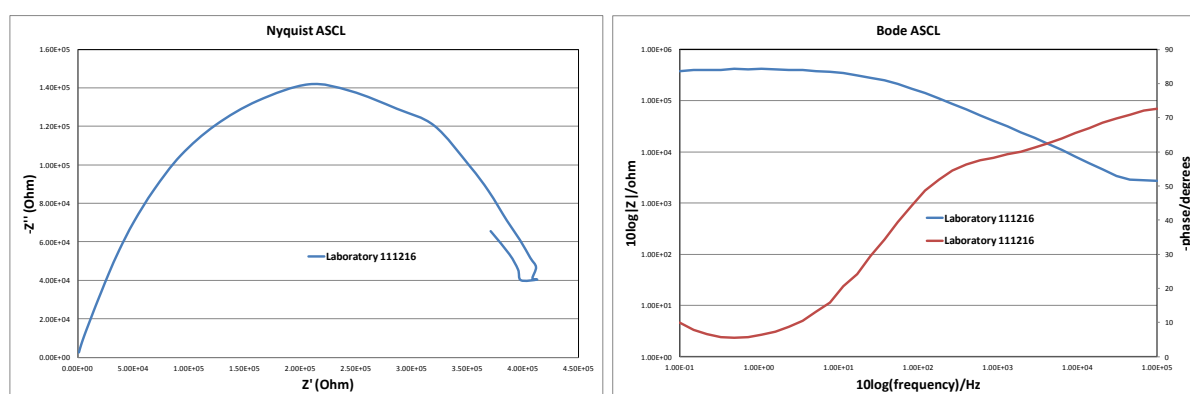
Figure 39. Nyquist + Bode plot recorded at green circles.

Result interpretation of the laboratory coupons degraded in the UV condensation cabinet coupons
Figure 40 shows the CV and PV results of the coupons degraded in the UV condensation cabinet. The results for the PV are displayed in dark blue for the handheld measurements and in blue for the laboratory measurements. The results for the CV are displayed in purple for the handheld measurements and in pink for the laboratory measurements.
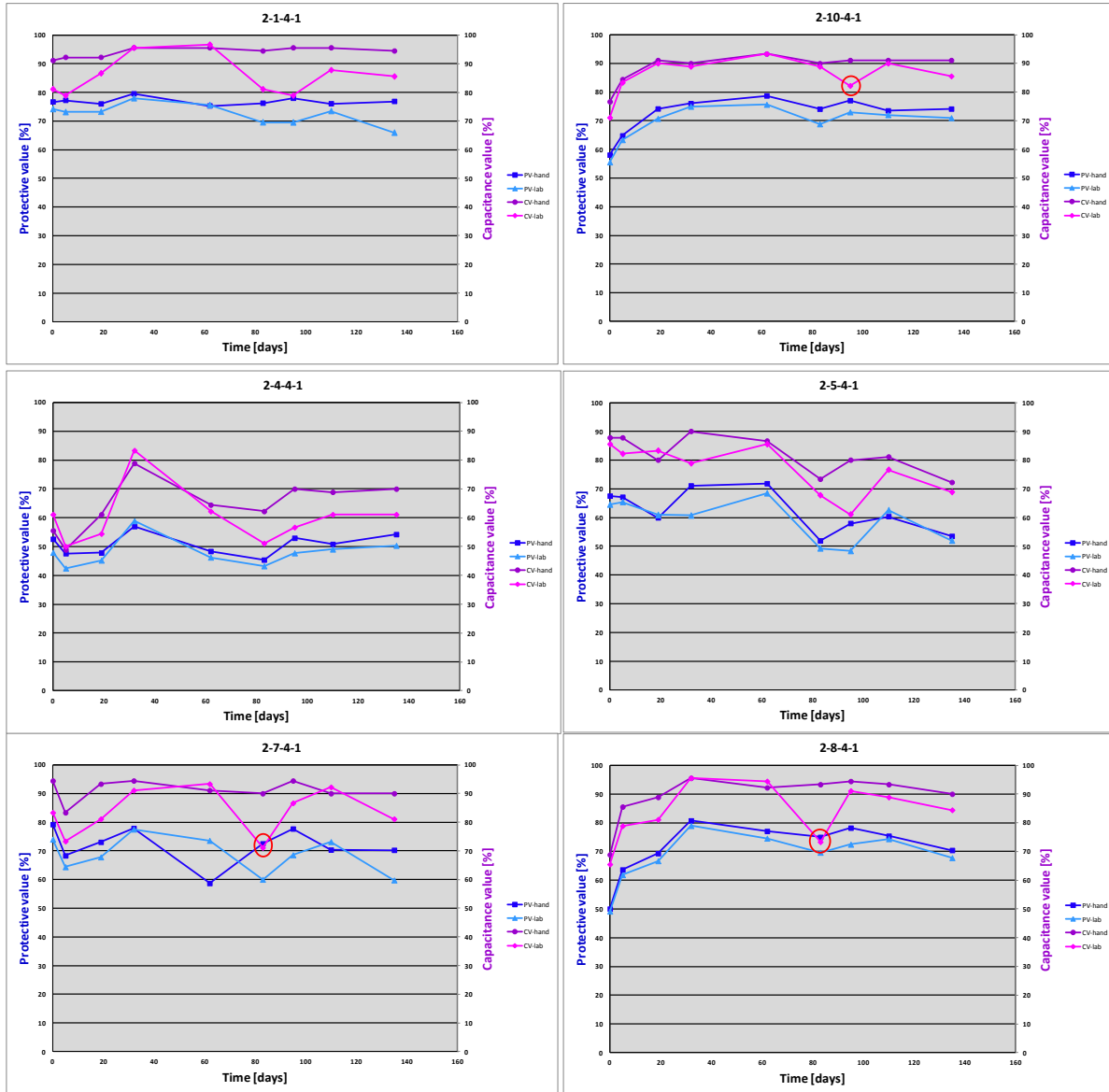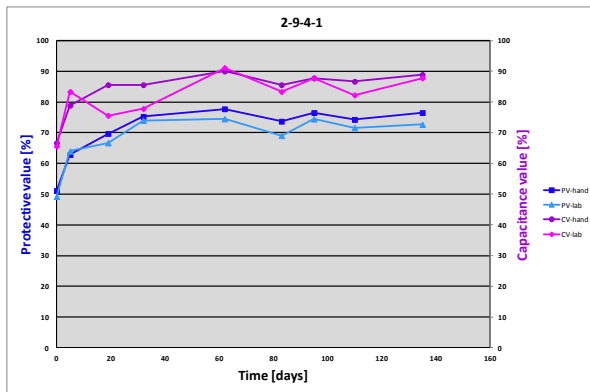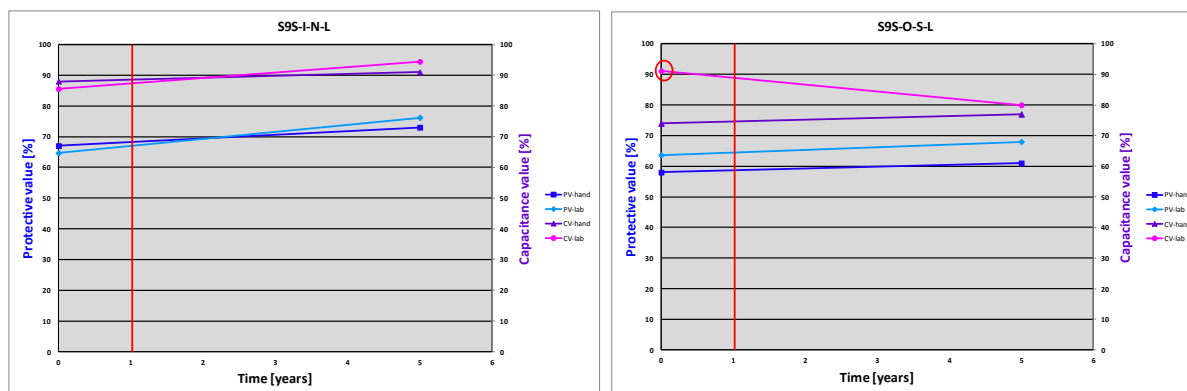
Figure 40. Handheld setup and laboratory setup comparison of the UV condensation coupons.

The coupons results of the UV condensation cabinet show very similar degradation patterns, especially coupon 2-10-4-1, 2-8-4-1 and 2-9-4-1. The results from these coupons recorded with the handheld setup and the ones recorded with the laboratory setup show very little difference and indicate that the handheld setup is capable of producing results that are comparable with the results generated with a traditional laboratory setup.

The graphs of laboratory coupon 2-10-4-1, 2-8-4-1 and 2-7-4-1 all have a data point with a black circle. Figure 41 shows the recorded Bode plots for these data points. It shows a sudden drop of the phase angle in the high frequency range. This indicates that the potentiostat is switching between current ranges, this makes the recorded values unreliable in that frequency range unreliable. In section 7.5 this phenomena will be discussed in more detail section 7.5.
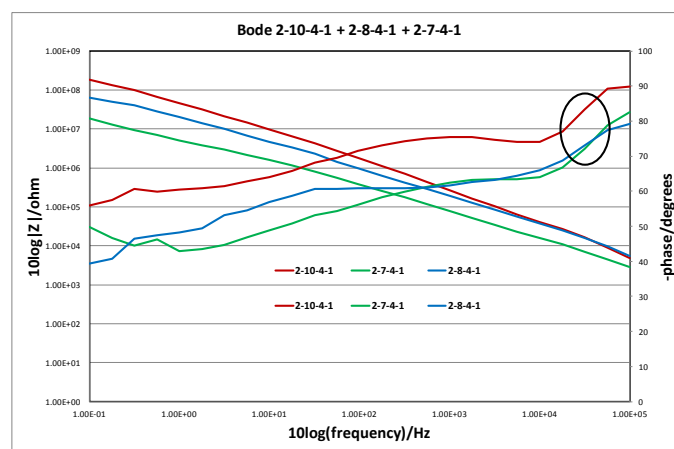
Figure 41. Recorded Bode plots of the datapoints with the black circle.

Result interpretation of the measurements on the Oosterscheldekering degraded in a natural environment.

Figure 37 shows the CV and PV results of the measurement locations on the Oosterscheldekering degraded in a natural environment. The results for the PV are displayed in dark blue for the handheld measurements and in blue for the laboratory measurements. The results for the CV are displayed in purple for the handheld measurements and in pink for the laboratory measurements.

Figure 42. Handheld setup and laboratory setup comparison of the Oosterscheldekering measurements.

As described in section 5.3, the red line indicates a new coating layer, the graphs of both positions show an increase of the PV and CV measured with the handheld and laboratory setup. Except CV marked with the red circle, the recorded Bode plot for this point is shown in Figure 43. In the high frequency range around 10^5 Hz (marked with the red circle) a disturbance is recorded. This distortion is responsible for the higher CV. It is hard to say what caused this distortion, most likely the potentiostat switches between different current ranges. As described in section 4.3.2 this measurement was performed 5 years ago by C-Cube, the exact reason for this deviation is therefore unclear.

The measurement results show that the values of the measurements at location S9S-O-S-L are overall lower compared to the values of location S9S-I-N-L. Location S9S-I-N-L is positioned inside the pillar, as shown in Figure 23, which is surrounded by other beams and therefore better protected against the environment as opposed to location S9S-O-S-L. Location S9S-O-S-L is on the outside face of the beam and therefore in direct contact with the environment. Especially wind, which is almost always present on the Oosterschelkering, can have a big impact on the lifespan of a coating.
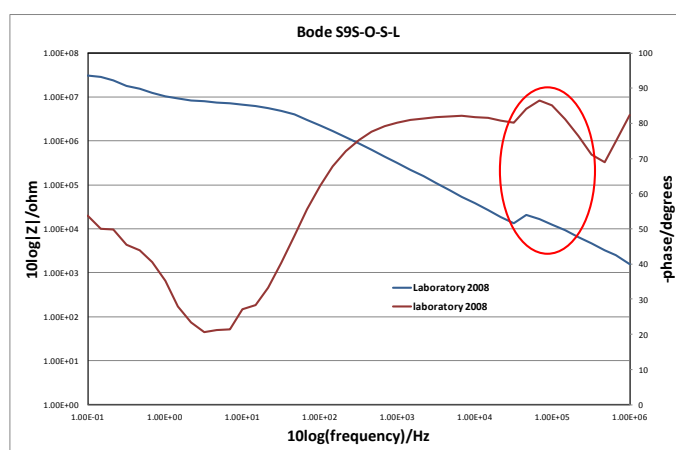

Figure 43. Bode plot recorded of the data point with the red circle.

5.6   Blister formation

The laboratory coupon labeled AACN was not selected for the comparison of the measurement setups and interpretation methods. Although the coupon does not show a logical degradation pattern, it shows a sudden drop of all values, indicated with the red circle in Figure 44. The point indicated with the red circle is the moment the laboratory coupons were removed from the salt-spray cabinet in NLR, after two weeks they were put back in salt-spray cabinet at C-Cube.
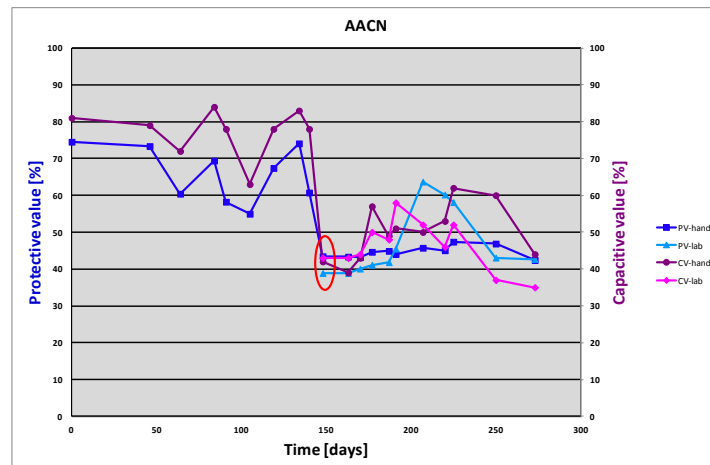

Figure 44. Handheld setup and laboratory setup measured PV and CV of coupon AACN.

The difference with this coupon, in comparison with the used coupons for the interpretation and method comparison, is the presence of blisters at the moment the coupon was removed from the salt spray cabinet. Figure 45 shows pictures of the blister propagation of coupon AACN in time the picture marked '140 days' shows the blisters present at the moment the coupons was removed from the cabinet. During the period the coupon was outside the salt spray cabinet the water in the blisters evaporated and the blisters disappeared. When the coupon was then put back into the cabinet the blisters swelled again, which lead to a severe mechanical movement of the coating. This movement lead to cracks on the edges of the blisters which causes lowering of the PV and CV.
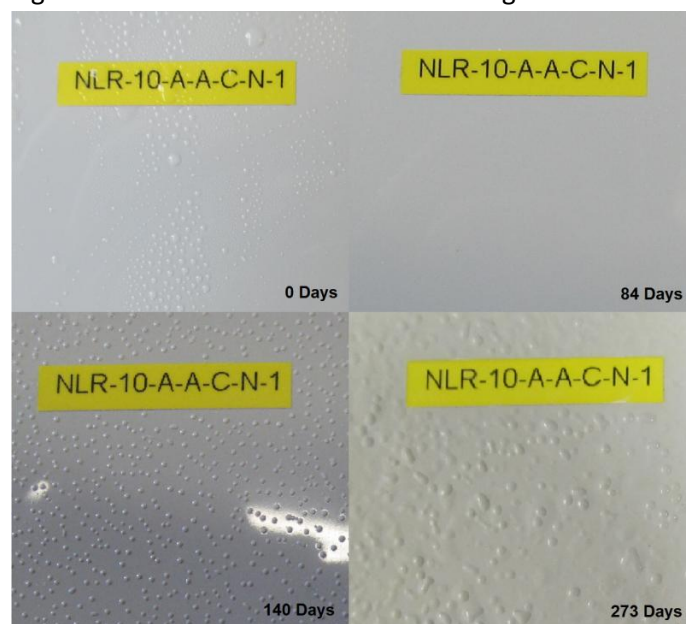

Figure 45. Blister formation in time on laboratory coupon AACN.

5.7 Measurement difference between laboratory setup and handheld setup.

Figure 46 and Figure 47 show the difference between the PV and CV measured with the handheld and laboratory setup for the coupons degraded by salt spray. The orange line indicates the absolute difference of each separate measurement, it is hard to discover a general trend in these lines and all lines lay close to the black zero line.
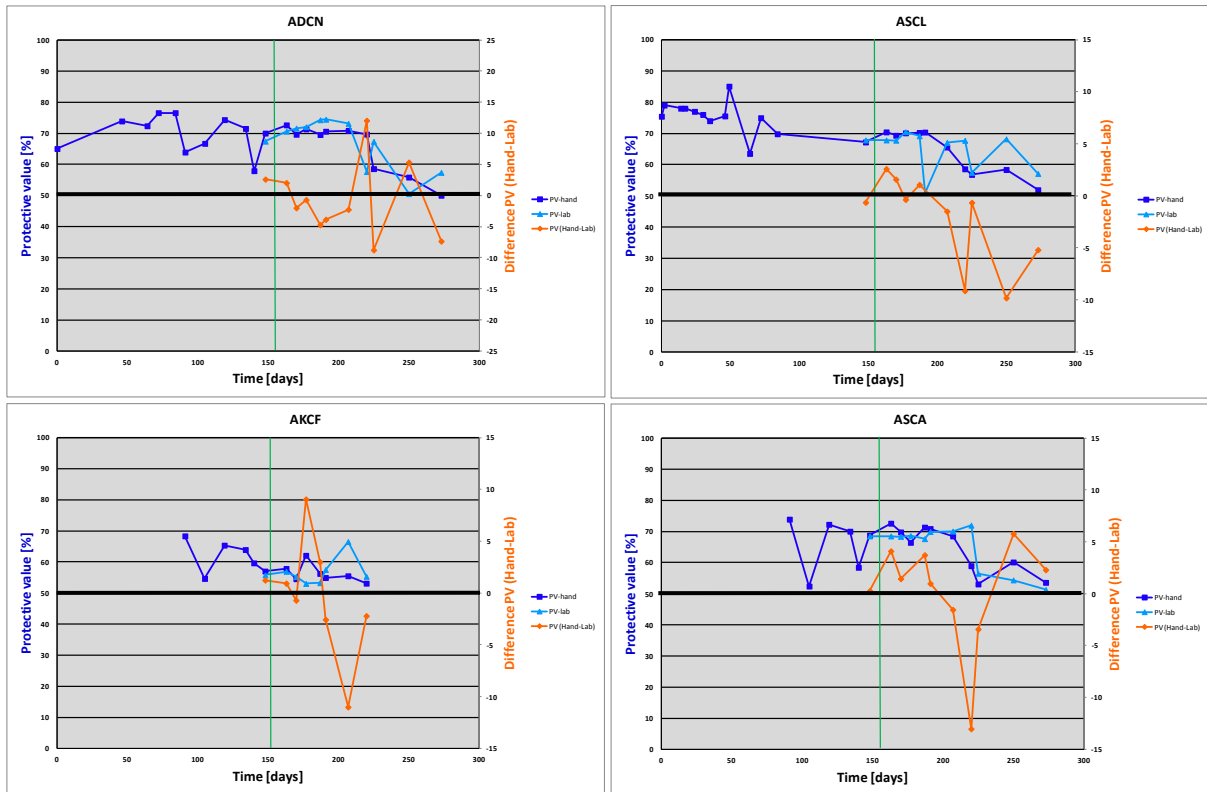

Figure 46. Difference between the PV measured with handheld and laboratory setup for the coupons degraded with salt spray.
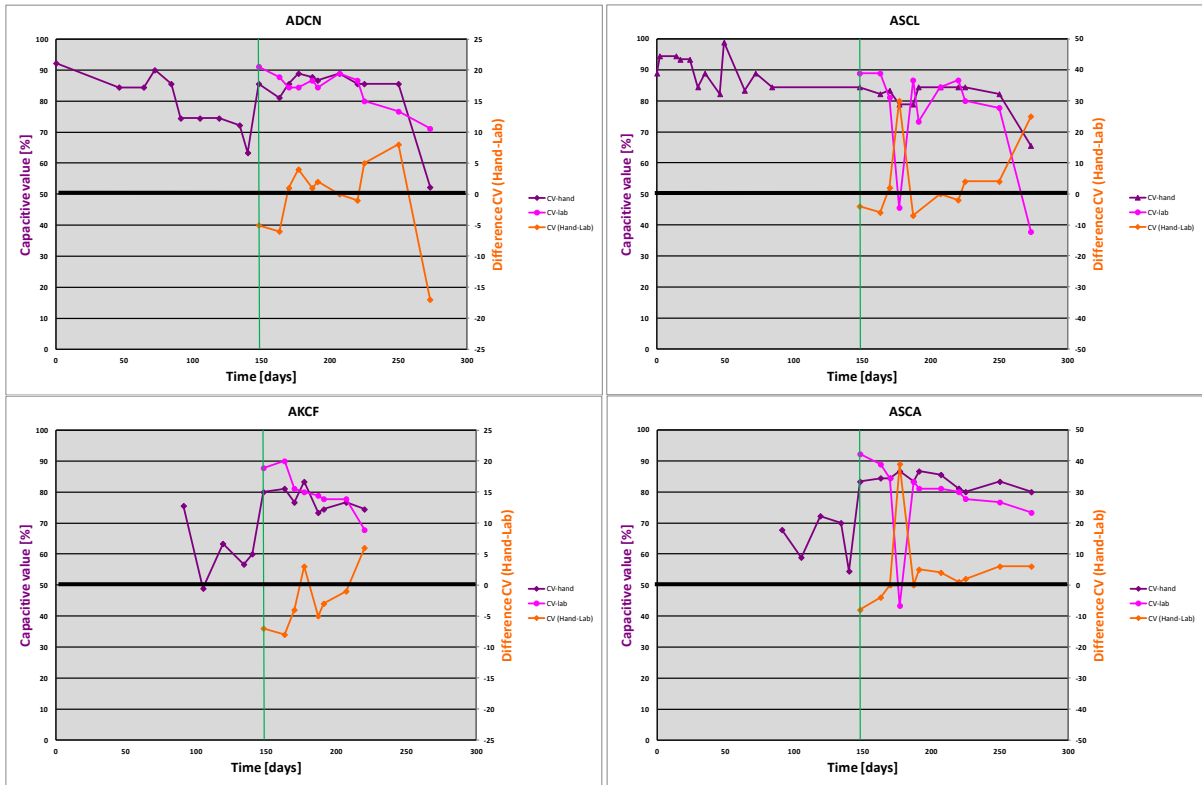
Figure 47. Difference between the CV measured with handheld and laboratory setup for the coupons degraded with salt spray.

Table 7 shows the average difference of the result values of the handheld setup compared with the result values generated with the laboratory setup. For the calculation of the average values the discussed data points with an extreme deviation from the degradation profile are left out. These values show that the handheld setup generate result values for the PV that overall are -0.62 % lower than the results generated with the laboratory setup and 0.35 % lower for the CV results.

Table 7. Average difference in % between the result values of the handheld and the laboratory setup for the coupons degraded with salt spray.

	NLR-10-A-D-C-N-1	NLR-10-A-S-C-L-1	NLR-10-A-K-C-F-1	NLR-10-A-S-C-A-1	Overall
PV	-0.04	-2.21	-0.29	0.06	-0.62
CV	0.90	-1.13	-2.38	1.20	-0.35

Figure 48 and Figure 49 show the difference between the PV and CV measured with the handheld and laboratory setup for the coupons degraded by UV-condensation. The orange line indicates the absolute difference of each separate measurement. These lines show that for both results the PV and the CV the values that were produced with the handheld are systematic higher than the results produced with the laboratory setup. This suggests that the handheld is less sensitive compared to the

laboratory setup. There are several reasons that can lead to the less sensitive character of the handheld measurements. In a traditional three-electrode setup the signal passes the coating thickness ones. The reference electrode measures with respect to the substrate. In the handheld setup, this is with respect to the second sensor the signal passes therefore trough the coating trough the substrate and again there coating. In the calculation of the result values, there is compensation for the fact that the signal passes the coating thickness twice. The distance the signal travels through the substrate is not compensated for and this resistance may be responsible for sensitivity difference. Another important distinction between the setups is the fact that in the laboratory setup the electrolyte is in 'direct' contact with the coating. Under pressure of the electrolyte column, it might penetrate easier into the coating in comparison with the electrolyte in the sponge of the handheld setup.
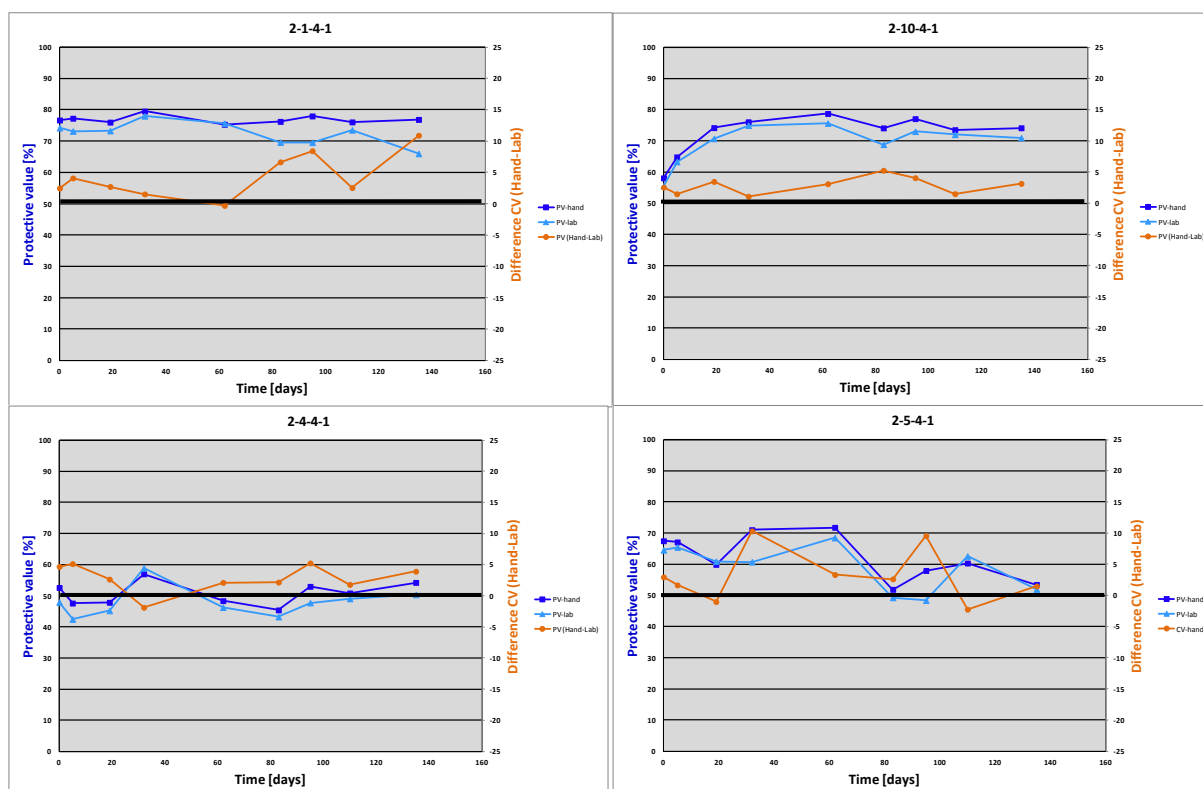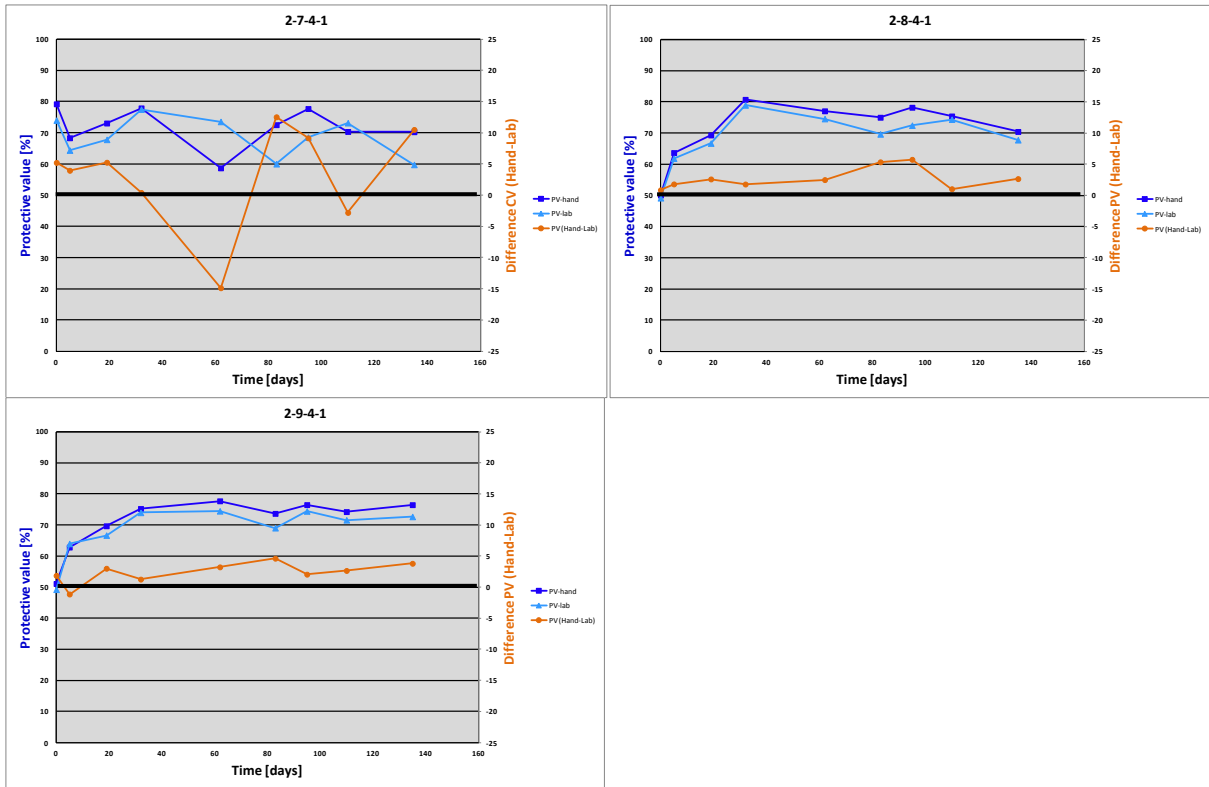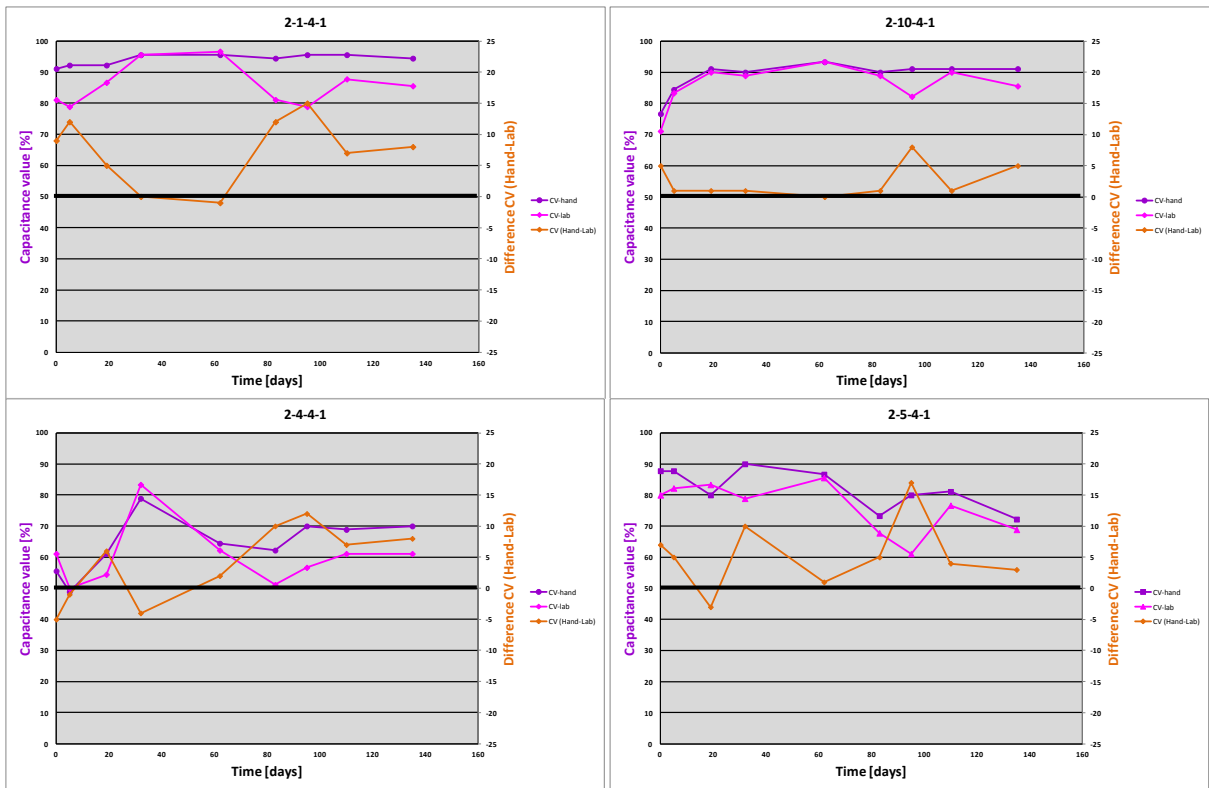
Figure 48. Difference between the PV measured with handheld and laboratory setup for the coupons degraded with UV-condensation.
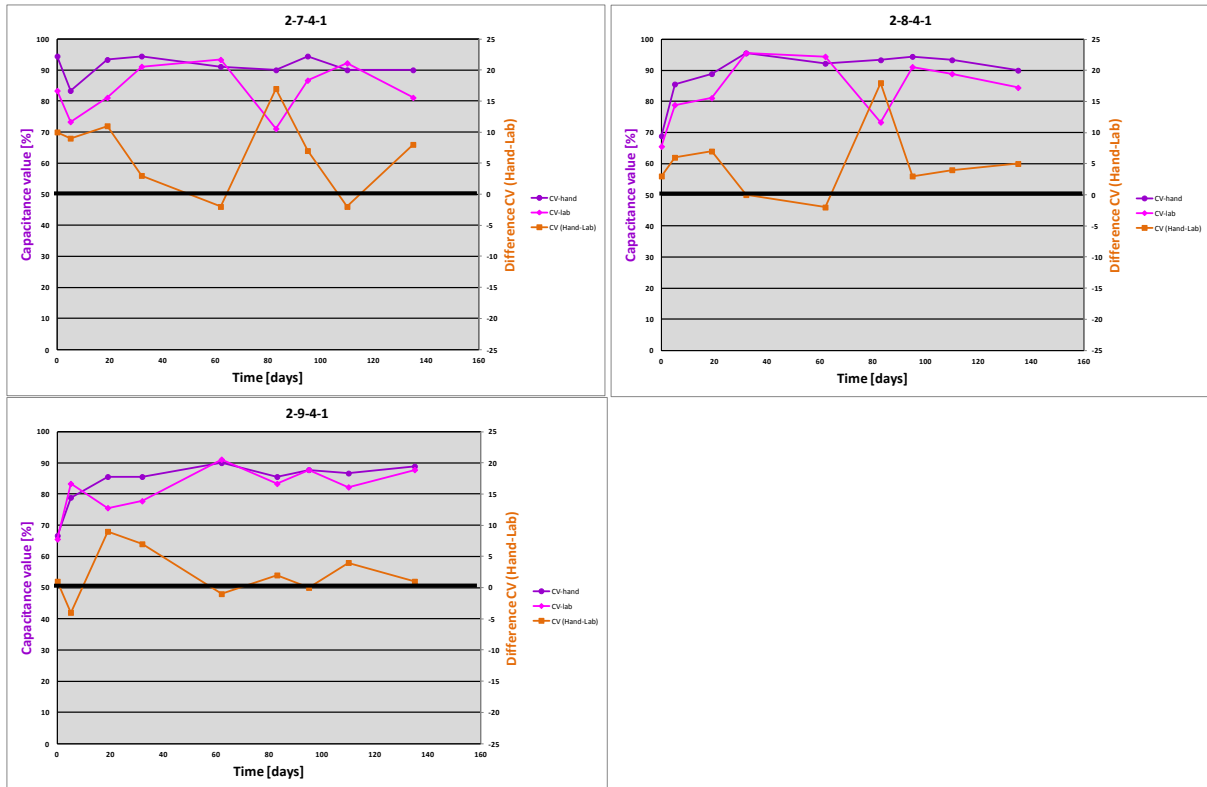
Figure 49. Difference between the CV results measured with handheld and laboratory setup for the coupons degraded with UV-condensation.

Table 8 shows the average error of the result values of the handheld setup compared with the result values generated with the laboratory setup. For the calculation of the average values the discussed data points with an extreme deviation from the degradation profile are left out. These values show that the handheld setup generate result values for the PV that overall are 3.08 % higher than the results generated with the laboratory setup and 4.73 % higher for the CV results.

Table 8. Average difference in % between the result values of the handheld and the laboratory setup for the coupons degraded with UV-condensation.

	2-1-4-1	2-10-4-1	2-4-4-1	2-5-4-1	2-7-4-1	2-8-4-1	2-9-4-1	Overall
PV	4.33	2.86	2.87	3.18	3.26	2.71	2.38	3.08
CV	7.44	2.56	3.89	5.44	6.78	4.89	2.11	4.73

The results for the measurements performed on the Oosterscheldekering can be found in Appendix B as these only consist of two measurements it has little scientific relevance.

6   Conclusion

The goal of this research was to validate a new handheld sensor setup and interpretation method developed for in situ degradation studies of coated metals with electrochemical impedance spectroscopy. The results in section 5.5 show that the sensor setup is very capable for in situ application of electrochemical impedance spectroscopy. The technique has been successfully used to collect EIS spectra of coatings without any damage to the coating or substrate. The simplified interpretation method was compared with two traditional interpretation methods. The results in section 5.3 show that the generated values with the simplified interpretation method are very similar to the modelled values. The results in section 5.4 show that the result values compared to the coating capacitance show little correlation.

For this research a lot of EIS spectra were recorded in the laboratory with different measurement setups performed on different types of coatings degraded by different environments. This in combination with the measurements performed on the Oosterscheldekering lead to a good understanding of how an in situ EIS measurement should be performed.

For the qualification of an in situ organic coating with electrochemical impedance spectroscopy the following requirements should be met:
- Fluctuation of coating thickness can have a large influence on the interpreted EIS results. It is therefore important to determine the fluctuations in coating thickness, with a coating thickness measurement. If large fluctuations are present it is important the EIS measurements are on thinnest spots.
- To get a good picture of the whole coating condition of an object it is important that the measurement location and the number of measurements are well chosen. Visual inspection of the object is therefore vital, in the selection process everything must be taken into account, common wind directions presence of sand, (sea)water, etc.
- For reliability all result values must be based on three stable recorded EIS spectra.

Overall it can be concluded that the handheld sensor setup with the simplified interpretation method is very good technique for in situ organic coating assessment on metal substrates. With the caveat that the measurements are performed by someone who is experienced in the use of Electrochemical Impedance Spectroscopy and understands the discussed shortcomings of the system.

7 Remarks

7.1 Power grid induced noise.

In several EIS spectra a noise round the 50 Hertz frequency range was exhibit as shown on the left in Figure 50. Experience showed that this noise was only present when the laptop charger was plugged into the grid. Since the power grid operates on this frequency this seems a logical explanation. In Figure 50 the difference is shown between a measurement with a charging laptop and a measurement performed while the laptop runs on solely the battery.
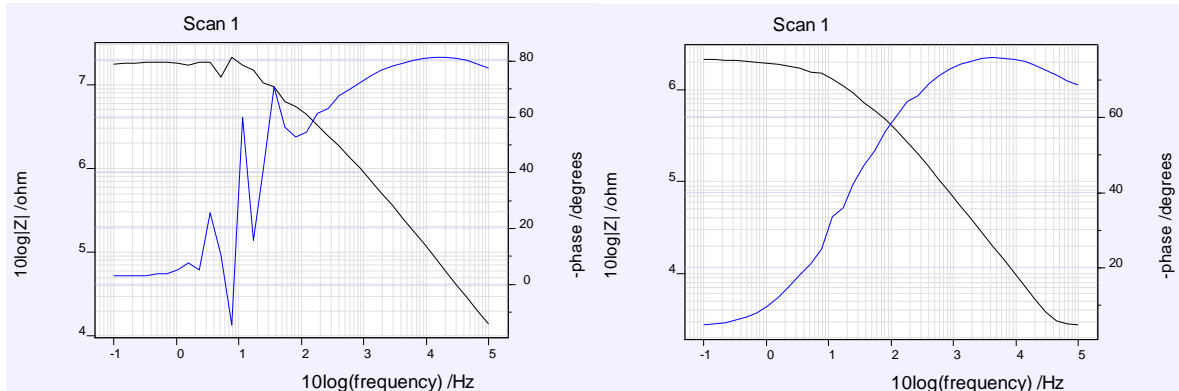

Figure 50. Difference between the recorded spectra while laptop is charging (left) and while laptop runs on the battery (right).

This recorded noise makes modeling of the equivalent circuits within acceptable chi squared margins impossible. This noise was not a big problem in the result value calculation with the other interpretation methods.

7.2 Reduced surface contact

The dimensions of the laboratory coupons used in the salt-spray cabinet were 100mm x 100mm. The thick epoxy coating used for protection of the underside and edges of the coupon as described in 4.2.1 caused a little 'bump' on the topside of the coupon, as shown on the left in Figure 51.
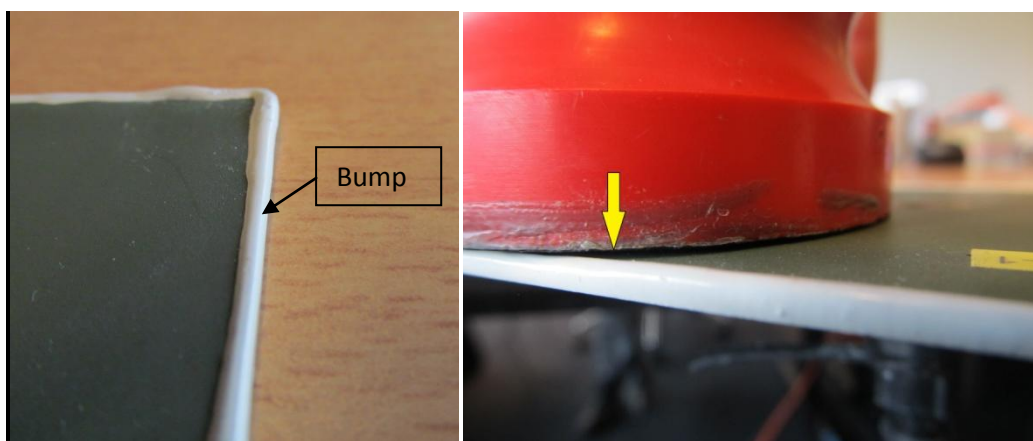

Figure 51. Left: Protective coating creates a bump on the edge of the coupon Right: Space under the handheld sensor caused by the 'bump'.

On the left of Figure 52 a view of how the handheld sensors are placed on a laboratory coupon can be seen. This shows that the edges of the sensor overlap the edges of the coupon. The bump on the edges of the coupons creates a small space underneath the handheld sensor marked by the yellow arrow in Figure 51. This makes that the contact of the handheld sensor with the coating is not optimal. To overcome this problem a new design of the handheld sensor was made and better contact with the surface was achieved. On the right of Figure 52 the new slimmer design is shown that overcomes the problem.

Figure 52. Left: Placement on the laboratory coupon of old handheld sensor design. Right: Placement on the laboratory coupon of new handheld sensor design.

7.3   Coating condition before measurement

The laboratory coupons were periodically measured after the wet cycle of the different degradation tests as described in section 4.3.1. Since the cabinets were located in Marknesse the timing to arrive from Delft at the right moment, just after the wet cycle, was not always perfect. In order to get correct measurements it is important that the coatings are saturated with an electrolyte. A mismatch in timing leads to drying of the coating. An EIS measurement performed on a dried coating may result in a higher PV and CV, while in reality the coating quality is lower. This phenomenon could not directly be related to the results, but it is important to make sure saturation of the coating is obtained before a measurement is executed.

7.4   Result interpretation with incorrect set resolution

7.5   Switching current range up versus down

In performing EIS measurements, it is important that the correct current range is set in the EIS software. The selection of current range is determined by the quality of the organic coating. The

current sensitivity used by the potentiostat is determined by the quality of the coating. High quality coatings are measured with a high current sensitivity as the quality drops the current sensitivity does the same. The used potentiostat is capable of switching to a less sensitive current range during recording, but it is less capable of switching the other way around. In certain boundary situations this can have a huge effect on the recorded EIS spectra. For the operator it is therefore important to recognize this phenomenon, as shown in Figure 53.
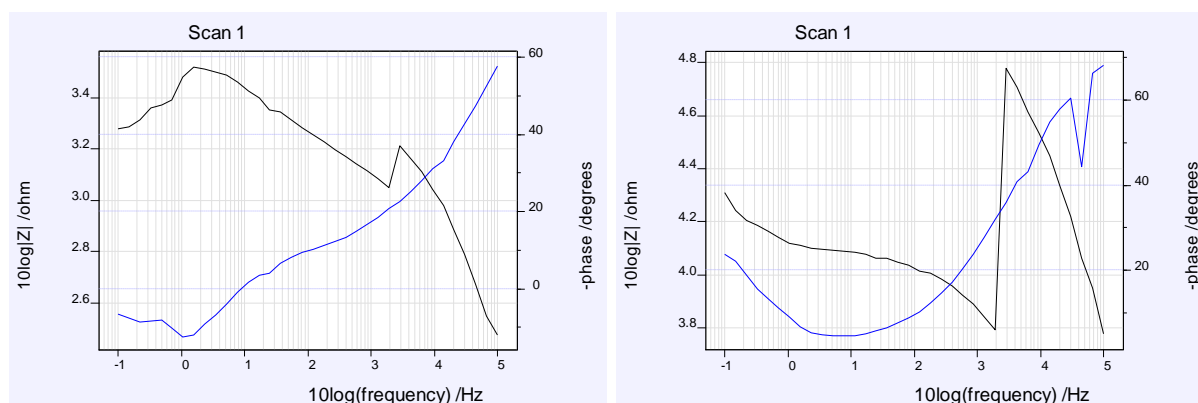
Figure 53. Two examples of incorrect current range switching.

7.6 Surface area of electrolyte contact

In order to interpreter to correct values from an recorded EIS spectrum it is important to know the exact surface area of the coating in contact with the electrolyte. The construction of the used electrochemical cell with the laboratory setup makes this surface area very controlled. The silicon seal of the electrochemical cell provides a good barrier for keeping the electrolyte inside the defined surface of the cell. Figure 54 shows the defined surface area shielded by the silicon seal.
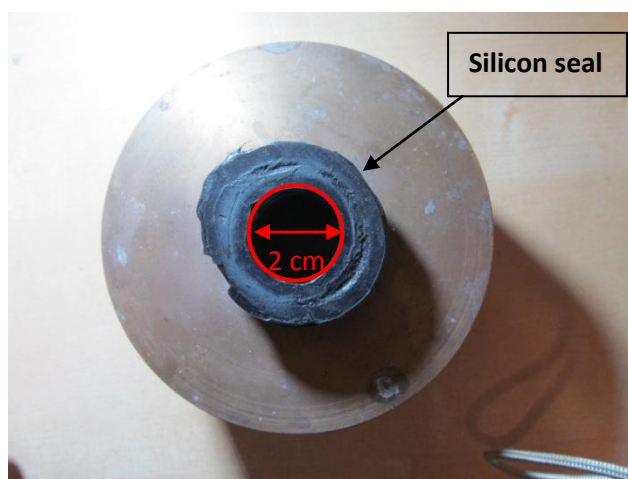

Figure 54. Red circle indicates the surface area defined by the silicon seal.

8 Recommendations

8.1 Identical measurement surface area between handheld and laboratory setup.

To get a better comparison between the EIS results collected with the handheld setup and that of collected with the laboratory setup, a further research could include a laboratory cell in which the electrolyte contact surface is the same as in the handheld setup. An option to achieve this is to make an electrochemical cell consisting of two separate cells and connect them with an electrolyte bridge. Figure 56 shows a schematic of the proposed setup, the surface area of the two electrochemical cells should be the same as the two handheld sensors. In all individual measurements the both setups need to be placed on the coating at the same location.
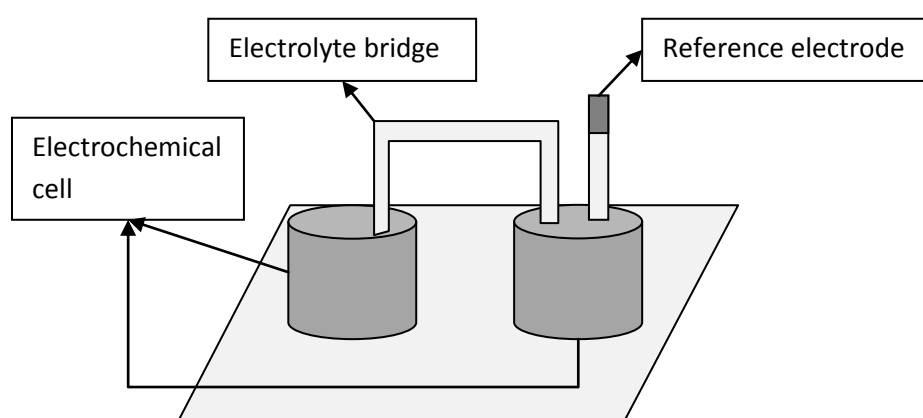
Figure 55. Schematic representation of the proposed setup.

8.2 Generate PV and CV with the help of a computer script

The simplified interpretation method used in this research to generate the PV and CV is done 'by hand' this means that all recorded EIS spectra are individually analyzed to calculate both values. To make this process commercial more interesting, a relative simple computer script can make the interpretation of an individual EIS spectrum much quicker. It is in important that boundaries for such a script are well defined and validated. For example a multiple time-constants detection, which would indicate that the calculated values are not correct, due to the single time constant limitation of the simplified interpretation method.

8.3   Electrolyte diffusion

To be able to perform an EIS measurement with the handheld setup that provides information of an in situ coating condition, it is important the coating is conditioned before a measurement is performed. In this research this was achieved with stickers containing electrolyte which were applied two weeks before executing the EIS measurements. It would be helpful to get insight in the diffusion characteristics of the coating in an in situ situation. This can be achieved by placing the handheld sensor on the unconditioned coating and record EIS spectra in batch mode till a stable spectrum is reached. The diffusion coefficient may be estimated from the reduced water volume fraction as described in section 3.4.3. Since the duration of this measurement can be a couple of days, the measurement setup needs to be capable of performing this without an operator present.

8.4   Surface area of electrolyte contact of the handheld sensor

9 Measurement protocol

9.1 Introduction

In this section a guideline is described of how to perform EIS measurements with the handheld setup on an in-situ application. For this guideline a steel bridge is taken as example shown in Figure 56. In general, it is important to take enough pictures and to keep a detailed logbook.

Figure 56. Typical steel bridge

9.2 Guideline

Preparation

1. An overview of the coating system applied on the construction has to be made. Important is to know what type of coating is used and on what protective principle it is based (chromates, pigments, etc). The history of the coating, when is it applied, known defects or repairs, have been an overlaying in the past.

2. Make an assessment of the measurement positions and the quantity of measurement positions, in order to get a insight of the condition of the coating system. There are multiple issues that need to be addressed in this assessment. It is advised is to divide the construction into sections as shown in the schematic in Figure 57. Then determine which sectors are most likely to have to withstand the hardest conditions, general wind directions, presence of sand, sea, other aggressive media, weld lines, defects, etc. need to be taken into account.

   These sections should all contain multiple measurement positions. Make sure the measurement   positions do not contain local defects for overall qualification of the coating. It is not required to include measurement positions in all other sections. All measurement positions need to have a unique code, to be able to trace back measurement results to the exact position.
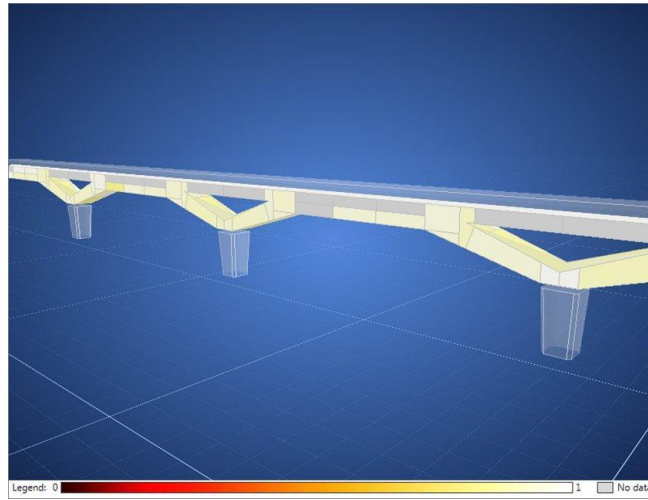
Figure 57. Schematic with the different sections of a steel bridge.

EIS measurements on location

10 Bibliography

[1] H. Lenderink, Filiform Corrosion of coated Aluminium Alloy "a study of mechanism", Delft, 1995.

[2] S. Pappa, Oldest Human Paint-Making Studio Discovered in Cave, Live Science, 2011.

[3] W. Hamer, Environmentally friendly corrosion protection of steel: (im)possibilities, Delft: Polypyrrole Electrochemistry, 2005.

[4] J. de Wit, D. der Weijde and G. Ferrari, Organic coatings, Delft.

[5] Z. Wicks Jr., F. Jones, S. Pappas and D. Wicks, Organic Coatings: Science and Technology, Third Edition, Wiley, 2007.

[6] E. Westing, "Determination of coating performance with impedance measurements," Delft, 1992.

[7] S. sytems, "Epoxy and polyurethane coating systems for marine applications," juni 2001. [Online]. Available: http://www.pondussnickeri.se/.

[8] A. Forsgren, Corrosion control trough organic coatngs, CRC Press.

[9] T. Bos, Prediction of coating durability, Delft, 2008.

[10] G. Grundmeier, W. Schmidt and M. Stratmann, "Corrosion protection by organic coatings: electrochemical mechanism and novel methods of investigation," vol. 2000, no. 45, pp. 15-16, 1999.

[11] G. Bayer and M. Zamanzadeh, "Failure Analysis of Paints and Coatings," 2004.

[12] B. Boelen, B. Schmitz, J. Defourny and F. Blekkenhorst, "A literature survey on the development of an accelerated laboratory test method for atmospheric corrosion of precoated steel products," no. 34, 1993.

[13] G. Bierwagen, L. He, J. Li, L. Ellingson and D. Tallman, "Studies of a new accelerated evaluation method for coating corrosion resistance," *Progress in organic coatings,* no. 39, pp. 67-78, 2000.

[14] F. Geenen, "Characterisation of organic coatings with impedance measurements: a study of coating structure, adhesion and underfilm corrosion," Delft, 1991.

[15] B. Appleman, "Survey of accelerated test methods for anti-corrosive coating performance," vol. 1990, no. 67.

[16] "Method of Salt Spray (Fog) Testing". Patent ASTM B 117.

[17] E. Fekete and B. Lengyel, "Accelerated testing of waterborne coatings," 2005.

[18] B. Heffer and B. Lee, "Braving the Elements Analyzing the weathering performance of chromate-free coating systems," vol. 2005.

[19] S. Boocock, "Meeting industry needs for improved tests," vol. 1995.

[20] M. Morcillo, J. Simanacas, J. Bastidas, S. Feliu, C. Blanco and F. Camón, "Comparison of laboratory tests and outdoor tests of paint coatings for atmospheric exposure.," in *Polymeric Materials for Corrosion control*, American Chemical Society, 1986.

[21] M. Aamodt, "New water-borne products matching solvent-borne coatings in corrosion protection," [Online].

[22] ASTM, "Standard practice for testing water resistance of coatings in 100% relative humidity". Patent D2247.

[23] ASTM, "Standard specification for reagent water". Patent D1193.

[24] B. Carlozzo, J. Andrews, F. Anwari, M. DiLorenzo, R. Glover, S. Grossman, C. Harding, J. McCarthy, B. Mysza, R. Raymond, B. Skerry, P. Slifko, W. Stipkovich, J.

Weaver and G. Wilson, "Correlation of accelerated exposure testing and exterior exposure sites," vol. 1996.

[25] L. Fedrizzi, A. Bergo, F. Deflorian and L. Valentinelli, "Assessment of protective properties of organic coatings by thermal cycling," vol. 2003.

[26] G. Bierwagen, D. Tallman, J. Li, L. Hea and C. Jeffcoate, "EIS studies of coated metals in accelerated exposure," vol. 2003.

[27] ASTM, "Standard practice for cyclic salt fog/UV exposure of painted metal, (alternating exposures in a fog/dry cabinet and a UV/condensation cabinet)". Patent D5894-10.

[28] D. Macdonald, Transient techniques in electrochemistry, New York: Plenum, 1977.

[29] M. Sluyters-Rehbach and J. Sluyters, Electroanalytical chemistry, New York, 1970.

[30] D. Macdonald, Reflections on the history of electrochemical impedance spectroscopy, Pennsylvania, 2005.

[31] E. Warburg, Ueber das verhalten sogenannter unpolarisirbarer elektroden gegen, 1899.

[32] A. de Jong, "Characterization of coatings inside food and beverage cans," Delft, 2000.

[33] D. Loveday, P. Peterson and B. Rodgers, "Evaluation of organic coatings with electrochemical impedance spectroscopy," Warminster, 2005.

[34] M. McKubre, D. MacDonald and J. MacDonald, Impedance Spectroscopy: Theory, Experiment, and Applications, New York: John Wiley & Sons, 1987.

[35] Z. Stoynov, "Impedance modelling and data processing: Structural and parametrical," *Electrochimica Acta,* no. 35, pp. 1493-1499, 1990.

[36] T. Nguyen, J. Hubbard and J. Pommersheim, "Unified model for the degradation of organic coatings in steel in a neutral elecrolyte," *Journal of coatings technology,* 1996.

[37] D. Weijde, "Impedance Spectroscopy and organic barrier coatings," Delft University of Technology, Delft, 1996.

[38] F. Mansfeld, "Use of electrochemical impedance spectroscopy for the study of corrosion protection by polymer coatings," *Journal of Applied Electrochemistry,* no. 25, pp. 187-202, 1995.

[39] C. Moren, S. Hernández, J. Santana, J. González-Guzmán, R. Souto and S. González, "Characterization of Water Uptake by Organic Coatings Used for the Corrosion Protection of Steel as Determined from Capacitance Measurements," *International Journal of electrochemical science,* vol. 2012.

[40] J. Mayne, The Mechanism of the Inhibition of the Corrosion of Iron and Steel by Means of Paint, Official Digest, 1952.

[41] C. Bacon, J. Smith and F. Rugg, Electrolytic resistance in evaluating protective merit of coatings on metals, Industrial and engineering chemistry, 1948.

[42] C. Wu, X. Zhou and Y. Tan, A study on the electrochemical inhomogeneity of organic coatings, Progress in organic coatings, 1995.

[43] E. Kinsella and E. Mayne, Ionic conduction in polymer films I. influence of electrolyte on resistance, British polymer journal, 1969.

[44] H. Leidheiser Jr., Corrosion control by organic coatings, NACE, 1981.

[45] J. Mayne and J. Scantlebury, Ionic conduction in polymer films: II. Inhomogeneous structure of varnish films, British polymer journal, 1970.

[46] R. Fernandez-Prini and H. Corti, Epoxy coal tar films: Membrane properties and film deterioration, Journal of Coatings Technology, 1977.

[47] H. Corti, R. Fernández-Prini and D. Gómez, Protective organic coatings: Membrane properties and performance, Progress in Organic Coatings, 1982.

[48] H. Leidheiser and P. Deck, "Chemistry of the metal-polymer interfacial region," *Science,* no. 241, pp. 1176-1181, 1988.

[49] J. Murray and H. Hack, "Testing organic architectural coatings in ASTM synthetic seawater immersion condition using EIS," *Corrosion,* no. 48, pp. 671-685, 1992.

[50] L. Gray and B. Appleman, "EIS electrochemical impedance spectroscopy - A tool to predict remaining coating life?," *Journal of protective coatings and linings ,* no. 20, pp. 66-74, 2003.

[51] J. Mcintyre and H. Pham, "Electrochemical impedance spectroscopy; a tool for organic coatings optimizations," *Progress in organic coatings,* no. 27, pp. 201-207, 1996.

[52] 3M, "MSDS 3M™ Scotch-Brite™ Products, 7447, 7467, General Purpose Pad," 2011.

[53] ASTM, "Standard practice for modified salt spray (fog) testing". 2011.

[54] ASTM, "Standard practice for operating fluorescent ultraviolet (UV) lamp apparatus for exposure of nonmetallic materials". 2012.

[55] I. technologies, "Iviumsoft manual," Eindhoven, 2010.

[56] H. Bao, J. Bahr, J. He, M. Stafslien, S. Balbyshev and B. J. Chisholm, "Novel Mg-rich primers based on a binder system derived from organically-modified silica nanoparticles," Department of coatings and polymeric materials, North Dakota State Univerity, 2010.

[57] D. Battocchi, A. Simoes, D. Tallman and G. Bierwagen, "Electrochemical behaviour of a Mg-rich primer in the protection of Al alloys," *Corrosion Science,* vol. 2006, no. 48, 2005.

[58] H. Ochs, J. Vogelsang and G. Meyer, "Enhanced surface roughness of organic coatings due to UV-degradation: an unknown source of EIS-artifacts," *Progress in organic coatings,* vol. 2003, no. 46-3, pp. 182-190, 2001.

[59] F. Lytle, R. Greegor, G. Bibbins, K. Blohowiak, R. Smith and G. Tuss, "An investigation of the structure and chemistry of a chromium-conversion surface layer on aluminum," *Corrosion Science,* vol. 1995, no. 37-3, pp. 349-369.

[60] G. Walter, The application of impedance spectroscopy to study the uptake of sodium chloride solution in painted metals, Corrosion science, 1991.

[61] T. Bos, "Prediction of coating durability," Delft, 2008.

[62] M. Morcillo, J. Simanacas, J. Bastidas, S. Feliu, C. Blanco and F. Camón, "Comparison of laboratory tests and outdoor tests of paint coatings for atmospheric exposure.," in *Polymeric Materials for Corrosion control*, American Chemical Society, 1986.

[63] B. Carlozzo, J. Andrews, F. Anwari, M. DiLorenzo, R. Glover, S. Grossman, C. Harding, J. Mc Carthy, B. Mysza, R. Raymond, B. Skerry, P. Slifko, W. Stipkovich, J. Weaver and G. Wilson, "Correlation of accelerated exposure testing and exterior exposure sites," vol. 1996.

[64] L. Fedrizzi, A. Bergo, F. Deflorian and L. Valentinelli, "Assessment of protective properties of organic coatings by thermal cycling," vol. 2003.

[65] G. Bierwagen, D. Tallman, J. Li, L. Hea and C. Jeffcoate, "EIS studies of coated metals in accelerated exposure," vol. 2003.

[66] G. Bierwagen, "Reflections on corrosion control by organic coatings," *Progress in organic coatings,* no. 28, pp. 43-48, 1996.

[67] J. Wang, Y. Zuo and Y. Tang, "The study on Mg-Al rich epoxy primer for protection of aluminum alloy.," *International Journal of Electrochemcal Science,* vol. 2013, no. 8, pp. 1-14, 2013.

[68] M. Ohman and D. Persson, "ATR-FTIR Kretschmann spectroscopy for interfacial studies of a hidden aluminum surface coated with a silane film and epoxy II.

Analysis by integrated ATR-FTIR and EIS during exposure to electrolyte with complementary studies by in situ ATR-FTIR and in sit," *Surface and Interface Analysis,* vol. 2012, no. 44, pp. 105-113, 2011.

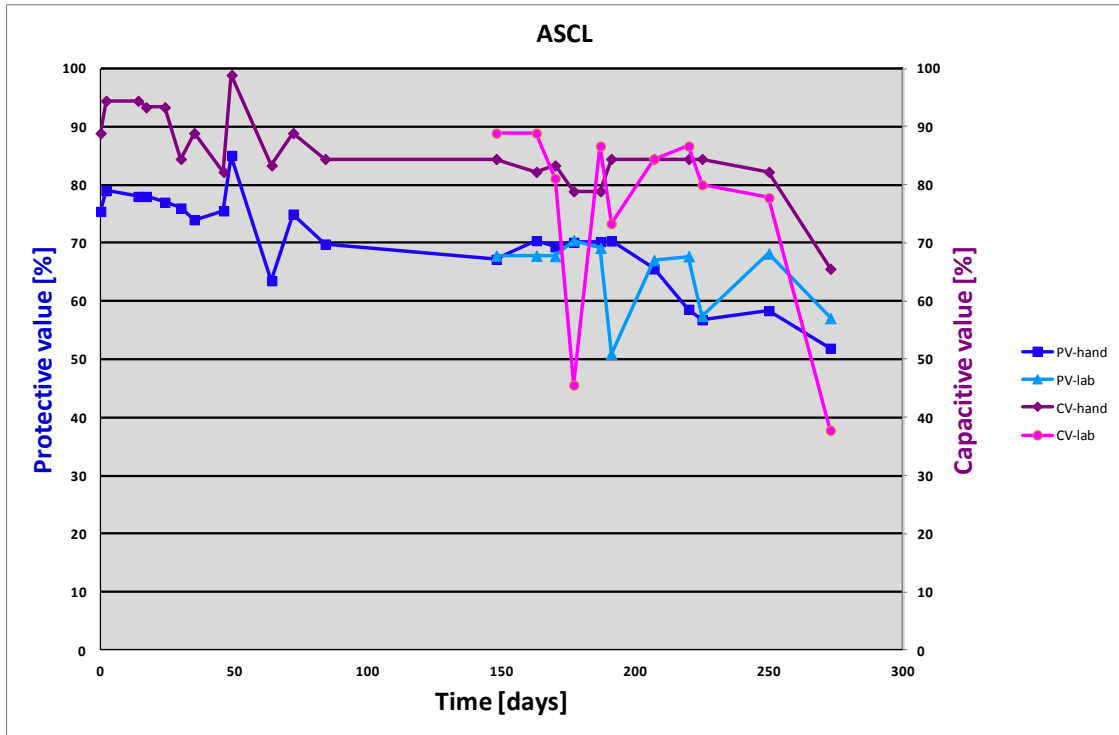# 11 Appendix

11.1 Appendix A

Figure 58. The result values PV and CV of the laboratory coupon ASCL degraded in the salt spray cabinet.
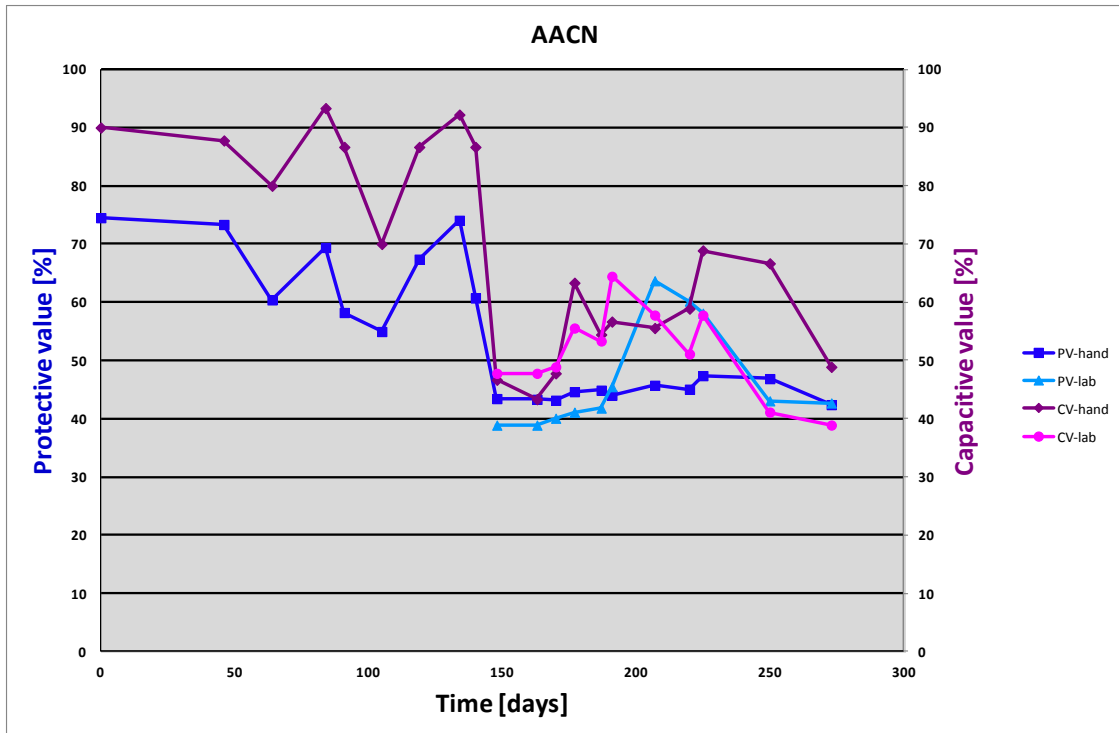

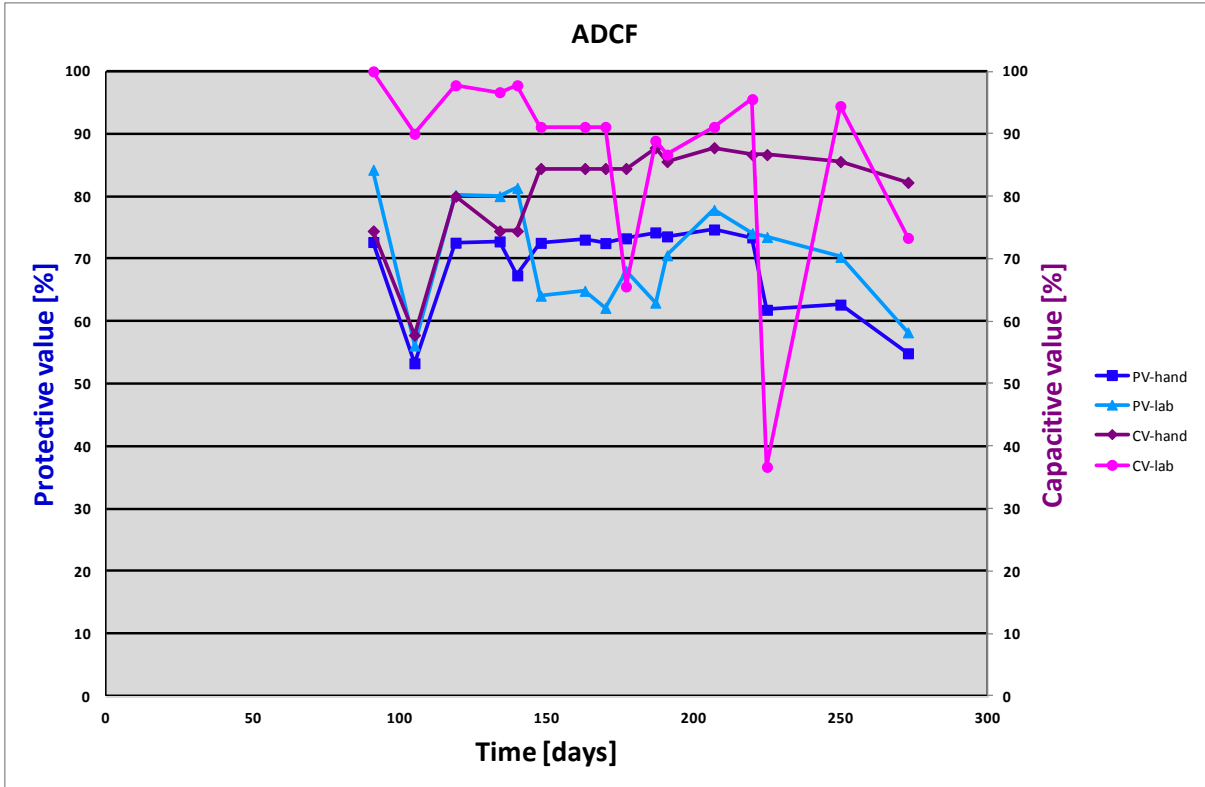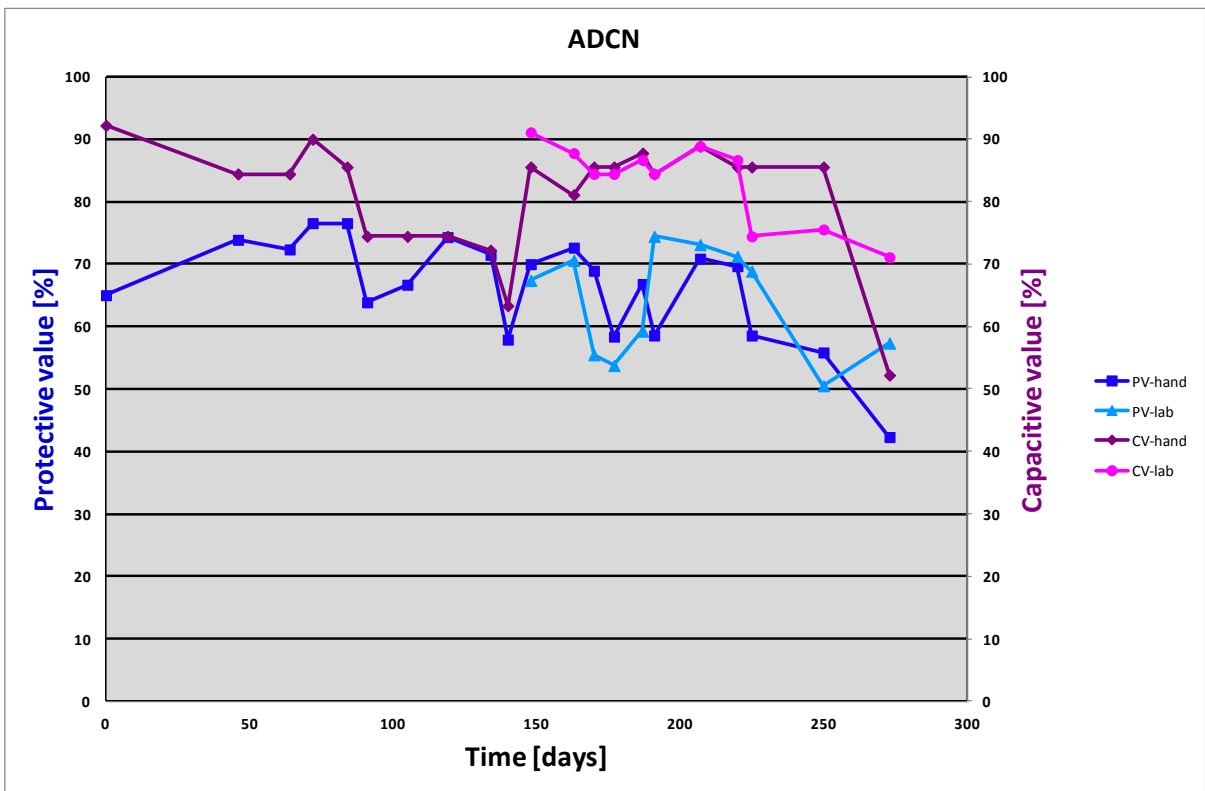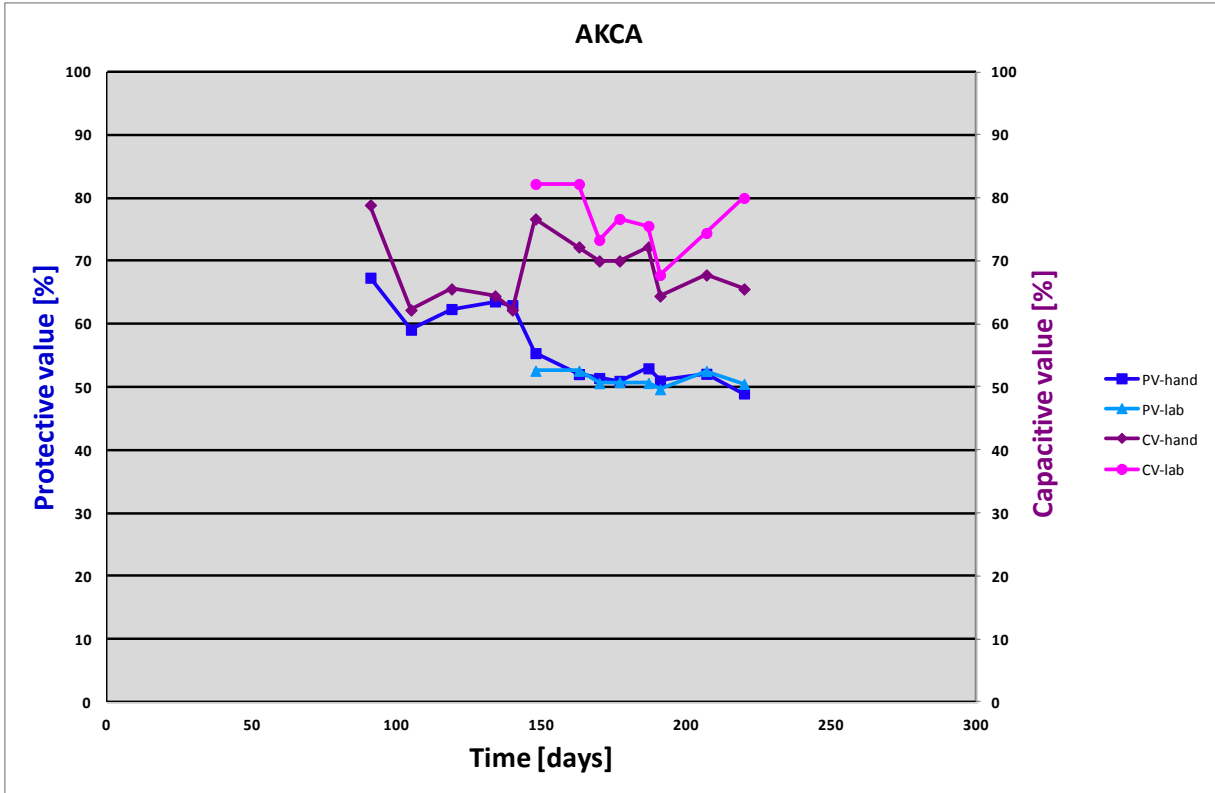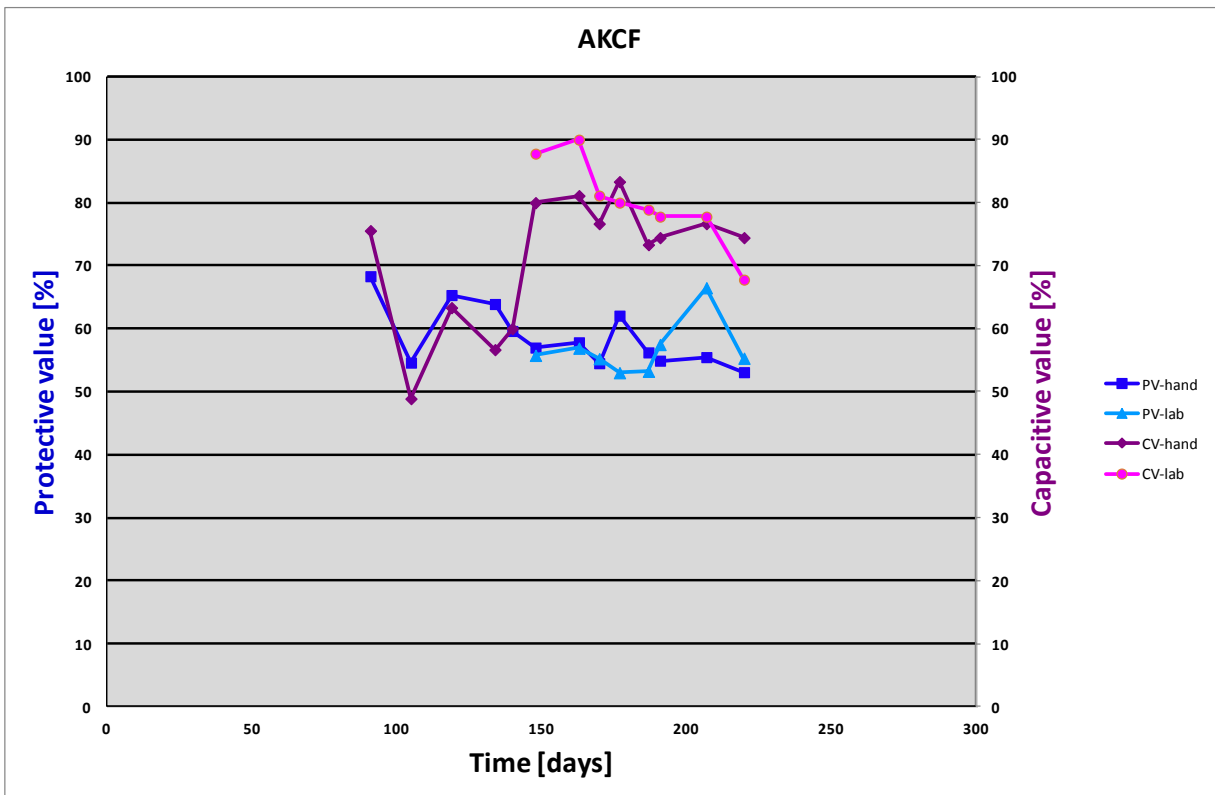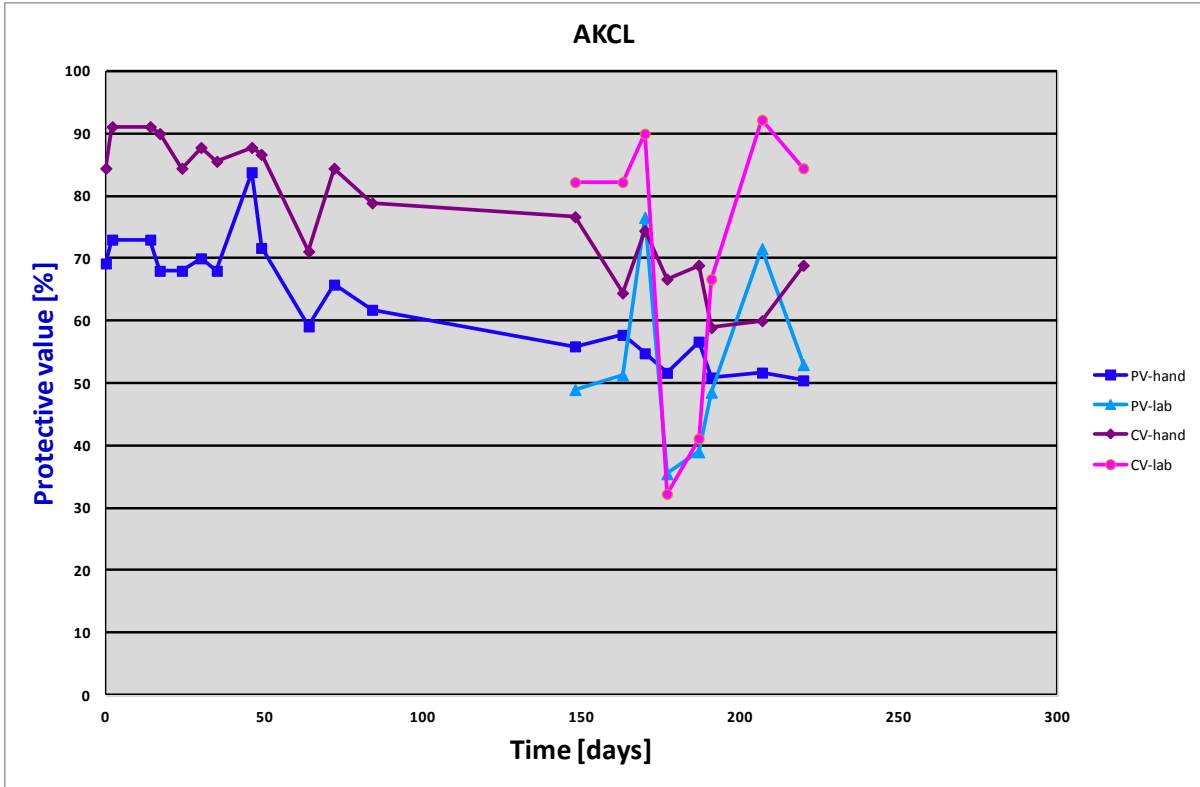**Figure 59. The result values PV and CV of the laboratory coupon AACN degraded in the salt spray cabinet.**
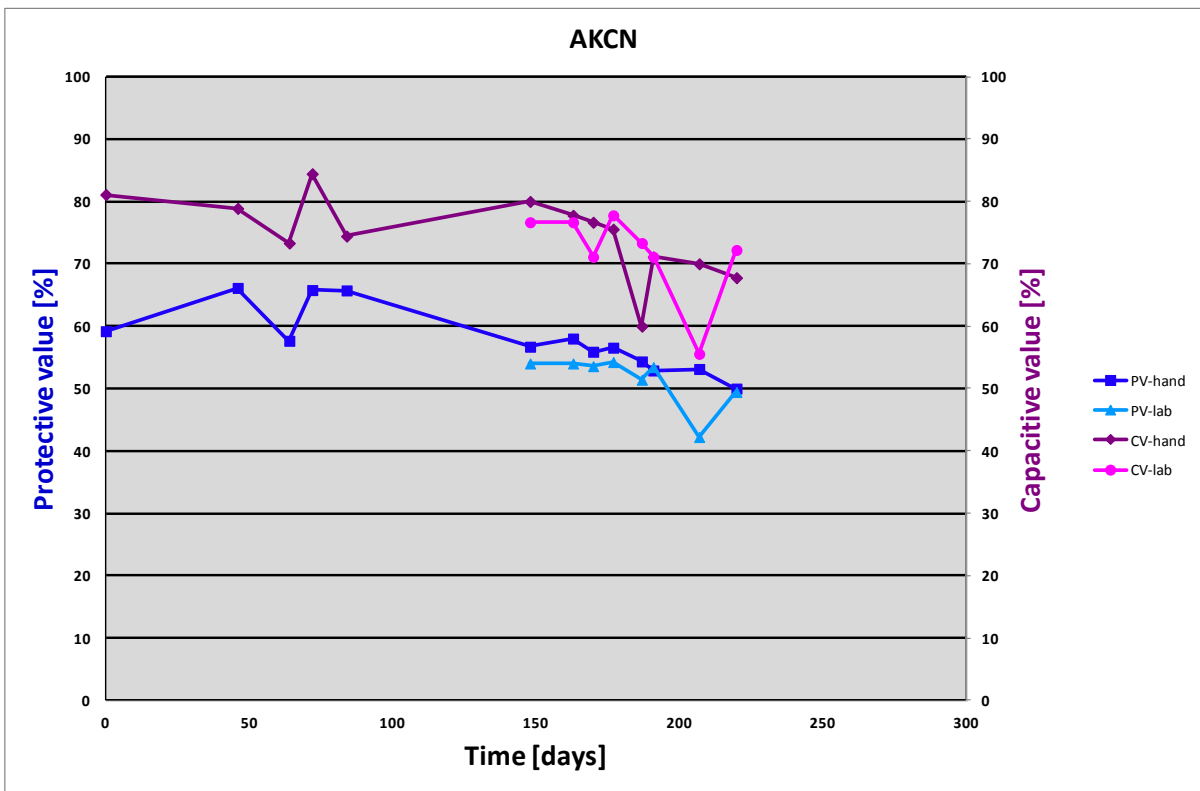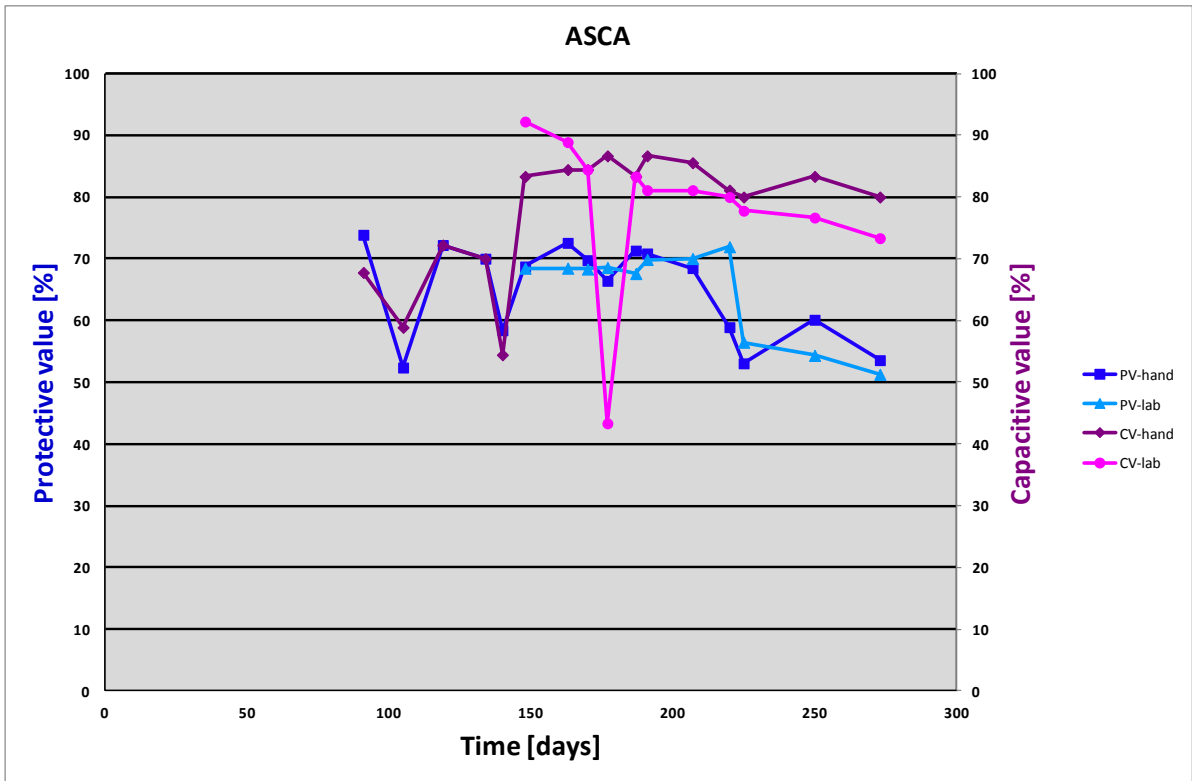
Figure 60. The result values PV and CV of the laboratory coupon ADCF degraded in the salt spray cabinet.

Figure 61. The result values PV and CV of the laboratory coupon ADCN degraded in the salt spray cabinet.

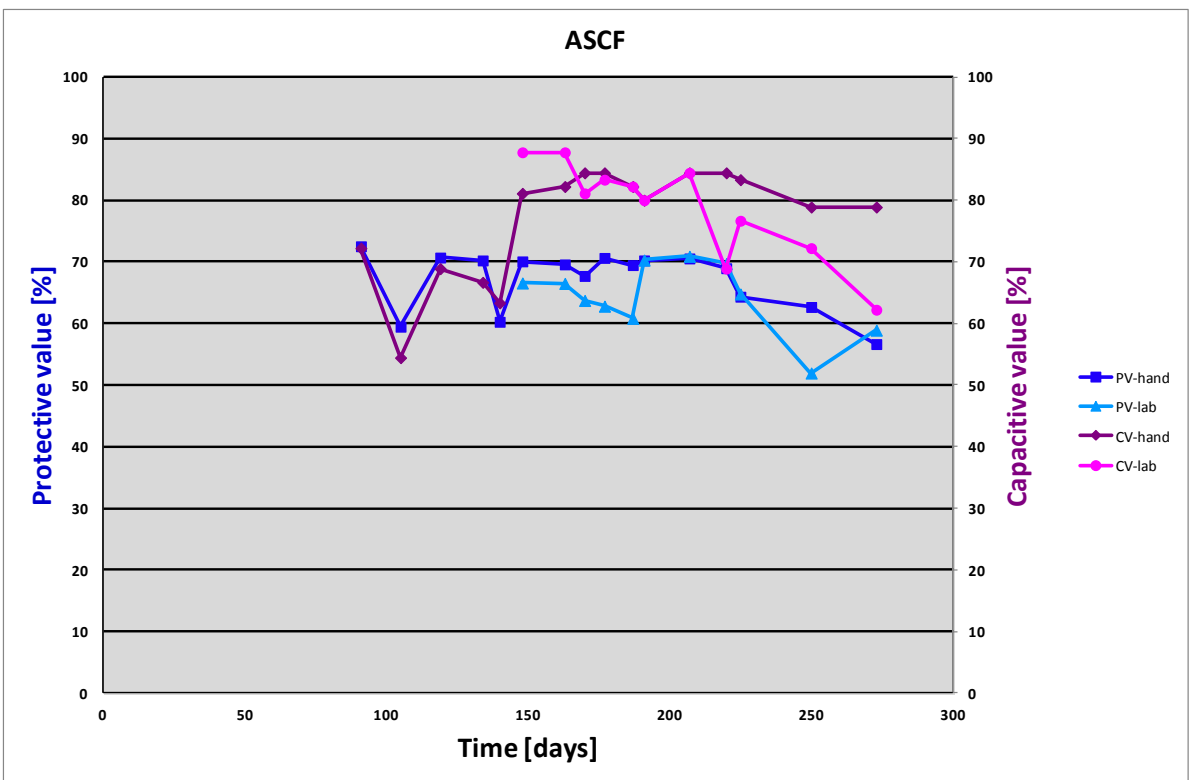Figure 62. The result values PV and CV of the laboratory coupon AKCA degraded in the salt spray cabinet.

Figure 63. The result values PV and CV of the laboratory coupon AKCF degraded in the salt spray cabinet.
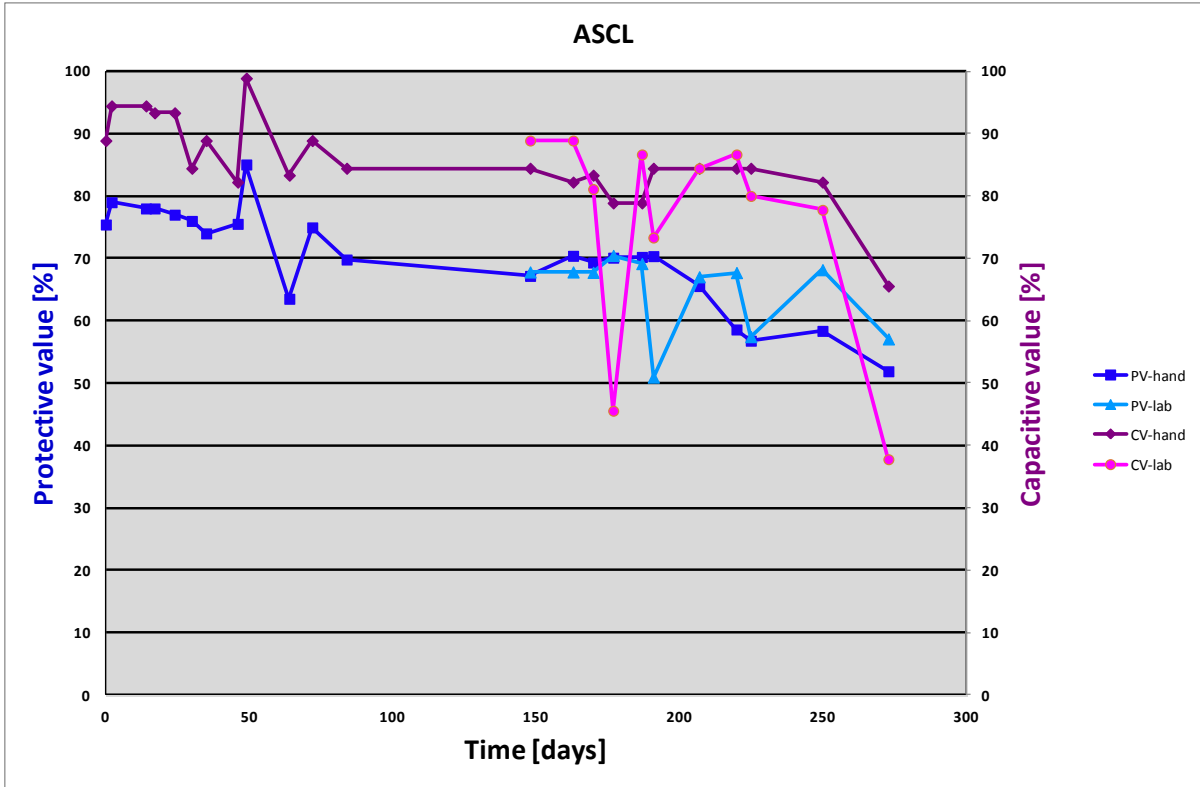
Figure 64. The result values PV and CV of the laboratory coupon AKCL degraded in the salt spray cabinet.

Figure 65. The result values PV and CV of the laboratory coupon AKCN degraded in the salt spray cabinet.

Figure 66. The result values PV and CV of the laboratory coupon ASCA degraded in the salt spray cabinet.

Figure 67. The result values PV and CV of the laboratory coupon ASCF degraded in the salt spray cabinet.

Figure 68. The result values PV and CV of the laboratory coupon ASCL degraded in the salt spray cabinet.
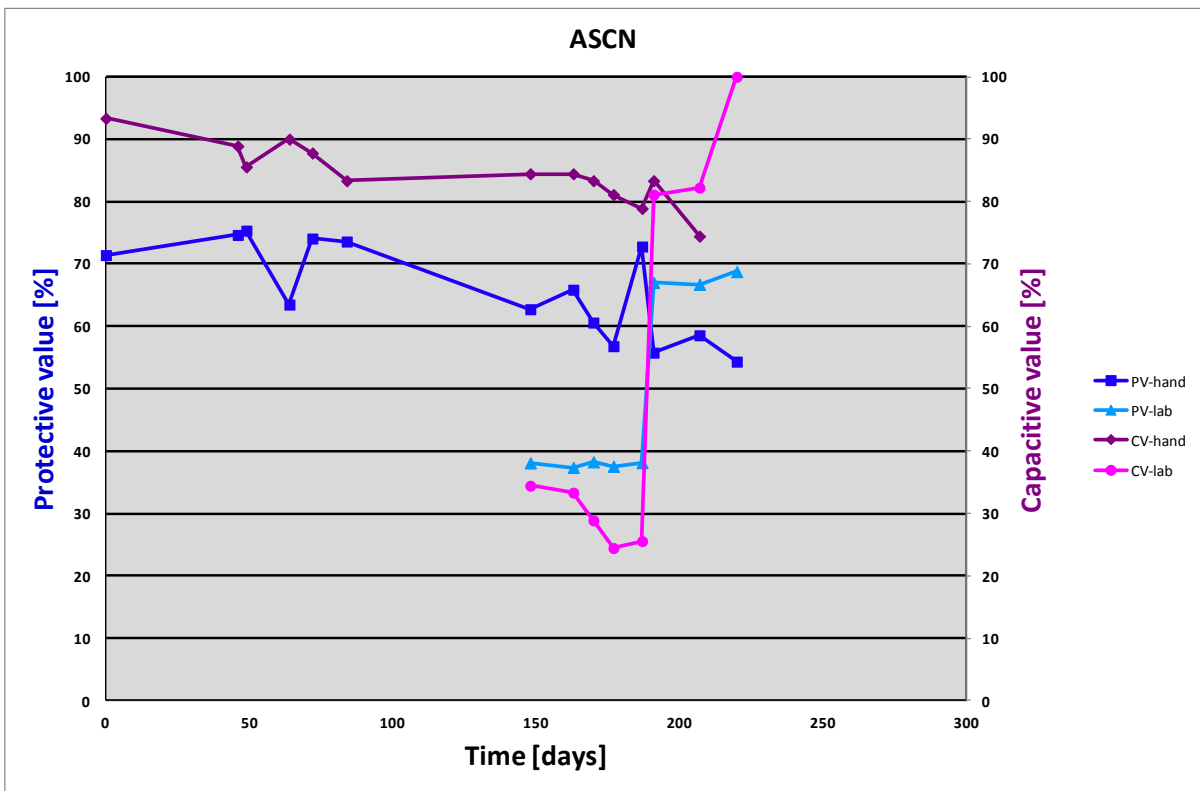

Figure 69. The result values PV and CV of the laboratory coupon ASCN degraded in the salt spray cabinet.
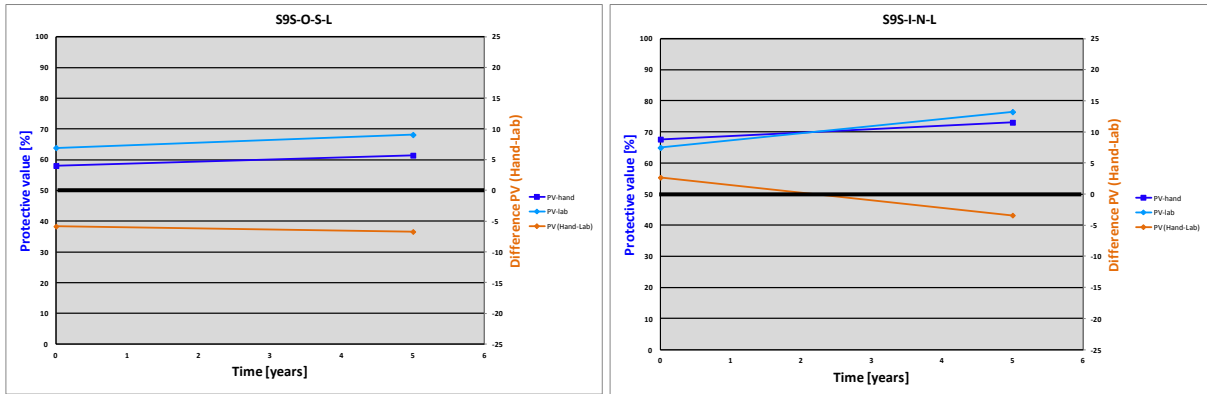
11.2 Appendix B

Figure 70. Difference between the PV results measured with handheld and laboratory setup for the coupons degraded in a natural environment.
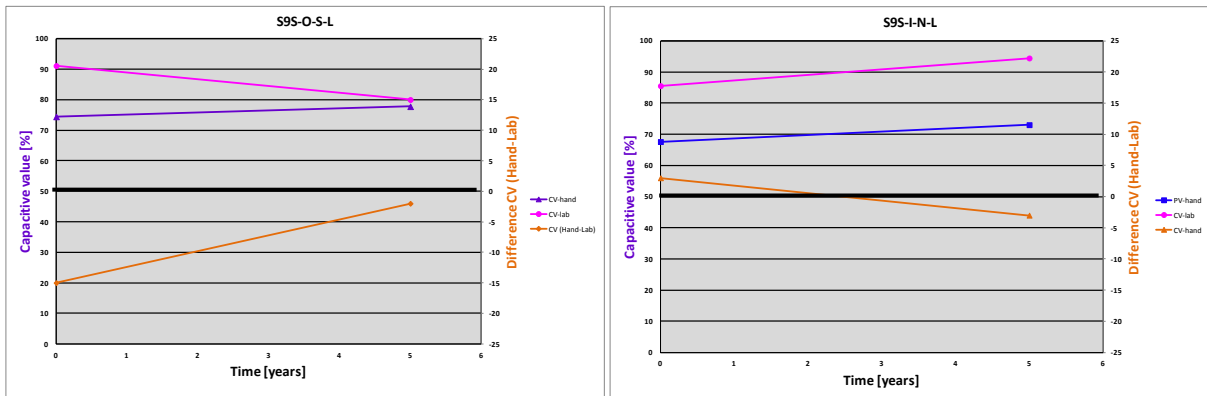

Figure 71. Difference between the CV results measured with handheld and laboratory setup for the coating positions degraded at the Oosterscheldekering.

Table 9. Average Average difference in % between the result values of the handheld and the laboratory setup for the coating positions degraded at the Oosterscheldekering.

	S9S-I-N-L	S9S-O-S-L	Overall
PV	-6.28	-0.37	-3.33
CV	-8.50	0.00	-4.25